

PRODUCTION OF PHOTOCATALYTICALLY ACTIVE  $\text{TiO}_2 - \text{P}_2\text{O}_5$  GLASSES  
BY THE SOL-GEL PROCESS

A THESIS SUBMITTED TO  
THE GRADUATE SCHOOL OF NATURAL AND APPLIED SCIENCES  
OF  
MIDDLE EAST TECHNICAL UNIVERSITY

BY

YIĞIT CANSIN ÖZTÜRK

IN PARTIAL FULFILLMENT OF THE REQUIREMENTS  
FOR  
THE DEGREE OF MASTER OF SCIENCE  
IN  
METALLURGICAL AND MATERIALS ENGINEERING

SEPTEMBER 2019



Approval of the thesis:

**PRODUCTION OF PHOTOCATALYTICALLY ACTIVE TIO<sub>2</sub> – P2O<sub>5</sub>  
GLASSES BY THE SOL-GEL PROCESS**

submitted by **YIĞIT CANSIN ÖZTÜRK** in partial fulfillment of the requirements  
for the degree of **Master of Science in Metallurgical and Materials Engineering**  
**Department, Middle East Technical University by,**

Prof. Dr. Halil Kalıpçılar  
Dean, Graduate School of **Natural and Applied Sciences**

\_\_\_\_\_

Prof. Dr. Cemil Hakan Gür  
Head of Department, **Met. and Mat. Eng.**

\_\_\_\_\_

Assist. Prof. Dr. Mert Efe  
Supervisor, **Met. and Mat. Eng., METU**

\_\_\_\_\_

Prof. Dr. Jongee Park  
Co-Supervisor, **Met. and Mat. Eng., Atılım Univ.**

\_\_\_\_\_

**Examining Committee Members:**

Prof. Dr. İshak Karakaya  
Met. and Mat. Eng., METU

\_\_\_\_\_

Assist. Prof. Dr. Mert Efe  
Met. and Mat. Eng., METU

\_\_\_\_\_

Prof. Dr. Caner Durucan  
Met. and Mat. Eng., METU

\_\_\_\_\_

Prof. Dr. Jongee Park  
Met. and Mat. Eng., Atılım Univ.

\_\_\_\_\_

Assoc. Prof. Dr. Volkan Kalem  
Met. and Mat. Eng., Konya Tech. Univ.

\_\_\_\_\_

Date: 09.09.2019

**I hereby declare that all information in this document has been obtained and presented in accordance with academic rules and ethical conduct. I also declare that, as required by these rules and conduct, I have fully cited and referenced all material and results that are not original to this work.**

Name, Surname: Yiğit Cansın Öztürk

Signature:

## ABSTRACT

### PRODUCTION OF PHOTOCATALYTICALLY ACTIVE TiO<sub>2</sub> – P<sub>2</sub>O<sub>5</sub> GLASSES BY THE SOL-GEL PROCESS

Öztürk, Yiğit Cansın

Master of Science, Metallurgical and Materials Engineering

Supervisor: Assist. Prof. Dr. Mert Efe

Co-Supervisor: Prof. Dr. Jongee Park

September 2019, 128 pages

TiO<sub>2</sub>-P<sub>2</sub>O<sub>5</sub> (TP) gels containing large amounts of TiO<sub>2</sub> were successfully synthesized by the sol-gel process. Influence of processing parameters such as pH, Ti precursor type, amount, H<sub>2</sub>O/Ti ratio, solvent type, concentration on the formation of homogeneous gels were investigated. Prepared gels were subjected to regulated heat-treatments at various temperatures, durations, and heating rates to obtain monolithic TP glasses. Binary glasses having compositions of xTiO<sub>2</sub> · (1-x)P<sub>2</sub>O<sub>5</sub> (x= 70, 80, 90, 95 mol %) were produced and evaluated in terms of their appropriateness for self-cleaning applications. The results revealed that photocatalytic activity of glasses could be customized by controlling processing and heat-treatment conditions carefully. TP glasses have effectively decomposed Methylene Blue (MB) under UV illumination and best MB degradation rate was 96.1 % after exposing to UV light for 90 min. Enhanced photocatalytic activity was attributed to compatibility of anatase crystallinity along with high specific surface area owing to the amorphous.

Keywords: Sol-gel, Glass, TiO<sub>2</sub>, P<sub>2</sub>O<sub>5</sub>, Photocatalytic, Self-cleaning

## ÖZ

### FOTOKATALİTİK OLARAK AKTİF TiO<sub>2</sub> – P<sub>2</sub>O<sub>5</sub> CAMLARININ SOL-JEL SÜRECİYLE ÜRETİLMESİ

Öztürk, Yiğit Cansın  
Yüksek Lisans, Metalurji ve Malzeme Mühendisliği  
Tez Danışmanı: Dr. Öğr. Üyesi Mert Efe  
Ortak Tez Danışmanı: Prof. Dr. Jongee Park

Eylül 2019, 128 sayfa

Yüksek miktarda TiO<sub>2</sub> içeren TiO<sub>2</sub>-P<sub>2</sub>O<sub>5</sub> (TP) jelleri sol-jel süreciyle başarıyla sentezlendi. pH, Ti prekürsör türü ve miktarı, H<sub>2</sub>O/Ti oranı, çözücü türü ve konsantrasyonu gibi işlem parametrelerinin homojen jel oluşumu üzerindeki etkisi araştırıldı. Hazırlanan jeller, monolitik ve şeffaf TP camlarını elde etmek için çeşitli sıcaklık, süre ve ısıtma koşullarında ısıtma işlemlere tabii tutuldu. xTiO<sub>2</sub> · (1-x)P<sub>2</sub>O<sub>5</sub> (x= 70, 80, 90, 95 mol %) kompozisyonuna sahip bir seri camlar üretildi ve kendi kendini temizleme uygulamalarına uygunluğunu araştırmak üzere değerlendirildi. Isıl işlem sıcaklığının kristal tipi, boyutu, morfolojisi ve yüzey alanı üzerindeki etkileri incelendi. Sonuçlar, TP camlarının fotokatalitik etkinliğinin, oluşturma ve ısıtma koşullarını dikkatlice kontrol ederek ayarlanabileceğini ortaya koydu. Üretilen camlar, UV ışık altında metilen mavisini etkin bir şekilde bozundurmıştır ve 90 dakikalık UV ışınma süresi sonunda %96.1 ile en iyi MB bozunumu elde edilmiştir. Camın sahip olduğu yüksek fotokatalitik etkinlik amorf içeriğe bağlı olarak yüksek spesifik yüzey alanına sahip olması ve beraberinde anataz kristalleri barındırmasındandır.

Anahtar Kelimeler: Sol-jel, Cam, TiO<sub>2</sub>, P<sub>2</sub>O<sub>5</sub>, Fotokatalitik, Kendi kendini temizleme

Dedicated to my beloved family,



## ACKNOWLEDGEMENTS

First, I would like to express my deepest gratitude for my supervisors Asst. Prof. Dr. Mert Efe and Prof. Dr. Jongee Park for their continuous support, patience, encouragement, motivation, advice, and guidance throughout this thesis study.

I am deeply grateful to Assoc. Prof. Dr. Volkan Kalem for his valuable contributions, advices, immense knowledge, life counsel, and technical guidance.

My thanks also extend to my examining committee members, Prof. Dr. İshak Karakaya and Prof. Dr. Caner Durucan for their enlightening comments and directions.

I would like to thank my old and current lab-mates from Photocatalytic Materials Laboratory for their infinite support and friendship for all time that we have shared.

This work was partially supported by TÜBİTAK with project number 216M391 and by METU BAP with project number BAP-03-08-2017-281. Their financial support is greatly appreciated.

Finally, and most importantly, sincere thanks go to my parents, Nimet and Abdullah Öztürk and my brother Mert Özcan Öztürk for their everlasting love, support, patience and understanding. Thank you for always being there for me.

## TABLE OF CONTENTS

ABSTRACT .....	v
ÖZ .....	vi
ACKNOWLEDGEMENTS.....	ix
TABLE OF CONTENTS .....	x
LIST OF TABLES.....	xv
LIST OF FIGURES .....	xvii
1. INTRODUCTION.....	1
2. LITERATURE REVIEW.....	5
2.1. General Remarks.....	5
2.2. Self-cleaning .....	5
2.2.1. Photocatalysis.....	5
2.2.2. Photo-induced Superhydrophilicity.....	8
2.3. Self-cleaning Materials .....	9
2.4. Self-cleaning Glasses .....	11
2.5. TiO <sub>2</sub> – P <sub>2</sub> O <sub>5</sub> (TP) Glasses.....	12
2.6. Properties of TP Glasses .....	13
2.7. Preparation of TP Glasses .....	13
2.7.1. Preparation of TP Glasses by Melt Quenching .....	14
2.7.2. Preparation of TP Glasses by Sol-gel Process.....	15
2.8. Steps in the Sol-gel Process .....	16
2.9. Factors Affecting the Sol-gel Process .....	17
3. EXPERIMENTAL PROCEDURE.....	19

3.1. Starting Materials .....	19
3.2. Preparation of TP Gels .....	20
3.3. Heat-treatment of TP Gels.....	23
3.3.1. Fast Heat-treatment Design (FHTD) .....	23
3.3.2. Slow Heat-treatment Design (SHTD).....	24
3.4. Characterization.....	25
3.4.1. X-Ray Diffraction (XRD).....	25
3.4.2. Field Emission Scanning Electron Microscope (FESEM) .....	25
3.4.3. Brauner-Emmett-Teller (BET) Specific Surface Area (SSA) Analysis ...	25
3.4.4. Differential Thermal Analysis (DTA) and Thermogravimetric (TG) Analysis .....	25
3.5. Property Measurements .....	26
3.5.1. Methylene Blue (MB) Photodegradation Test.....	26
3.5.2. Transmittance and Wettability Tests.....	27
4. RESULTS AND DISCUSSION OF SYNTHESIS STUDIES.....	29
4.1. Synthesis of TP Gels by the Sol-gel Process.....	29
4.1.1. Effect of TiO <sub>2</sub> Content.....	29
4.1.2. Effect of TiO <sub>2</sub> Precursor Type .....	31
4.1.3. Effect of Solvent Type .....	33
4.1.4. Effect of Solvent Content .....	35
4.1.5. Effect of Water Content.....	37
4.1.6. Effect of HCl Content .....	39
4.2. Effect of Drying.....	41
4.3. Differential Thermal and Thermogravimetric Analyses (DTA/TG).....	43

4.4. Effect of Heat-treatment Design .....	49
4.4.1. Effect of Fast Heat-treatment .....	49
4.4.2. Effect of Slow Heat-treatment.....	50
5. RESULTS AND DISCUSSION OF CHARACTERIZATION STUDIES.....	51
5.1. X-Ray Diffraction (XRD) .....	51
5.1.1. Effect of TiO <sub>2</sub> Content .....	51
5.1.2. Effect of TiO <sub>2</sub> Precursor Type.....	54
5.1.3. Effect of Solvent Type .....	56
5.1.4. Effect of Solvent Content .....	58
5.1.5. Effect of Water Content .....	60
5.1.6. Effect of HCl Content.....	62
5.1.7. Effect of Heat-treatment Design.....	65
5.1.7.1. Effect of Heat-treatment Temperature.....	65
5.1.7.2. Effect of Heat-treatment Duration .....	72
5.1.7.3. Effect of Heat-treatment Schedule and Heating Rate.....	74
5.2. Scanning Electron Microscope (SEM) and Energy Dispersive Spectroscopy (EDS) Analysis .....	76
5.2.1. Effect of TiO <sub>2</sub> Content .....	76
5.2.2. Effect of Solvent Type .....	80
5.2.3. Effect of Water Content .....	81
5.2.4. Effect of Heat-treatment Temperature .....	82
5.2.5. Effect of Heat-treatment Duration and Heating Rate .....	83
5.3. Brauner Emmett Teller (BET) Specific Surface Area (SSA) Analysis .....	84
5.3.1. Effect of TiO <sub>2</sub> Content .....	86

5.3.2. Effect of TiO <sub>2</sub> Precursor Type .....	86
5.3.3. Effect of Solvent Type .....	87
5.3.4. Effect of HCl Content .....	87
5.3.5. Effect of Heat-treatment Temperature .....	88
5.3.6. Effect of Heat-treatment Duration .....	91
5.3.7. Effect of Heating Rate .....	92
6. RESULTS AND DISCUSSION OF PROPERTY MEASUREMENTS.....	93
6.1. Photocatalytic Activity Measurements.....	93
6.1.1. Effect of TiO <sub>2</sub> Content.....	97
6.1.2. Effect of Solvent Type .....	98
6.1.3. Effect of Solvent Content .....	99
6.1.4. Effect of Water Content.....	100
6.1.5. Effect of HCl Content .....	101
6.1.6. Effect of Heat-treatment Schedule.....	102
6.1.6.1. Effect of Heat-treatment Temperature .....	103
6.1.6.2. Effect of Heat-treatment Duration .....	106
6.1.6.3. Effect of Heating Rate.....	108
6.2. Band Gap Measurements.....	108
6.2.1. Effect of TiO <sub>2</sub> Content.....	109
6.2.2. Effect of Heat-treatment .....	110
6.3. Transmittance Measurements .....	111
6.3.1. Effect of TiO <sub>2</sub> Content and Heat-treatment Temperature.....	112
6.3.2. Effect of Solvent Type .....	112
6.4. Hydrophilicity .....	113

7. CONCLUSIONS .....	117
REFERENCES .....	119

## LIST OF TABLES

### TABLES

Table 3.1. The solvents used in this study and their properties. ....	19
Table 3.2. Information on the chemicals used for the synthesis of TP gels.....	20
Table 4.1. Results for the TP gels synthesized by using different TiO <sub>2</sub> contents.....	30
Table 4.2. Results for the TP gels synthesized by using different TiO <sub>2</sub> precursors...32	
Table 4.3. Results for the TP gels synthesized by using different solvents. ....	34
Table 4.4. Results for the TP gels synthesized by using different solvent molarities. .....	36
Table 4.5. Results for the TP gels synthesized by using different water molarities. .37	
Table 4.6. Results for the TP gels synthesized by using different HCl molarities. ...39	
Table 5.1. Size of the anatase crystallites developed in the TP glasses with different TiO <sub>2</sub> contents.....	54
Table 5.2. Size of the anatase crystallites developed in the TP glasses with different TiO <sub>2</sub> precursors. ....	56
Table 5.3. Size of the anatase crystallites developed in the TP glasses produced by using different solvents. ....	58
Table 5.4. Size of the anatase crystallites developed in the TP glasses produced by using different solvent molarities.....	60
Table 5.5. Solution pH and size of the anatase crystallites developed in the TP glasses produced by using different HCl molarities.....	64
Table 5.6. Crystal sizes of the anatase and rutile crystallites developed during heat- treatment of the TP glasses at different temperatures, heating rates, and durations. .71	
Table 5.7. Batch and analyzed compositions of the TP glasses prepared by various TiO <sub>2</sub> contents.....	80
Table 5.8. Effect of preparation conditions and heat-treatment design on the SSA of the TP glasses prepared.....	85

Table 6.1. MB degradation values of the selected TP glasses after 90 min UV light illumination.....	94
Table 6.2. MB degradation values after 90 min UV light illumination for the TP glasses heat-treated at various temperatures for 1 h. ....	103
Table 6.3. The values for the direct $E_g$ for the TP glasses prepared by various $TiO_2$ content subsequently heat-treated at 600 °C for 1 h. ....	109
Table 6.4. Values for the direct $E_g$ for the TP glasses heat-treated at various temperatures.....	111
Table 6.5. Contact angle values of the TP glasses.....	114



## LIST OF FIGURES

### FIGURES

Figure 2.1. Schematic illustration of the band gap structure of a semiconductor [27]. .....	6
Figure 2.2. Schematic illustration of photoactivated processes [27]. .....	7
Figure 2.3. Effect of UV radiation on hydrophilicity and transparency of a glass slide coated with a TiO <sub>2</sub> thin film [35]. .....	9
Figure 3.1. Flowchart showing the steps involved in the synthesis of the TP gels....	22
Figure 3.2. Drying procedures of the wet gels derived by the sol-gel process. ....	22
Figure 3.3. The temperatures, durations, and heating rates applied in the FHTD of the dried gels. ....	24
Figure 3.4. The temperatures, durations, and heating rates applied in the SHTD of the dried gels. ....	24
Figure 3.5. Flowchart showing the transmittance and contact angle measurement steps of the TP gels. ....	27
Figure 4.1. Appearance of the dried TP gels synthesized by using different TiO <sub>2</sub> contents. ....	31
Figure 4.2. Appearance of the dried TP gels synthesized by using different TiO <sub>2</sub> precursors. ....	32
Figure 4.3. Appearance of the dried TP gels synthesized by using different solvents. ....	34
Figure 4.4. Appearance of the dried TP gels synthesized by using different solvent molarities. ....	36
Figure 4.5. Appearance of the dried TP gels synthesized by using different water molarities. ....	38
Figure 4.6. Appearance of the dried TP gels synthesized by using different HCl molarities. ....	40

Figure 4.7. Variation of weight retention of the gels with drying time at 60 °C. ....	42
Figure 4.8. Appearance of dried gels after 2 weeks of drying at 60 °C.....	43
Figure 4.9. DTA-TG thermograms of the TP gels synthesized by using different TiO <sub>2</sub> contents. a) 80 mol% TiO <sub>2</sub> and b) 95 mol% TiO <sub>2</sub> .....	44
Figure 4.10. DTA-TG thermograms of the TP gels synthesized by using different solvents. a) 2-propanol, b) 2-isopropoxy, c) 2-butoxy, and d) Ethylene glycol. ....	46
Figure 4.11. a) Appearance of the as dried TP gels of different TiO <sub>2</sub> contents, b) appearance of the TP gels of different TiO <sub>2</sub> contents after fast heat-treatment, and c) appearance of the TP gels of different TiO <sub>2</sub> contents after slow heat-treatment.....	50
Figure 5.1. XRD patterns of the dried TP gels synthesized by various TiO <sub>2</sub> contents. ....	52
Figure 5.2. The XRD patterns of the TP glasses prepared by various TiO <sub>2</sub> contents subsequently heat-treated at 600 °C for 1 h. ....	53
Figure 5.3. XRD patterns of the TP glasses prepared by different TiO <sub>2</sub> precursors and heat-treated at 600 °C for 1 h. ....	55
Figure 5.4. XRD patterns of the TP glasses prepared by using different solvents subsequently heat-treated at 600 °C for 1 h. ....	56
Figure 5.5. XRD patterns of the TP glasses prepared by using different solvent molarities subsequently heat-treated at 600 °C for 1 h. ....	59
Figure 5.6. XRD patterns of the TP glasses prepared by using different water contents subsequently heat-treated at 600 °C for 1 h. ....	61
Figure 5.7. Size of anatase crystallinities developed in the TP glasses prepared by using different water/alkoxide ratios. ....	62
Figure 5.8. XRD patterns of the TP glasses prepared by using different HCl molarities subsequently heat-treated at 600 °C for 1 h. ....	63
Figure 5.9. XRD patterns of the as dried gel and the gels subsequent heat-treated at various temperatures. A: Anatase, R: Rutile. ....	66
Figure 5.10. Calculated crystal sizes with respect to heat-treatment temperature.....	69
Figure 5.11. Calculated crystal sizes with respect to heat-treatment temperature.....	72

Figure 5.12. XRD patterns of the TP glasses prepared by applying different heat-treatment schedules. ....	74
Figure 5.13. SEM images of the TP glasses prepared by various TiO <sub>2</sub> contents subsequently heat-treated at 600 °C for 1 h. ....	77
Figure 5.14. SEM images of the TP glasses prepared by using 80 mol% TiO <sub>2</sub> subsequently heat-treated at 600 °C for 1 h.....	79
Figure 5.15. EDS spectra of the TP glasses prepared by various TiO <sub>2</sub> contents subsequently heat-treated at 600 °C for 1 h. a) 70 mol%, b) 80 mol%, c) 90 mol%, and d) 95 mol% TiO <sub>2</sub> . ....	79
Figure 5.16. SEM images of the TP glasses prepared by using a) 2-methoxyethanol, b) Ethylene glycol. The glasses were subsequently heat-treated at 600 °C for 1 h....	81
Figure 5.17. SEM images of the TP glass prepared by using different water content, subsequently heat-treated at 600 °C for 1 h. ....	81
Figure 5.18. SEM images of the TP glasses heat-treated at temperatures of a) 500, b) 550, c) 600, d) 700, and e) 800 °C.....	82
Figure 5.19. SEM images of the TP glasses heat-treated at 600 °C for different durations.....	84
Figure 5.20. Pore volume of the TP glasses heat-treated at a) 600 °C and b) 800 °C. ....	89
Figure 5.21. Pore size distribution of the TP glass heat-treated at 600 °C.....	90
Figure 6.1. MB absorbance spectra of the selected TP glasses a) EG70-601, b) EG80-601, c) EG90-601, d) EG95-601, e) EG80-602, f) 2M80-600, g) EG80-603, h) EG80-610, and i) P25 powder. ....	96
Figure 6.2. The variation of MB degradation after 90 min UV illumination for the TP glass prepared with different TiO <sub>2</sub> contents. ....	98
Figure 6.3. Effect of different solvent type on MB degradation.....	98
Figure 6.4. Effect of solvent content on photocatalytic activity. ....	99
Figure 6.5. The variation in MB degradation with the pH of the solution for the TP glasses prepared by using different solvent molarities. ....	101

Figure 6.6. Variation in MB degradation with heat-treatment temperature for the TP glasses heat-treated at various temperatures for 1 h. .... 103

Figure 6.7. Band-gap energy of the TP glasses. .... 109

Figure 6.8. The transmittance of a) 90 mol% 2-methoxyethanol 600 °C, b) 80 mol% 2-methoxyethanol 600 °C, c) 90 mol% ethylene glycol 600 °C, d) 80 mol% ethylene glycol 600 °C, e) 80 mol% ethylene glycol 800 °C, f) 80 mol% ethylene glycol 1000 °C. .... 112

Figure 6.9. The interaction between the distilled water droplets and the glass surface. .... 114

## CHAPTER 1

### INTRODUCTION

Titanophosphate ( $\text{TiO}_2\text{-P}_2\text{O}_5$ , TP) glasses containing  $\text{TiO}_2$  and  $\text{P}_2\text{O}_5$  are of interest because they offer high transparency in the ultraviolet (UV) region, high dispersion and low density, as well as photo-induced hydrophilicity [1]. Photocatalytic properties initiated from Titania ( $\text{TiO}_2$ ) crystallinity and high surface area originated from phosphate ( $\text{P}_2\text{O}_5$ ) make TP glasses very attractive for both optical and photocatalytic applications. In the last decade, glasses capable of photocatalytic degradation of organic chemical species such as dirt, dust, soot, odour, pollution, etc. have been investigated for self-cleaning applications.

Generally, self-cleaning glass is produced by applying a thin coating layer on glass surface. The coating layer of a few nanometer thickness is composed of a material with superhydrophobic or superhydrophilic properties.  $\text{TiO}_2$  has received much attention as coating material due to its exceptional potential in photocatalytic activity [2], chemical stability, and low cost [3].

Organic dirt and dust stacked or in contacted with the surface of glass are decomposed by the coating material and their connection to surface breaks off when they are exposed to UV light. However, the use of coated self-cleaning glasses becomes limited since the thin coating material suffers from the effects of sun light, wind, and dusts hence wears out and loses its self-cleaning ability or could easily peel off the substrate over time [4]. Research and development studies were addressed towards the innovation of new, efficient, and cost-effective bulk materials, instead of applying a coating layer on a glass substrate, for the remediation of polluted environment.

The bulk glass keeps its self-cleaning ability theoretically forever. Thus, there is an increasing and urgent need to produce bulk glasses offering improved self-cleaning properties.

The system  $\text{TiO}_2\text{-P}_2\text{O}_5$  is noteworthy of investigation for the materials whose properties might be useful in the field of photocatalysis as an alternative material to  $\text{TiO}_2$  photocatalyst [5]. In this regard, the TP composites were introduced to the research field of self-cleaning. Despite the benefits (e.g. lower costs, higher durability, good photocatalytic efficiency), the opacity and the complexity involved in the preparation of the TP composites are their major drawbacks.

For optical applications, an amorphous structure is preferred, due to the absence of optical anisotropy [6]. The glasses prepared in the  $\text{TiO}_2\text{-P}_2\text{O}_5$  system are transparent and are expected to show photocatalytic activity in the UV-light. They could be utilized in special applications like air/water purification and self-cleaning because of their oxidizing ability and hydrophilicity [2]. They have high potential to be commercialized especially for applications such as windows, winter gardens, skyscrapers, glass fronts, and glass roofs where dirt and dust are difficult to clean. In addition, these glasses disinfect the environment through the kill of bacteria and microbes by the radicals [7].

They have potential to protect environment from harsh pollution cleaning chemicals. Since large parts of construction materials are exposed anyway with sunlight or indoor light, the maintenance and cleaning costs of these materials could be lowered if they have self-cleaning ability. Self-cleaning glass saves time, energy, material, and money spend for cleaning expenses. Furthermore, service life of the glass will be extended as it will not be further damaged during the wiping and cleaning operations. As it rains or as the glass is washed, the glass cleans the surface by itself as soon as it comes contact with the water.

Preparation methods and conditions have a pronounced influence on the properties of TP glasses and consequently on their photocatalytic activity. TP glasses could be produced by melt-quenching method at temperatures ranging from 1300 to 1500 °C [8 - 11]. But, they are colored in purple due to the presence of  $Ti^{3+}$  ions formed during the glass melting process [12]. Also, they show limited photocatalytic activity and hydrophilicity. For that reasons, the TP glasses produced by melt-quenching are considered inappropriate for optical and self-cleaning applications.

Additionally,  $TiO_2$  content more than 74 mol% in TP glass would be advantageous for better self-cleaning properties. The sol-gel process extends the glass formation region and offers special advantages like ease of synthesis, better homogeneity, and production of high purity material and, good control over crystalline phases and morphology developed [13, 14]. By tailoring the synthesis conditions such as chemical concentration, precursor type, acid type, synthesis time, solvent type, water molar ratio, pH, aging time, calcination time, calcination temperature, heating rate etc. the photocatalytical properties of  $TiO_2$  could be optimized for better efficiency.

The abovementioned advantages of the sol-gel process over melt-quenching method encourage the synthesis of TP glasses even though it is difficult to produce them in bulk. The sol-gel process allows us to prepare TP glasses over a wide-range of compositions containing 30–90 mol%  $TiO_2$  [15]. TP gels containing 22.2 to 100 mol%  $TiO_2$  have been synthesized by the sol–gel process [16]. Nonetheless, most of the studies on TP glasses were on their optical, electrical, or biomedical properties [17 - 19]. There has been no systematic study on self-cleaning properties of the sol-gel derived TP glasses and uncertainty still exists.

It has been commonly known that self-cleaning properties of a material deeply depend on several characteristics such as crystal size [20], surface area [21, 22], morphology [23, 24] and crystal structure [25, 26]. Semiconductor materials with large surface area, high crystallinity, and small crystal size favor high photocatalytic activity [27, 28].

Ohtani et al. [29] reported that amorphous  $\text{TiO}_2$  has negligible photocatalytic activity due to the existence of high concentration of defects on the surface and in the bulk of the material which facilitate the rapid recombination of the photoexcited electron and hole.

The preparation of TP glasses with small amount of nano-size anatase crystals is a research challenge. The crystallinity, size and surface area of the crystals developed could be tailored by applying a regulated heat-treatment and varying the heat-treatment parameters such as temperature, time, and heating rate.

Hence, self-cleaning properties of TP glasses could be optimized to get a better performance in special applications. The objective of this study was to provide an insight on sol-gel synthesis of photocatalytically active transparent and monolithic TP glasses for self-cleaning applications and to explore the significance of synthesis and heat-treatment parameters on the preparation and self-cleaning properties of TP glasses.



## **CHAPTER 2**

### **LITERATURE REVIEW**

#### **2.1. General Remarks**

Self-cleaning material is a kind of material with special photocatalytic ability to clean dirt, dust, soot, odor, pollution, etc. without the help of a person or equipment. It interacts with the UV light of the solar spectrum to break down organic dirt through what is called a photocatalytic effect [2]. Self-cleaning issues have received considerable attention from researchers in recent years due to the increasing demands on hygiene concerns and increasing cleaning and maintenance costs and time. Self-cleaning is an inspiring sector with continuously developing self-cleaning properties. Many of the innovations involve the development of new materials, use of simple preparation methods and less expensive chemicals, and easiness to scale up. Novel preparation methods to enhance the self-cleaning performance of materials continue to emerge.

#### **2.2. Self-cleaning**

##### **2.2.1. Photocatalysis**

Photocatalysis is a process undertaken in the presence of a catalyst and produces surface oxidation to eliminate harmful substances such as organic compounds when exposed to light [30]. The photocatalytically active materials named “photocatalysts” are mostly semiconductors. During the photoactivated reaction, photocatalyst is not consumed and does not change, but plays a significant role by making the chemical reaction happen faster and increase the photoreaction.

In semiconductors and insulators, electrons are trapped to a number of bands of energy and can not move to other regions. The band with the highest energy that an electron can move is the valence band (VB). The next energy level is the conduction band (CB). The term band gap refers to the energy difference between the VB and CB. For an electron to jump from VB to CB, a specific minimum amount of energy for the transition is required. The required energy varies from material to material. Electrons can gain enough energy to jump to CB by absorbing either heat or light. After an electron reaches CB, a hole ( $h^+$ ) is created at VB and the material starts to conduct electricity. In a semiconductor, energy of photon is absorbed which results in generation of an electron ( $e^-$ ) from VB to CB with the concurrent generation of  $h^+$  in VB [30]. Therefore, band structure of the photocatalyst is crucial and must have low energy to yield an increased efficiency of photocatalytic system.

The band gap structure of a typical semiconductor is illustrated schematically in Figure 2.1. The photo-generated  $e^-$  and  $h^+$  can recombine without participating in photocatalytic reactions which severely limits performance of the photocatalysis [31]. The charge carriers travel to the surface and react with the species adsorbed on the surface to decompose them. The photodecomposition process involving intermediate species  $OH$ ,  $O^2$ ,  $H_2O_2$ , or  $O^\bullet$  plays important roles in the photocatalytic reaction mechanisms [31].

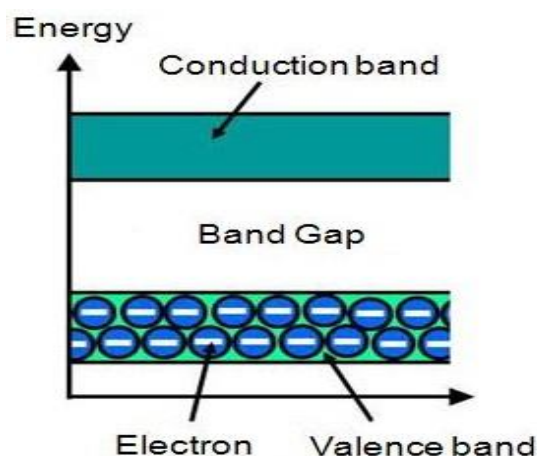


Figure 2.1. Schematic illustration of the band gap structure of a semiconductor [27].

The photocatalysis reaction initiates with the formation of  $e^-$  and  $h^+$  pairs which need photon energy ( $h\nu$ ) to overcome band gap energy ( $E_g$ ) between VB and CB of semiconductor [30]. When  $E_g$  is greater than  $h\nu$ , charge will transfer between generated  $e^-$  and  $h^+$  pairs and reactants on semiconductor surface and photo-oxidation reaction happens only if redox potentials of  $e^-$  and  $h^+$  are suitable for generating redox processes [32]. Thus, probability and rate of charge transfer directly related with redox potentials of adsorbate species and respective positions of band edges of VB and CB [32].

The competition between these processes controls the overall photocatalytic efficiency of the semiconductor. The photogenerated VB hole converts the surface hydroxyl group and adsorbed water molecules to highly reactive OH radicals, which have strong oxidizing power to rapidly degrade a variety of organic contaminants [33]. A schematic illustration of photoactivated photocatalysis processes is shown in Figure 2.2.

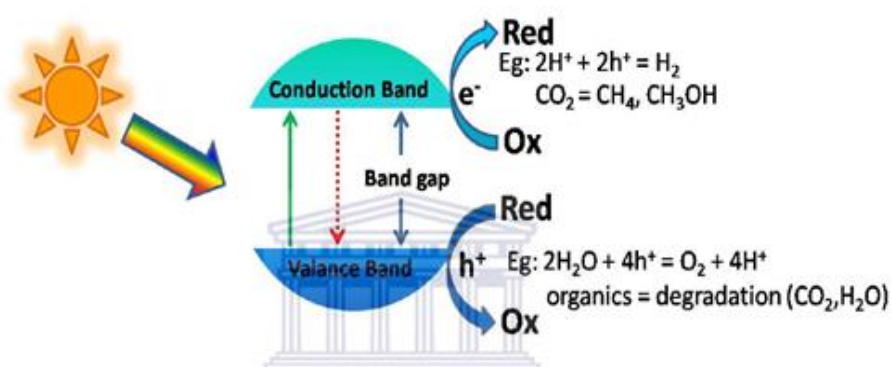


Figure 2.2. Schematic illustration of photoactivated processes [27].

In order to develop efficient photocatalyst, it is necessary to bring the light where it is needed and bring the reactants into contact with the catalyst at the right time and provide sufficient surface area for efficient reaction rates. The most photocatalysts are formed as nanoparticles because it is easy to get the photo  $e^-/h^+$  that are usually generated below the surface and then migrated to the surface, recombination depth [33].

Chen and Mao [31] reported that a large surface area catalyst with a constant surface density of adsorbents leads to faster surface photocatalytic reaction rates. In this sense, the larger the specific surface area, the higher the photocatalytic activity is. Conversely, the surface is an imperfect site. Hence, the larger the surface area, the faster the recombination is.

### **2.2.2. Photo-induced Superhydrophilicity**

The terms superhydrophilicity and superwetting were introduced to describe the complete spreading of water or liquid on substrates. The term superhydrophobicity was introduced to describe water-repellent fractal surfaces on which water drops remain as almost perfect spheres and roll off such surfaces leaving no residue. A hydrophilic surface has strong affinity to water whereas hydrophobic surface repel water [34].

Hydrophobic and hydrophilic surfaces are classified according to their contact angle with water. The contact angle is defined as “the value of the amount of wetting of a solid by a liquid”. If the contact angle is less than  $90^\circ$ , the liquid wets the surface. If it is greater than  $90^\circ$ , it is considered not to wet. If the liquid drop tends to spread on the surface, the surface is called “a hydrophilic surface”. If the water drop is completely spread and the angle with the surface is less than 5 degrees (0 is approaching the stream) it is “superhydrophilic”. If the drop is almost spherical in the surface and the angle with the surface is greater than  $150^\circ$  (approaching  $180^\circ$ ), it is called “superhydrophobic”.

In 1997, Wang et al. [35] demonstrated superhydrophilic effect on a glass slide coated with a thin  $\text{TiO}_2$  polycrystalline film. The effect is shown in Figure 2.3. The  $\text{TiO}_2$  film acquires superhydrophilic properties after UV illumination. Water remains in shape of lenses with contact angle of  $70\text{-}80^\circ$  on the  $\text{TiO}_2$ -coated glass when stored in dark (Figures 2.3 a and c), but it spreads completely when exposed to UV radiation (Figures 2.3 b and d).

The spreading of water was the result of hydrophilic properties of TiO<sub>2</sub> exposed to UV radiation, although the effect of water spreading was entirely attributed to photoinduced self-cleaning capability of TiO<sub>2</sub>. Under UV radiation, a hydrophobic surface rather rapidly re-convert to the hydrophilic state [35].

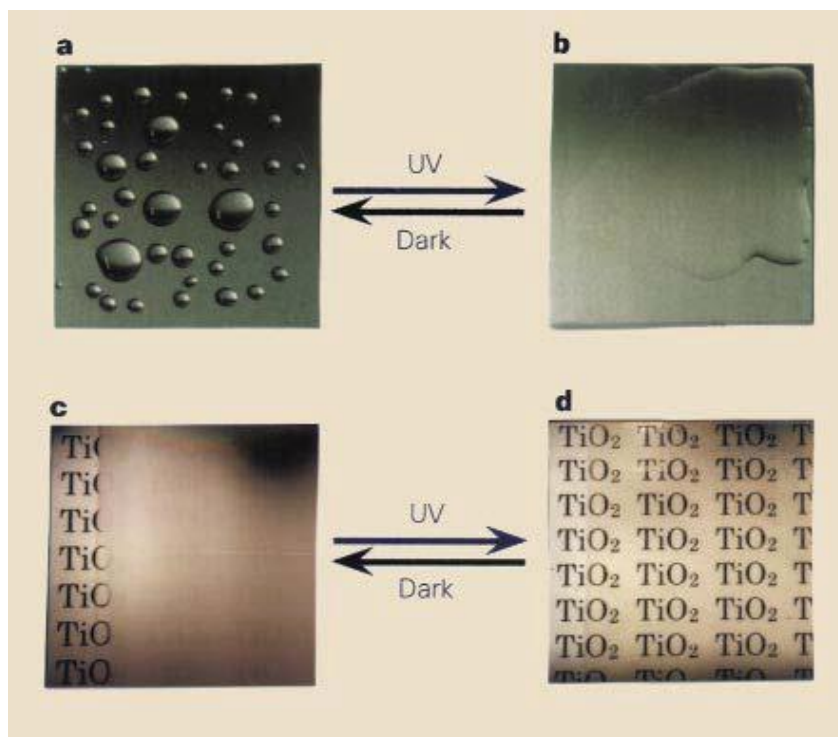


Figure 2.3. Effect of UV radiation on hydrophilicity and transparency of a glass slide coated with a TiO<sub>2</sub> thin film [35].

### 2.3. Self-cleaning Materials

Several semiconductors including TiO<sub>2</sub>, SiO<sub>2</sub>, ZnO, CdS, ZrO<sub>2</sub>, V<sub>2</sub>O<sub>5</sub>, CuO, Fe<sub>2</sub>O<sub>3</sub>, Al<sub>2</sub>O<sub>3</sub>, etc. have been investigated as potential self-cleaning materials. Among them, TiO<sub>2</sub> is the most suitable semiconductor for photocatalytic decontamination of water. Wang and co-workers demonstrated TiO<sub>2</sub> coating on the surface of ceramic tile for self-cleaning ability [35]. TiO<sub>2</sub> is able to absorb energy from light, and then use that energy to catalyze the degradation of organic molecules and the oxidation of some inorganic pollutants like nitrogen oxides (NO<sub>x</sub>) [36].

Photocatalytic features of  $\text{TiO}_2$  has been widely used in many applications including; industrial wastewater treatment, air purification, self-cleaning coatings and glasses, anti-fogging and recently in medical applications to destroy the bacteria and viruses [37].

$\text{TiO}_2$  is used in self-cleaning application areas as the exterior construction material that require periodical cleaning to maintain desired optical properties and visual aspects, which can be very costly, particularly when the accessibility to the exposed surface is difficult. That is, skyscrapers, roofs, etc. Investigations on photocatalytic construction materials showed that utilization of self-cleaning materials as concrete, wallpaper, gypsum, and paint in the buildings will significantly decrease the concentration of the pollutants [2]. If construction materials have self-cleaning ability and illuminated anyhow with sunlight the maintenance costs could be extremely lowered. Also, with the help of the hydrophilicity effect provided by  $\text{TiO}_2$ , degraded contaminants will be effectively removed with rain. Self-cleaning products including tiles, glass, siding, plastic films, tent materials, cement, etc., have already been commercialized in USA, Japan, and European countries [38].

Despite good peculiarities, it is not possible to produce  $\text{TiO}_2$  in amorphous form in bulk and polycrystalline  $\text{TiO}_2$  is not transparent. Therefore,  $\text{TiO}_2$  can not be used for the applications requiring high degree of transparency such as windows, winter gardens, balcony windows, glass fronts, and glass roofs. For such applications self-cleaning ability is achieved by applying transparent coatings on the surface of the ordinary soda lime silica glass. The coating material, usually  $\text{TiO}_2$ , forms a thin film of a few nanometer thickness on the surface. The amount of  $\text{TiO}_2$  needed could be quite low since the photocatalysis occurs on the light exposed surface that is in contact with the contaminant [36]. Self-cleaning ability of the coatings decreases with degrading surface functionality of the coatings. Under harsh environmental conditions where scratches and breaks occur, coatings lack the regeneration of the self-cleaning function.

Also, it is hard to synthesize well crystallized anatase phase in such coatings and films. Another bad feature is their relatively small surface which will not provide a good interaction with the pollutants [39]. Providing a glass that contains titanium (Ti) ions in it will resolve such problems and it has a great importance when its potentials for practical applications is considered. Therefore, in order to eliminate the drawbacks of the ordinary glasses, there is an urgent need to produce glasses exhibiting self-cleaning properties in bulk form.

The advantages of using self-cleaning glasses instead of conventional glasses include saving of cleaning time and the reduction in the expenditure on the cleaning products. Also, the environment is saved due to the rare use of the potentially harmful chemical detergents. Self-cleaning windows should also reduce the need for ladders and industrial cleaning equipment that must be operated at extreme heights [2].

#### **2.4. Self-cleaning Glasses**

The photocatalytic ability of the TiO<sub>2</sub> containing glasses has been overlooked despite their benefits mostly because of the complexity of the production of TiO<sub>2</sub> glasses in bulk form. A bulk glass is defined as “a single glass piece with the smallest dimension of several millimeters or larger”. TiO<sub>2</sub> does not form a glass alone in conventional glass forming i.e., melt quenching [11]. Therefore, in order to produce glass by the conventional glass forming, a glass former such as SiO<sub>2</sub> and P<sub>2</sub>O<sub>5</sub> must be incorporated to the composition.

The idea behind that is, TiO<sub>2</sub> will provide the required properties for the photocatalytic performance and contribute to the glass structure by the same stabilization mechanism provided by the Al<sub>2</sub>O<sub>3</sub> and B<sub>2</sub>O<sub>3</sub> additions to the ordinary glass compositions [40]. P<sub>2</sub>O<sub>5</sub> acts as a good glass former by successfully dissolving TiO<sub>2</sub> up to 95 mol% and due to the strong chemical bonds between the materials, closely packed P-O-Ti bonds, will increase the stability and the density of the glass [17].

## 2.5. TiO<sub>2</sub> – P<sub>2</sub>O<sub>5</sub> (TP) Glasses

Investigations on TiO<sub>2</sub>-P<sub>2</sub>O<sub>5</sub> system might be useful in the field of glass. However, dissolving TiO<sub>2</sub> at high percentage in glass formers is not an easy task. P<sub>2</sub>O<sub>5</sub> alone is not easy to obtain a glassy form by itself because it is very hygroscopic and volatile. Therefore, modifying oxides and network intermediates are added to the phosphate glass system to stabilize the glass network [41]. TiO<sub>2</sub> acts as intermediate network former in TP glass and stabilizes the phosphate network [40]. Ti<sup>4+</sup> ion has a small ionic radius and can penetrate into the phosphate network [41]. When Ti is integrated into the phosphate network, it can easily attract oxygen from the PO<sub>4</sub> tetrahedron and create Ti-O-P links [42]. Thus, the bonding between different chains becomes stronger. Ti<sup>4+</sup> ion participation to the network improves the glass forming ability and strengthens the glass network [43]. Consequently, the glasses with large TiO<sub>2</sub> content could be synthesized in less P<sub>2</sub>O<sub>5</sub> amounts. Structural studies on the TP glasses showed that the P-O-P bonds are gradually replaced by the P-O-Ti and Ti-O-Ti bonds with increasing TiO<sub>2</sub> additions. The addition of TiO<sub>2</sub> increases the O/P ratio and creates stronger Ti-O-P cross-linking within the glass network. In rich TiO<sub>2</sub> glasses, no more P-O-P links exist. The network includes TiO<sub>6</sub>-PO<sub>4</sub>-TiO<sub>6</sub> polyhedra and Ti-O-Ti linkages of TiO<sub>6</sub> octahedra along with PO<sub>4</sub><sup>-3</sup> ions [42].

TP glasses could make photocatalytic products cost-effective. To get the same photocatalytic efficiency, fewer resources are invested for TP glass as compared to pure TiO<sub>2</sub>. Also, TP glass retains photocatalytic efficiency for longer durations due to its increased durability. The photocatalytic efficiency of the material can be increased for a longer time than pure TiO<sub>2</sub> since P<sub>2</sub>O<sub>5</sub> has larger specific surface area. Therefore, utilization of TP glasses in water and air cleaning applications offers an improvement of the quality of air and water. Introducing cheaper material such as P<sub>2</sub>O<sub>5</sub> to the system, production costs will be greatly reduced too. In order to produce this cost-effective photocatalytic material, TP glass needs to be produced by a low costs production method.



## 2.6. Properties of TP Glasses

Besides the price-cutting role that the  $P_2O_5$  plays in the glasses, it has other favorable features.  $Ti^{+4}$  ion participation to the network improves the chemical durability, thermal stability, optical, physical and mechanical properties as well as self-cleaning properties of the final product [43].

Being amorphous, TP glass will not reflect light and light passes unabsorbed through the glass, which makes it transparent. As a result of the amorphous background provided by the addition of  $P_2O_5$ , large specific surface area is introduced to the TP glass, which will help the product to adsorb and react with more pollutants than pure  $TiO_2$ . Therefore, the same level of the photocatalytic activity could be obtained.

As TP glass is used instead of pure  $TiO_2$ , self-cleaning ability lasts for longer periods with higher efficiencies. Furthermore, thanks to the higher durability of the glass, it is expected that  $TiO_2$  will have extended functioning time. Enhanced thermal stability allows TP glasses to be used in the applications requiring higher temperatures. TP glasses have attracted attention from science world due to their good electronic conduction sourced by  $Ti^{+3}$  and  $Ti^{+4}$  ions. In addition, TP glasses have been investigated extensively for killing or growth inhibition of bacteria [44].  $TiO_2$  has a potential to be used in commercial optical glasses instead of toxic heavy metals.

## 2.7. Preparation of TP Glasses

The relative concentrations of both ‘P’ and ‘Ti’ structural units present in the TP glass are strong functions of the composition of different constituents making up the glass. Therefore, understanding the details of the TP glass preparation under different preparation conditions and their effect on the photocatalytic efficiency with respect to composition is essential. Also, in order to produce cost-effective photocatalytic material, the self-cleaning TP glass must be produced by using an inexpensive method having low production costs. Previously produced TP glasses were not suitable for photocatalytic applications and some of them were produced using very expensive synthesis methods.

Many different methods namely, melt quenching, sol-gel process, hydrothermal process, chemical vapor deposition, etc., are available for producing TP glasses. Each method has their own parameters and preparing conditions hence, advantages and disadvantages. When all these factors are taken into consideration, the sol-gel process is selected to be the ideal and the most successful method for synthesizing TP glasses having such desirable features.

### **2.7.1. Preparation of TP Glasses by Melt Quenching**

Rapid quenching of a melt is historically the most established and still most widely used technique for preparing glasses. In this method, usually high purity powders are melted at temperatures above 1000 °C and then the melt is exposed to a rapid quench. To ensure homogenization, melt is continuously rocked.

The melting temperature of the glass depends on its initial composition. As the melt cools at a rate higher than the nucleation and crystal growth rates, the disordered state of melt is maintained in the solid state [45]. That is, an amorphous solid form. Phosphate-based glasses are very easy to prepare by conventional melting since they have low melting temperature and low viscosity at melting temperatures. Similarly, TP glasses are mostly prepared by conventional melt quenching. The biggest technological challenge is that melts of P<sub>2</sub>O<sub>5</sub> are hygroscopic and appeal water upon exposure to air. The absorption of small amounts of water can promote crystallization and devitrification [11].

P<sub>2</sub>O<sub>5</sub> can dissolve TiO<sub>2</sub> up to about 70 mol%. Pickup et al. [15] studied the structure of binary TP glasses with TiO<sub>2</sub> content of 60-65 mol%. Hashimoto et al. [8] prepared colorless, Ti<sup>+3</sup>-free binary TP glasses containing TiO<sub>2</sub> up to 74 mol% by the melt quenching method at temperatures between 1300 and 1500 °C. They reported that the glasses obtained are blackened due to the Ti<sup>+3</sup> ions. This achievement has triggered the use of TP glass in photonic and optical devices [46].

### 2.7.2. Preparation of TP Glasses by Sol-gel Process

The sol-gel process involves the transition of a system from a liquid “sol” into a solid “gel” phase. The gel is dried and heat-treated to form the desired product. Upon heat-treatment, the porous gel is converted into a dense glass or ceramic [47]. Due to its low cost, easiness, and utilization of low temperatures, the sol-gel technique is among the convenient methods to prepare glasses with specific properties.

Also, it allows close control over many preparation parameters and wide variety of shapes and morphologies are obtained [45]. This is very useful in optimizing the morphology, size, crystallinity, and porosity of the resultant product. Such extensive control on the products features is not available neither in melt-quench method nor in the other synthesizing techniques. Since the microstructure of the nanoparticles is controllable, materials with high specific surface area could be synthesized.

The interest in producing glasses via sol-gel process has been increasing very rapidly since the processing temperature is usually below the crystallization temperature of the oxides that allows for the production of novel glass compositions [48]. Nonetheless, the precipitation is encountered in the sols or xerogels when the TiO<sub>2</sub> content exceeds 80 mol% [16]. Because of the non-trivial chemistry involved in phosphate synthesis, studies performed on the sol-gel synthesis of TP glasses are few.

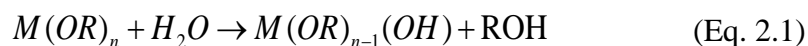
A comparison of the structure of the binary TP glasses of the same composition prepared by the sol–gel and melt–quench routes revealed that, in the sol–gel derived glass, the Ti<sup>4+</sup> ion has an average coordination number of 6 and tends to form TiO<sub>6</sub> octahedron, whereas, in the melt-derived glass, the same ion has an average coordination number of between 4 and 5 since it exists predominantly in the fourfold and fivefold coordination states as TiO<sub>4</sub> tetrahedral and TiO<sub>5</sub> pyramidal units, respectively, while only a small number of Ti<sup>4+</sup> ions are present as TiO<sub>6</sub> octahedra [15].

Furthermore, the Ti–O bond length in the melt-derived glass is slightly shorter than that in the sol–gel derived glass; this may possibly be attributed to the presence of TiO<sub>5</sub> pyramidal units in the melt-derived glass in addition to the TiO<sub>4</sub> tetrahedral and TiO<sub>6</sub> octahedral units [18]. Thus, for binary TP glasses, the sol-gel process creates a more consistently ordered structure than melt-quenching.

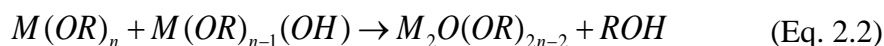
## 2.8. Steps in the Sol-gel Process

The sol-gel process consists of four steps namely; hydrolysis, condensation, gelation, and drying. The hydrolysis reaction leads to the formation of original nuclei or basic units of TiO<sub>2</sub> while the condensation reaction leads to the growth of network system of the original basic units [49]. The reactions involved in these steps are shown in Eq. 2.1 - 2.4 [39]. Metal alkoxide precursor is represented as M(OR)<sub>n</sub>; where M is the metal and R is the alkyl group.

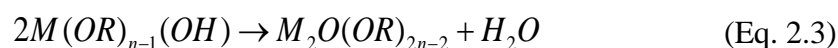
### Hydrolysis



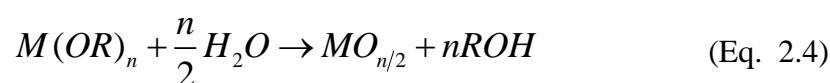
### Condensation



### Gelation



### Net Reaction



The alkoxide reacts with water and forms M-OH bonds. After that, condensation process starts. Condensation creates a compact structure. In this stage, hydrolysis species polymerize to form higher molecular weight products that is, nuclei and particles [49]. As the particle growth occurs, gelation starts.

After gel is formed, condensation proceeds in two ways through water elimination and through alcohol elimination. Depending on the reaction (equation), water and alcohol are the two possible by-products. After the gel is formed, it starts to shrink with time due to the loss of water and alcohol and pores occur. Reaction rate of the dehydration process is expected to be much faster compared to the gelation process. However, the dominant mechanism depends on the hydrolysis rates, condensation reactions, and the number of hydroxyl groups [49].

Gelation of the solution is the basis of the sol-gel method. The formation and properties of the gel are affected by the gelation conditions, even if the composition of the starting solution is the same. In order to obtain a gel with desirable microstructure and properties, many factors such as the solubility of precursor (must be high), concentration and type of solvent, pH of the solution, water content etc. must be precisely controlled. Upon heat-treatment of the gel, the remaining solvent evaporates and a glass with several millimeters or larger could be obtained.

The preparation of larger pieces is not an easy task. Cracks and fracture are often encountered when wet gels consisting of pores filled with solvent start drying because of the generation of a capillary pressure gradient in the liquid phase of the gel. The pressure difference causes differential shrinkage of the gel network and this causes cracking [50].

## **2.9. Factors Affecting the Sol-gel Process**

The most important parameters affecting the structure and morphology of the sol-gel derived products are: the type and concentration of precursor used, pH, the type and amount of solvent used, water/alkoxide ratio, solution viscosity, calcination regime, drying and aging conditions, calcination temperature [47]. Each parameter has a distinctive influence on the hydrolysis, condensation, and gelation reactions. By optimizing these parameters, it is possible to change the reaction kinetics thus, the molecular structure of the product.

By such optimizations, a control over the morphology and uniformity could be achieved. In this thesis work, effects of pH, titanium precursor source, solvent type and amount, water/precursor ratio, catalyst amount, drying conditions and heat-treatment regime on crystal structure, size, microstructural properties, surface area and the self-cleaning properties of TP glasses have been studied.

## CHAPTER 3

### EXPERIMENTAL PROCEDURE

#### 3.1. Starting Materials

In order to synthesize  $\text{TiO}_2\text{-P}_2\text{O}_5$  (TP) gels by the sol-gel process, analytical grade titanium tetraisopropoxide (TTIP) and titanium tetra-butoxide (TBOT) were used as titanium precursor. Triethyl phosphate (TEP) was taken as phosphate precursor. Various solvents having different molecular weight, carbon content, and boiling point were used to suppress capillary pressure in the drying stage. Table 3.1 summarizes the solvents used and their properties.

Table 3.1. The solvents used in this study and their properties.

Solvent	Molecular weight (g/mol)	Boiling Point ( $^{\circ}\text{C}$ )
Methanol	32.04	64.70
Ethanol	46.07	78.37
2-Propanol	60.10	82.50
Ethylene glycol	62.07	197.60
2-Methoxyethanol	76.09	124.00
2-Ethoxyethanol	90.04	135.60
1-2 Dimehoxyethanol	90.12	85.00
2-Isopropoxyethanol	104.15	44.00
Benzyl alcohol	108.14	205.00
2-Butoxyethanol	118.17	171.00

Distilled water was used for promoting hydrolysis. HCl was used as a catalyst. At the mixing stage, extra pure N,N-dimethylformamide (DMF) was introduced as drying control chemical additive to avoid crack formation and as catalyst to prevent precipitation and foaming so that the monolithicity of the resultant gels was retained.

All chemicals were analytical grade and used in as received form without any chemical treatment. Supplier and product number of the chemicals used for the synthesis of TP gels was shown in Table 3.2.

Table 3.2. Information on the chemicals used for the synthesis of TP gels.

Material name	Chemical formula	Supplier (Product code)
Titanium tetraisopropoxide	Ti(OCH(CH <sub>3</sub> ) <sub>2</sub> ) <sub>4</sub>	Sigma-Aldrich (87560)
Triethyl phosphate	PO(OC <sub>2</sub> H <sub>5</sub> ) <sub>3</sub>	Sigma-Aldrich (240893)
Methanol	CH <sub>3</sub> OH	Merck Millipore (106002)
Ethanol	C <sub>2</sub> H <sub>5</sub> OH	Merck Millipore (100980)
Ethylene glycol	C <sub>2</sub> H <sub>6</sub> O <sub>2</sub>	Merck Millipore (100949)
2-propanol	C <sub>3</sub> H <sub>8</sub> O	Merck Millipore (100272)
2-methoxyethanol	C <sub>3</sub> H <sub>8</sub> O <sub>2</sub>	Sigma-Aldrich (88907)
2-ethoxyethanol	C <sub>4</sub> H <sub>10</sub> O <sub>2</sub>	Sigma-Aldrich (128082)
1-2 dimethoxyethane	C <sub>4</sub> H <sub>10</sub> O <sub>2</sub>	Sigma-Aldrich (72405)
2-isopropoxyethanol	C <sub>5</sub> H <sub>12</sub> O <sub>2</sub>	Sigma-Aldrich (107891)
Benzyl alcohol	C <sub>7</sub> H <sub>8</sub> O	Sigma-Aldrich (305197)
2-butoxyethanol	C <sub>6</sub> H <sub>14</sub> O <sub>2</sub>	Sigma-Aldrich (53071)
N,N-dimethylformamide	HCON(CH <sub>3</sub> ) <sub>2</sub>	Sigma-Aldrich (227056)
Hydrochloric acid	HCl	Sigma-Aldrich (320331)
Distilled water	H <sub>2</sub> O	Laboratory product
P25 <sup>®</sup> (Degussa)	TiO <sub>2</sub>	Sigma-Aldrich (718467)

### 3.2. Preparation of TP Gels

TP gels in the system  $x\text{TiO}_2 \cdot (1-x)\text{P}_2\text{O}_5$  ( $x = 70, 80, 90, 95$  mol%) were synthesized in accord with the work reported by Tang et al. [17]. First, TTIP was diluted in 1/3 of the solvent in a glass beaker and TEP was added slowly while magnetic stirring at 300 rpm for 20 min. After allowing precursors to react with each other for a while, stirring rate was increased to 500 rpm and 1/3 of the solvent was added. Adding solvent step by step was crucial for preventing foaming of the sol and retaining transparency. After addition of 1/3 of the solvent, DMF (with molar ratio of 1) was introduced to the solution.



Addition of DMF had a critical role in the preparation of monolithic (crack free) gels. After keeping the solution stirred for 10 min, 1/3 of the solvent and predetermined amount of HCl was added dropwise into the solution that was stirred for additional 10 min. After adding all the chemicals except distilled water, the solution was kept stirred for 1 h to assure complete mixing.

Finally, distilled water was introduced into the resulting solution to initiate the hydrolysis and condensation reactions dropwise using a burette while stirring gently at 300 rpm until a homogeneous and transparent sol was achieved. Slow addition of distilled water was necessary for preventing instant gelation of the sol. As the added water amount and aging time increased, sol viscosity increased. Then, the resultant sol was transferred into an ice-water bath for cooling and kept there until gelation was visually observed. Just before the gelation, pH of the sol was measured by using pH strips. Upon cooling, the sol set to a gel in 1 to 15 min depending on the Ti/H<sub>2</sub>O molar ratio, i.e. TiO<sub>2</sub> content of the solution.

The sols prepared with optimized parameters were gelled in a few minutes. Complete gelation was taken as the state where gels preserved their shape after 90° tilt of the beaker containing the gel. Resultant gels were removed from the ice-bath, loosely covered with a parafilm and kept 1 day at room temperature for aging and relaxation.

1 day aging resulted in complete gelation even for the sols prepared with undesirable parameters which does not favor gelation such as excess water, pH etc. The steps involved in the synthesis of TP gels are shown in Figure 3.1.

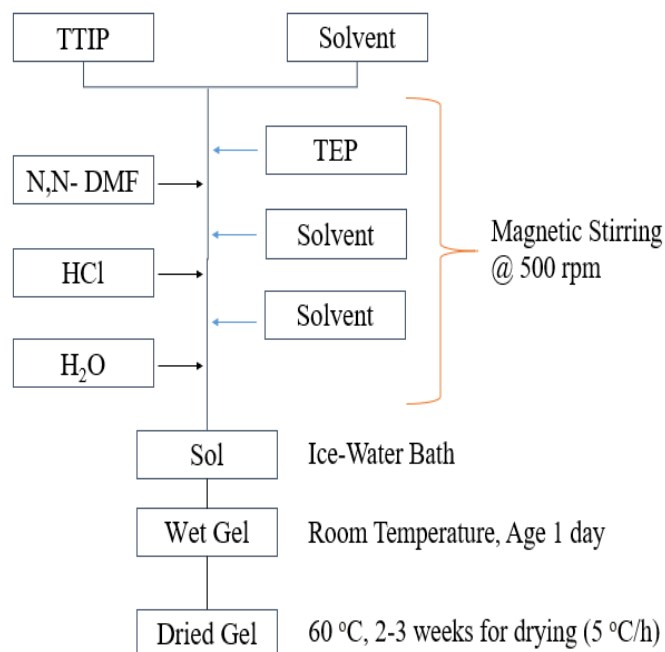


Figure 3.1. Flowchart showing the steps involved in the synthesis of the TP gels.

After aging, the wet gels were dried in a drying oven in two steps. First, oven temperature was raised slowly to 40 °C for 1 week. After removing the parafilm and allowing the wet gels to contact with air, oven temperature was gradually increased to 60 °C at a slow heating rate to prevent water evaporation and crack formation. The wet gels were kept at that temperature for 2 more weeks for complete drying. The drying procedure for the wet gels is shown in Figure 3.2.

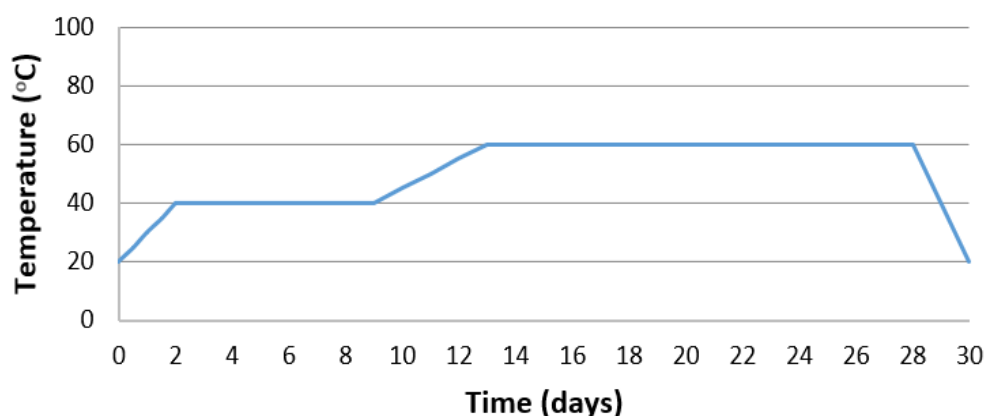


Figure 3.2. Drying procedures of the wet gels derived by the sol-gel process.

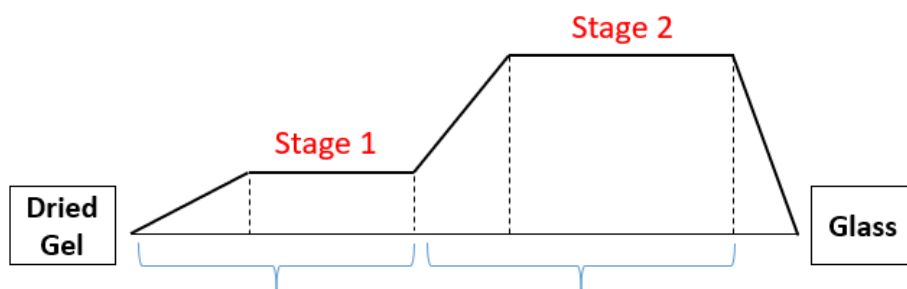
### **3.3. Heat-treatment of TP Gels**

Dried gels were subjected to a regulated heat-treatment schedule where water and solvent were removed to get the TP glasses containing small amount of nano size anatase TiO<sub>2</sub> crystals. Heat-treatment parameters (temperature, time, heating and cooling rates) are vital for the removal of the organic molecules from the gels and to initiate the crystallization. In order to obtain monolithic glass, i.e., bulk glass, slow removal of the organics is a must for preventing the excess volume shrinkage and the crack formation during heat-treatment [51]. Two different heat-treatment schedules were designed and applied to dry gels in order to satisfy the success criteria given below.

- Gels become water free
- Solvent is removed
- Amorphous TiO<sub>2</sub> converts to anatase
- Complete crystallization is prevented
- Anatase to rutile transformation is prevented
- High specific surface area is obtained
- Bulk and transparent glasses is obtained. Bulk glass is defined as the glass of a single piece with nominal dimensions of several millimeters or larger.

#### **3.3.1. Fast Heat-treatment Design (FHTD)**

Different heat-treatment temperatures, durations, and heating rates applied in the FHTD of the dried gels are shown in Figure 3.3. FHTD consisted of 2 main stages. At the first stage, gel became water free and solvent was removed. At the second stage crystallization took place. After reaching the predetermined target temperature, power of the furnace was turned off and samples were cooled naturally in the furnace.



	<u>Stage 1</u>	<u>Stage 2</u>
Heat-treatment temperature (°C)	250, 280	400, 450, 500, 550, 600
Heat-treatment duration (h)	2, 10	1, 2, 3, 4, 10
Heating rate (°C/h)	2, 12, 300	2, 150, 180, 250, 300

Figure 3.3. The temperatures, durations, and heating rates applied in the FHTD of the dried gels.

### 3.3.2. Slow Heat-treatment Design (SHTD)

A much slower heat-treatment design than FHTD was applied to overcome the cracking problems and to get the desired transparency. The temperatures, durations, and heating rates applied in SHTD of the dried gels are shown in Figure 3.4. The SHTD was completed in 4 steps. a heating rate of 6 °C/h was applied up to 280 °C. Relatively longer durations at 280 °C were adopted. Such long heating durations were essential for the removal of the solvent and other organics. From 280 °C up to the predetermined target temperature in the range from 400 to 1000 °C, a heating rate of 180 °C/h was applied to the dried gels to increase the growth rate of the anatase crystals. After reaching the predetermined target temperature, power of the furnace was turned off and samples were cooled naturally in the furnace.

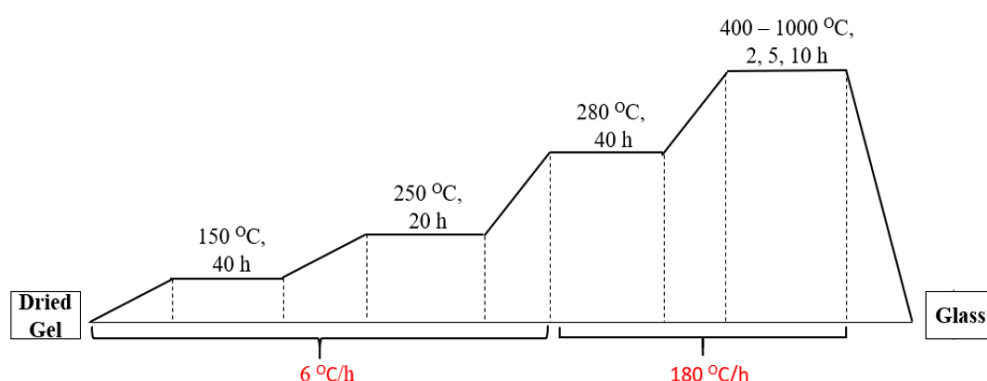


Figure 3.4. The temperatures, durations, and heating rates applied in the SHTD of the dried gels.

### **3.4. Characterization**

#### **3.4.1. X-Ray Diffraction (XRD)**

The phase(s) present in the samples was identified using XRD analysis. XRD patterns were scanned in the range from  $2\theta$  of  $10^\circ$  to  $80^\circ$  at a scanning speed of  $2^\circ/\text{min}$  using Cu-K $\alpha$  radiation,  $\lambda=1.5406 \text{ \AA}$ , 40 kV, 40 mA by means of an X-ray diffractometer (Rigaku, D/MAK/B). The size,  $d_{hkl}$ , of the crystallites developed during heat-treatment was calculated employing the Scherrer's equation [52] by assuming the crystallites are spherical in shape.

#### **3.4.2. Field Emission Scanning Electron Microscope (FESEM)**

FESEM (Nova Nanosem 430) was employed to examine the surface morphology of the gels and glasses. Operation voltage was varied between 10 to 20 kV. All samples were coated with a thin layer of gold by a sputter coating prior to SEM examination. FESEM is equipped with Energy Dispersive X-Ray Spectroscopy (EDS) that provides the information of the elemental composition of the samples. The elemental analysis was done at a voltage of 10 kV.

#### **3.4.3. Brauner-Emmett-Teller (BET) Specific Surface Area (SSA) Analysis**

SSA analysis was performed to measure the total surface area of the glass samples. The SSA was measured using multipoint Brauner-Emmett-Teller (BET), Quantachrome NOVA-3000 analyzer. Samples were degassed in N at  $110^\circ\text{C}$  for 12 h prior to the analysis.

#### **3.4.4. Differential Thermal Analysis (DTA) and Thermogravimetric (TG) Analysis**

The DTA and TG analyses were done by heating the dried TP gels up to  $1000^\circ\text{C}$ . The heating rate was  $10^\circ\text{C}/\text{min}$ . The analyses were performed under nitrogen/air atmosphere using TG/DTA (S II Exstar 7300).

### 3.5. Property Measurements

#### 3.5.1. Methylene Blue (MB) Photodegradation Test

The photocatalytic activity of the TP glasses was evaluated based on the variation in the absorbance of the aqueous methylene blue (MB) solution under UV illumination with time. The absorbance was measured using an ultraviolet-visible (UV/Vis) spectrophotometer (Scinco). Photocatalytic measurements were executed using 100 mL MB solution. First, a 10 mg/L of MB solution was prepared by dissolving 0.01 g of MB powder (Fluka) in 1 L of de-ionized water in a glass beaker.

Then, 0.1 g glass powder was added into 25 mL of MB solution. Before irradiation, the suspension containing the glass powder and the aqueous MB solution was stirred continuously in dark for 30 min to ensure adsorption/desorption equilibrium using a magnetic stirrer.

Initial concentration of MB before dark mixing was used as the initial value for further kinetic treatment of the photodecomposition processes to identify adsorption values. After dark stirring for 30 min, a 3 mL of the test solution were removed using a syringe filter (Millex Millipore, 0.22  $\mu\text{m}$ ) and analyzed. Then, a 100 W UV lamp at a wavelength of 365 nm was turned on, representing the start of the exposure to UV radiation. A 3 mL of the test solution was removed in every 30 min to determine the concentration of MB. The samples were stirred continuously during the total testing time of 90 min. The MB degradation efficiency of the sample was calculated according to the equation;

$$\text{Efficiency}=(C_0-C_t)/C_0 \times 100 \quad (\text{Eq. 3.1})$$

where,  $C_0$  and  $C_t$  are the concentrations of MB at initial and different irradiation times, respectively. The percent reflection against wavelength graph was transformed using the Kubelka–Munk method to an  $[\text{eV}]^{1/2}$  against  $[\text{eV}]$  graph. Band gap energy of the powder sample was calculated by extrapolating the mid-section of the graph to the x axis.

### 3.5.2. Transmittance and Wettability Tests

A piece of glass was placed to Scinco S-3100 UV-Vis single beam spectrophotometer for transmittance measurements. Graphs were drawn according to the refractive index of the photon passing through the glass and the calculation was made. Wettability of the glasses was examined via contact angle measurements. Contact angle of the samples were measured using SEO Phoenix 300 contact angle measurement equipment. A drop of distilled water was dropped on the surface of glass sample to find the value of contact angle to determine the hydrophilicity of the sample.

The flowchart for the measurements of the transmittance and contact angle of the TP glass is shown in Figure 3.5.

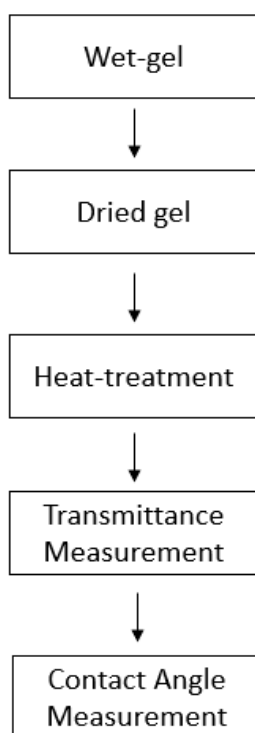


Figure 3.5. Flowchart showing the transmittance and contact angle measurement steps of the TP gels.





## CHAPTER 4

### RESULTS AND DISCUSSION OF SYNTHESIS STUDIES

#### 4.1. Synthesis of TP Gels by the Sol-gel Process

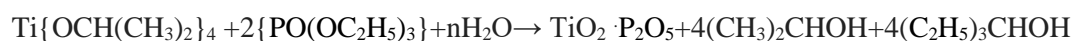
Optimization of the synthesis parameters is a key step for obtaining transparent and monolithic TP gels. In order to investigate the effects of the synthesis parameters on the transparency and monolithicity (or resistance against crack formation), TiO<sub>2</sub> concentration, H<sub>2</sub>O content, HCl molarity, and solvent content as well as solvent type of the solutions were changed systematically. The gel monolithicity is very important and has a crucial impact on preparation and properties of bulk glasses.

##### 4.1.1. Effect of TiO<sub>2</sub> Content

The optimization of TiO<sub>2</sub> content was made by changing the TEP content in the solution to synthesize the TP gels containing different TiO<sub>2</sub> percentages. A solution expected to yield 70 mol% TiO<sub>2</sub> in the gel was selected as the starting composition. It was reported by various researchers that TP glass is produced from the prescribed solution by the sol-gel process [17, 45].

In addition to this solution, three other solutions of progressively higher TiO<sub>2</sub> content (80, 90, and 95 mol% TiO<sub>2</sub>) were prepared. Other synthesis parameters were kept constant. All TP gels were synthesized by using TTIP and 2-methoxyethanol as TiO<sub>2</sub> precursor and solvent, respectively. The effects of TiO<sub>2</sub> content on transparency and monolithicity of the wet and dried gels were investigated visually. The solutions prepared by using different TiO<sub>2</sub> contents were clear. By carefully controlling the processing conditions such as stirring and aging, hydrolysis, condensation, and gelation reactions were favored. Stirring process enhanced the crosslinking probability of the chains and promoted the gelation.

As a result, each solution of different TiO<sub>2</sub> contents set to monolithic and transparent wet gels. The proposed net reaction leading to the formation of the TP gel from TTIP and TEP is;



Results for the TP gels with the projected compositions of 70 to 95 mol% TiO<sub>2</sub> is shown in Table 1. All the wet gels retained their transparency but, crack formation was encountered in the gels synthesized by using 90 and 95 mol% TiO<sub>2</sub> upon drying at 60 °C as shown in Figure 1.

It is obvious that the gels synthesized by using 90 and 95 mol% TiO<sub>2</sub> were not proper for retaining the monolithicity of the gel. Therefore, the gel with the projected composition of 80 mol% TiO<sub>2</sub> was taken as the most appropriate TiO<sub>2</sub> content for the synthesis of the TP gels and was used in the optimization studies for the other synthesis parameters.

Table 4.1. Results for the TP gels synthesized by using different TiO<sub>2</sub> contents.

TTIP (M)	TEP (M)	Solvent (M)	TiO <sub>2</sub> content (mol%)	H <sub>2</sub> O (M)	HCl (M)	Appearance		Satisfaction Sign
						Wet gel	Dried gel	
1	0.86	20	70	8	0.05	Transparent	Transparent	✓✓
1	0.50	20	80	8	0.05	Transparent	Transparent	✓✓
1	0.22	20	90	8	0.05	Transparent	Transparent	✓✓
1	0.11	20	95	8	0.05	Transparent	Transparent	✓✓

✓✓: Very good.

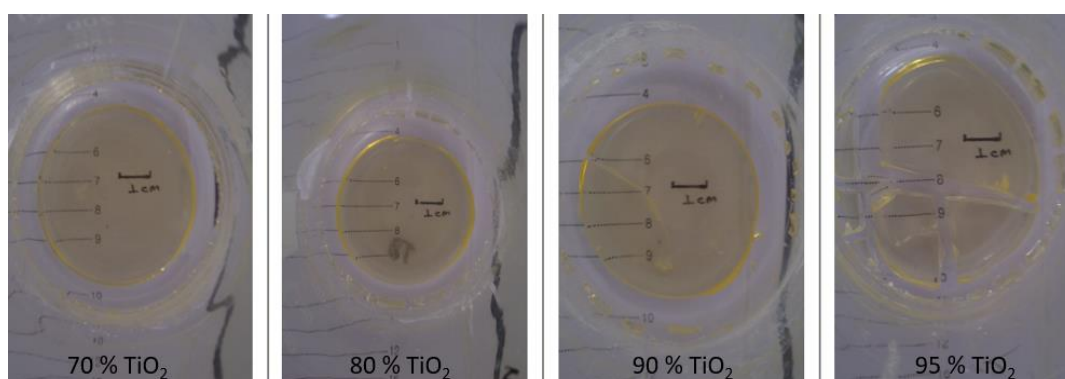


Figure 4.1. Appearance of the dried TP gels synthesized by using different  $\text{TiO}_2$  contents.

The concentrations of TTIP and TEP affect the stability, and morphology of the gel produced. As  $\text{TiO}_2$  concentration increases, initially Ti ions incorporated into the phosphate network attract oxygen from the  $\text{PO}_4$  tetrahedron and create Ti-O-P linkages. The network is composed of Ti-O-P and P-O-P bonds. Closely packed, strong Ti-O-P bonds provide extra monolithicity to the gels. Further increase in  $\text{TiO}_2$  concentration causes to the formation of Ti-O-Ti bonds. The TP gels containing high amount of  $\text{TiO}_2$  contains no P-O-P bonds. The increase in  $\text{TiO}_2$  concentration also changes the water/titanium alkoxide molar ratio ( $R = [\text{H}_2\text{O}]/[\text{Ti alkoxide}]$ ) which affects the gel stability [53]. The effect of R on the development and stability of the TP gels will be discussed in Section 4.1.5.

#### 4.1.2. Effect of $\text{TiO}_2$ Precursor Type

Two of the most commonly used Ti alkoxide precursors namely TTIP and TBOT were used to see the effects of  $\text{TiO}_2$  precursor type on the synthesis of the TP gels. The other synthesis parameters were kept constant. The evaluation was made for the TP gels containing 80 mol%  $\text{TiO}_2$ . Solvent used was 2-methoxyethanol. The influence of  $\text{TiO}_2$  precursor type on transparency and monolithicity of the wet and dried gels were investigated visually. Results for the TP gels synthesized by using both precursors were tabulated in Table 4.2. Appearance and visual transparency of the gels were displayed in Figure 4.2.

Visual inspection revealed that the dried gels synthesized by using both precursors showed monolithicity and satisfactory transparency although the gel synthesized by using TBOT was slightly cloudy after drying. Therefore, TTIP was taken as more appropriate  $\text{TiO}_2$  precursor for the synthesis of the TP gels and was used in the optimization studies of the other synthesis parameters.

Table 4.2. Results for the TP gels synthesized by using different  $\text{TiO}_2$  precursors.

TTIP (M)	TBOT (M)	TEP (M)	Solvent (M)	$\text{H}_2\text{O}$ (M)	HCl (M)	Appearance		Satisfaction Sign
						Wet Gel	Dried Gel	
1	-	0.50	20	8	0.05	Transparent	Transparent	✓✓
-	1	0.50	20	8	0.05	Transparent	Slightly Cloudy	✓

✓: Satisfactory, ✓✓: Very good.

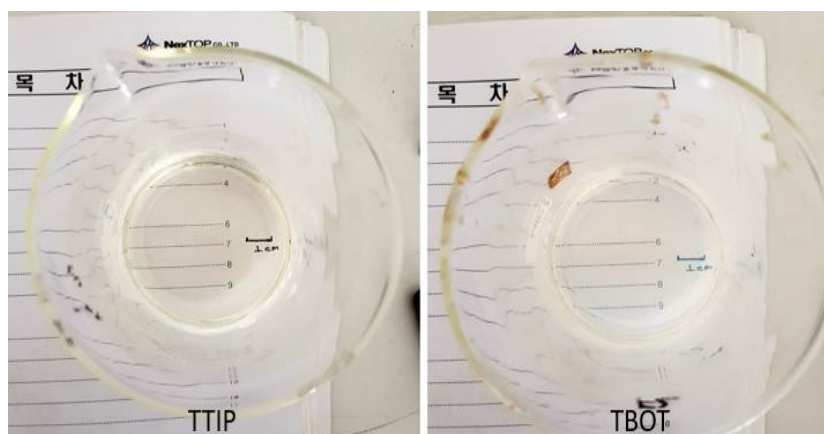


Figure 4.2. Appearance of the dried TP gels synthesized by using different  $\text{TiO}_2$  precursors.

The number of Ti ions varies with alkoxide type. The influence of the Ti precursor is due to differences in the reactivity of the alkoxides that influence the size and structure formed during the synthesis [54]. Ethoxy group has the highest reactivity and butoxy group has the lowest reactivity [54]. High reactivity of TTIP led higher hydrolysis and condensation rates probably due to its shorter carbon chain. The difference in the hydrolysis and condensation rates of the Ti precursors resulted in variation in the setting time of the gels as well as in their physical appearance.

### 4.1.3. Effect of Solvent Type

Solvent type is an important parameter in terms of synthesizing the gels with desired outlook and properties as it affects the hydrolysis and condensation rates. The hydrolysis rate decreases as the alkoxy group becomes more complicated. Commonly, alcohols are used as solvents since they promote condensation reaction by increasing the oxide content of the material [49]. Alkoxy groups having non-primary structures also contribute to slower reaction rates [49]. Moreover, solvents with different surface tension have a role in overcoming the cracks by suppressing the capillary forces and in obtaining bulk gels after drying.

In order to find out the best solvent, many solvents having different surface tensions were utilized to synthesize TP gels. The effect of solvent type was investigated only for the TP gels containing 80 mol% TiO<sub>2</sub>. Solvent type was changed while the other synthesis parameters were kept constant. Solvent molarity was 25 M. The effects of the solvent type on transparency and monolithicity of the wet and dried gels were investigated visually. Results for the TP gels synthesized by using different solvents are tabulated in Table 4.3. Appearance and visual transparency of the gels were shown in Figure 4.3.

Ethanol and methanol are the most common alcohols used as solvents. When ethanol or methanol was used as solvent, wet gels in milky-white color were synthesized. Hence, desired transparency was not achieved. Ethanol derived gels formed powders upon drying. Synthesis of bulk dried gels was not possible due to the fast evaporation rate of ethanol. When methanol, lower viscosity higher polarity than ethanol was used as solvent yellow colored semi-transparent gels were obtained after drying. Severe cracks formed in these gels during drying were attributed to the low boiling point and fast evaporation rate of methanol.

Table 4.3. Results for the TP gels synthesized by using different solvents.

Solvent type	Color	Wet gel	Dried gel	Satisfaction Sign
Methanol	Yellow	Transparent	Transparent	✓
Ethanol	Milky-white	Opaque	Cloudy	✗
2-Propanol	Yellow	Transparent	Transparent	✓
Ethylene glycol	No color	Transparent	Transparent	✓✓✓
2-Methoxyethanol	No color	Transparent	Transparent	✓✓✓
2-Ethoxyethanol	Yellowish	Transparent	Transparent	✓✓
1-2 Dimethoxyethanol	Yellow	Transparent	Foamed	✗
2-Isopropoxyethanol	Yellow	Transparent	Transparent	✓
Benzyl Alcohol	No color	Transparent	Transparent	✓
2-Butoxyethanol	Yellow	Opaque	Cloudy	✗

✗: Unsatisfactory, ✓: Satisfactory, ✓✓: Good, ✓✓✓: Very good.

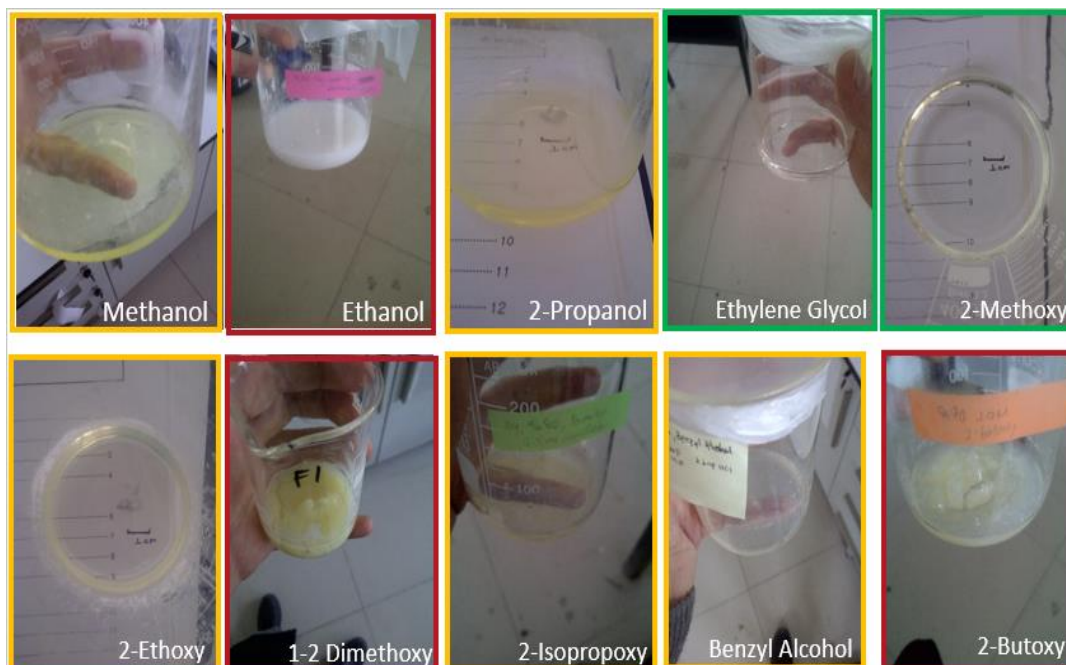


Figure 4.3. Appearance of the dried TP gels synthesized by using different solvents.

When 2-propanol, 2-ethoxyethanol, 1-2 dimethoxyethanol, 2-isopropoxyethanol, and 2-butoxyethanol were used as solvent, the gels synthesized appeared yellow in color. The yellow coloration was attributed to the presence of captured alkoxy groups. The high molecular weight (MW) solvents such as 1-2 dimethoxyethanol, benzyl alcohol, 2-isopropoxyethanol, and 2-butoxyethanol caused foaming and precipitation probably due to the lower solubility and enhanced tanglements.

The gels synthesized by using ethylene glycol and 2-methoxyethanol revealed exceptionally transparent gels, without any colorization. Ethylene glycol is a nucleophilic reagent. Through chemical modifications, specifically by occupying the coordination sites of  $Ti^{4+}$  ions, it controls the hydrolysis reaction [55]. Occupied coordination sites create higher resistance against substitution of the hydroxyl groups and slow down the hydrolysis reactions. Slow hydrolysis and condensation rates made precipitation process more controllable and provided gels with desired outlook. The use of 2-methoxyethanol suppressed the hydrolysis rate and provided the synthesis of transparent, homogeneous, and stable gels without any color. Pickup et al. [15] used 2-methoxyethanol instead of simple alcohols to avoid the precipitation by suppressing the rate of hydrolysis and polycondensation. In the light of the observations and from the appearance of the gels synthesized, 2-methoxyethanol and Ethylene Glycol were chosen as the most appropriate solvents for preparing TP gels.

#### **4.1.4. Effect of Solvent Content**

Interaction between the ions became much stronger with increasing solvent content. However, excessive addition of solvent decreases the growth rate by covering the surfaces. The optimization of solvent content was made for the TP gels containing 80 mol%  $TiO_2$ . Solvent used was 2-methoxyethanol. Solvent molarity was varied from 5 to 30 M while the other synthesis parameters were kept constant. The effects of solvent molarity on transparency and monolithicity of the wet and dried gels were investigated visually.

Results for the TP gels containing 80 mol% TiO<sub>2</sub> synthesized by using different solvent molarities tabulated in Table 4.4. Appearance and visual transparency of the gels were shown in Figure 4.4.

Table 4.4. Results for the TP gels synthesized by using different solvent molarities.

TTIP (M)	TEP (M)	Solvent (M)	H <sub>2</sub> O (M)	HCl (M)	Appearance		Satisfaction sign
					Wet gel	Dried gel	
1	0.5	5	8	0.05	Foamed	Opaque	✗
1	0.5	10	8	0.05	Transparent	Cloudy	✓
1	0.5	15	8	0.05	Transparent	Cracked	✓✓
1	0.5	20	8	0.05	Transparent	Cracked	✓✓
1	0.5	25	8	0.05	Transparent	Transparent	✓✓✓
1	0.5	30	8	0.05	Transparent	Cracked	✓✓

✗: Unsatisfactory, ✓: Satisfactory, ✓✓: Good, ✓✓✓: Very good.

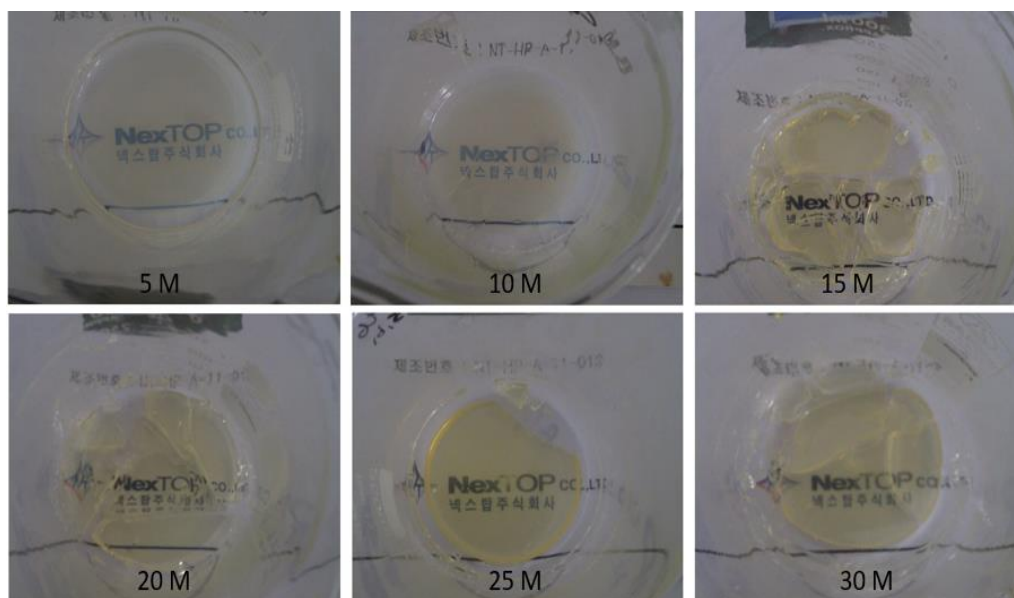


Figure 4.4. Appearance of the dried TP gels synthesized by using different solvent molarities.

The gel synthesized by using 5 M solvent had some crystalline precipitates in wet form and cracked intensively upon drying. Precipitation was observed also as the molarity of solvent was increased to 10 M.



Low solvent molarity was probably not sufficient to dissolve the TiO<sub>2</sub> and P<sub>2</sub>O<sub>5</sub> precursors totally, which caused precipitation rather than gelation. Increase in the solvent molarity increased the solubility of the chemicals in the system and led to the formation of transparent gels. Large cracks were observed in the dried gel when the solvent molarity was 30 M, due probably to the extensive evaporation of the solvent from the system. Pores and large capillary pressure difference created an observable pattern of crack formation. In addition, 30 M solvent molarity resulted in the formation of too thick gels. It was reported that using excess solvent decreases the alkoxide concentration hence, decreases the rate of chemical reactions [55]. Such relation results in formation of more close-packed agglomerates with lower open porosities. In the light of the observations and from the appearance of the gels synthesized, 25 M solvent molarity was selected as the optimum solvent molarity for the preparation of the TP gels.

#### 4.1.5. Effect of Water Content

The optimization of water content was made for the TP gels containing 80 mol% TiO<sub>2</sub>. Water content was varied from 1 to 10 M. The solvent used was 2-methoxyethanol. The effects of water content on transparency and monolithicity of the wet and dried gels were investigated visually. Results for the TP gels containing 80 mol% TiO<sub>2</sub> synthesized by using different water molarities were tabulated in Table 4.5. Appearance and visual transparency of the gels were shown in Figure 4.5.

Table 4.5. Results for the TP gels synthesized by using different water molarities.

TTIP (M)	TEP (M)	Solvent (M)	H <sub>2</sub> O (M)	HCl (M)	Appearance		Satisfaction sign
					Wet gel	Dried gel	
1	0.5	20	1	0.05	Foamed	Opaque	✗
1	0.5	20	4	0.05	Foamed	Transparent	✓
1	0.5	20	8	0.05	Transparent	Transparent	✓✓✓
1	0.5	20	10	0.05	Transparent	Transparent	✓✓

✗: Unsatisfactory, ✓: Satisfactory, ✓✓: Good, ✓✓✓: Very good.

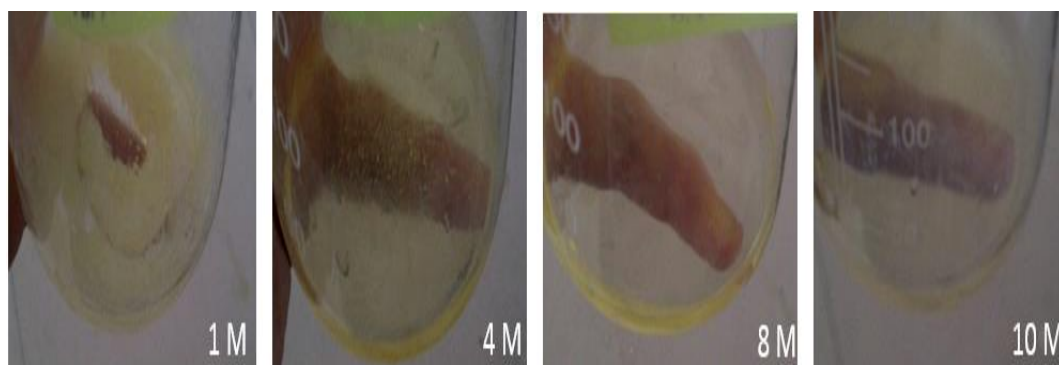


*Figure 4.5.* Appearance of the dried TP gels synthesized by using different water molarities.

Visual observations suggest that water content influence the appearance and transparency of the TP gels as it affects the interaction between chemical species and provides a control over molecular size and the morphology [56]. Also, water content changes the water/alkoxide ratio (R) that has profound effect on the hydrolysis. In the sol-gel hydrolysis, reaction rates are limited by the diffusion of atoms. It has been shown that increasing R increases the atomic mobility, promotes the hydrolysis reactions, which favor the gelation process [53].

For the gels containing low amount of water, i.e. 1 and 4 M, foaming and clouding was observed and evidently the transparency of the gels was poor. All the sols containing different water contents set to gels in less than 5 min. Increase in water content significantly decreased the gelation time, to even 1 min. With the addition of water, structure became looser, atomic mobility increased and chances of forming interactions that promote gelling increased. For the gels containing 4 M water, a colloidal suspension was formed from precipitated crystallites. Such behavior was also observed by Carp et al. [7] who stated that the utilization of Ti alkoxides as starting material involves the formation of  $\text{TiO}_2$  sols, gels, or precipitates by hydrolysis and condensation reactions. The appearances of the wet gel containing 8 M water suggested that 8 M water is a good interval for procurement of transparent gels. Above 8 M water, gelation occurred immediately during the stirring. Nevertheless, at the drying stage, dehydration occurred much faster.

In high water content, too fast formation of the network results in lower interconnectivity among atoms while in low water content, network formation is slow, and structure is more close-packed and denser. Also, increasing water content creates more space for  $[\text{TiO}_6]^{n+}$  units to have more regular arrangement and enables a long range ordered structure [3]. Enhanced capillary forces led to higher shrinkage and resulted in the formation of more cracked gels. Although the transparency was sufficient, gel monolithicity was not preserved as much. Therefore, 8 M water content was taken as the optimum water content for further optimization studies. Increasing water concentrations also decreases the solution pH by decreasing the  $\text{H}_3\text{O}^+$  and  $\text{OH}^-$  ions concentration.

#### 4.1.6. Effect of HCl Content

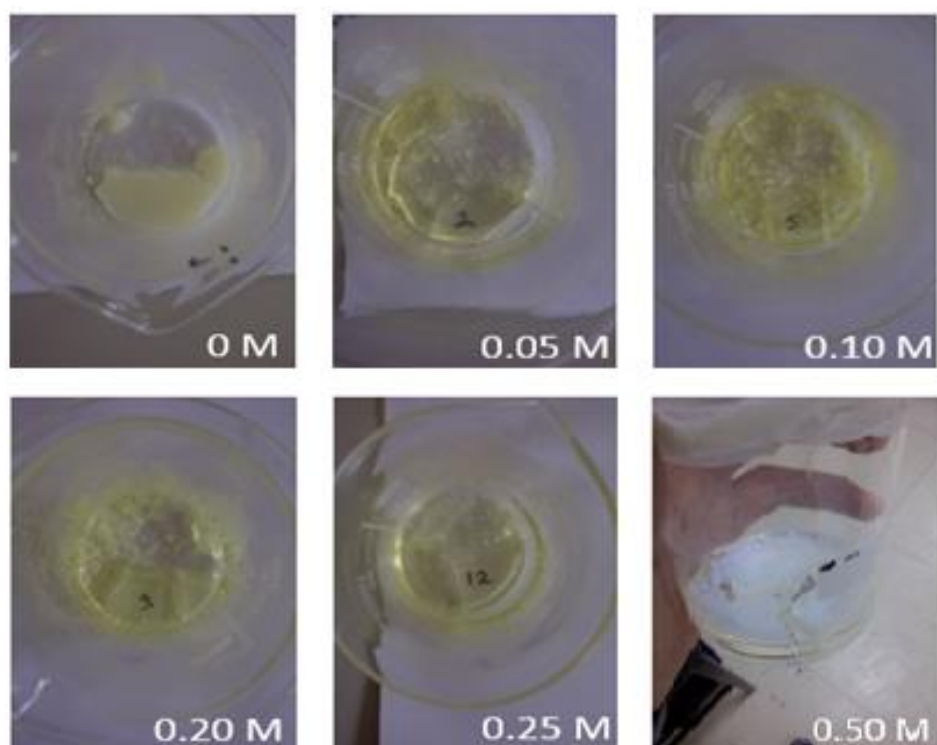
HCl is one of the most commonly used acid for adjusting and lowering the pH of the sol-gel solutions. The optimization of HCl molarity was made for the TP gels containing 80 mol%  $\text{TiO}_2$ . HCl molarity was varied from 0 to 0.5 M while the other synthesis parameters were kept constant. Solvent used was 2-methoxyethanol. The effects of HCl molarity on transparency and monolithicity of the wet and dried gels were investigated visually. Results for the TP gels containing 80 mol%  $\text{TiO}_2$  synthesized by using different HCl molarities are presented in Table 4.6.

Table 4.6. Results for the TP gels synthesized by using different HCl molarities.

TTIP (M)	TEP (M)	Solvent (M)	$\text{H}_2\text{O}$ (M)	HCl (M)	Appearance		Satisfaction sign
					Wet gel	Dried gel	
1	0.5	20	8	0	Foamed	Opaque	✗
1	0.5	20	8	0.05	Transparent	Transparent	✓✓✓
1	0.5	20	8	0.10	Transparent	Transparent	✓✓✓
1	0.5	20	8	0.20	Transparent	Transparent	✓✓
1	0.5	20	8	0.25	Transparent	Transparent	✓✓
1	0.5	20	8	0.50	Foamed	Opaque	✗

✗: Unsatisfactory, ✓: Satisfactory, ✓✓: Good, ✓✓✓: Very good.

Data suggest that as small as 0.05 M HCl is necessary to get transparent TP gels but, excessive addition of the HCl decreases the atomic mobility, affects the solution stability, and significantly reduces the transparency of the gel. This can be observed with naked eye as the solution becomes white-milky colored and opaque. Appearance and visual transparency of the gels were shown in Figure 4.6.



*Figure 4.6.* Appearance of the dried TP gels synthesized by using different HCl molarities.

All the gels, except the one synthesized by using 0.5 M HCl kept their monolithicity after drying. Cracks were observed in the gel synthesized by using 0.5 M HCl because of the pH change that influenced the stability of the solution. Excessive use of HCl caused precipitation and self-condensation which significantly reduced the transparency of the gel. The findings suggest that water content has more influence on the monolithicity of the gels than HCl molarity. Furthermore, the addition of HCl and with the increase in HCl molarity, gelation time of the solution decreased. The increase in HCl molarity decreased the gelation time due to the development of precipitated crystallites with less ionic charges [57].

It is possible to give two explanations for the role of HCl; one involves a catalytic role in the hydrolysis reaction, and the other one is a modifier of the formed polymer structure which influences the degree of hydrolysis [57]. As the HCl molarity increases,  $H^+$  ions in the solution increase. Increasing HCl additions also decrease the residual alkyls amount. At acidic environment, positively charged ions repel OR groups and attach to OH groups [58]. Such interaction promotes hydrolysis rate and slows the condensation rate. The appearance of the gels suggested that the TP gels synthesized by using HCl molarities between 0.05 and 0.25 were satisfactory in terms of the required transparency and monolithicity. Therefore, judgment for the best HCl molarity was done based on the literature information. It has been reported that an increase in pH leads to an increase in the active hydroxyl groups on the  $TiO_2$  surface [58]. At low pH values there is more chance for gelation since the crystallites have less ionic charges [58]. Additionally, low pH generally results in lower solubility. Therefore, more Ti precursor is needed for solutions containing high HCl molarity.

It is obvious that, HCl is necessary for the realization of the required transparency.  $H^+$  adsorption in acidic conditions make the surface positively charged and electrostatic repulsion forces break down the amorphous agglomerates to primary octahedron [26]. Therefore, when the equilibrium has been established, product becomes optically transparent. Besides, by preventing the precipitation, HCl could play a role in obtaining transparent  $TiO_2$  gels. Consequently, 0.05 M HCl was taken as the optimum HCl molarity for further optimization studies.

#### **4.2. Effect of Drying**

Drying behavior of the TP gels synthesized with various synthesis parameters were quite different. Some of the gels cracked during drying while some of them kept their monolithicity. Cracking during drying was attributed to the capillary pressure phenomena. Pressure difference between the exterior and interior gel network results in a shrinkage since exterior of the gel usually contracts faster than the interior [50].

The variation in the weight loss of the gels synthesized by using 2-methoxyethanol, ethylene glycol, and 2-propanol as solvent with drying time is shown in Figure 4.7. 30 day drying caused large loss in weight and volume of the wet gels due to the evaporation of water and solvent used. Weight loss occurred during drying was significantly higher for the gels synthesized by using low MW solvents with low carbon content. Decreasing MW of the solvents in the order of 2-methoxyethanol, ethylene glycol, 2-propanol ended up with weight losses of 11.3%, 23.8%, and 35.3%, respectively after 30 day drying probably due to the lower boiling point and weaker C-O bonds. As seen in Figure 4.8, the gels synthesized with high MW solvents were deeply colored upon drying due to their high carbon content.

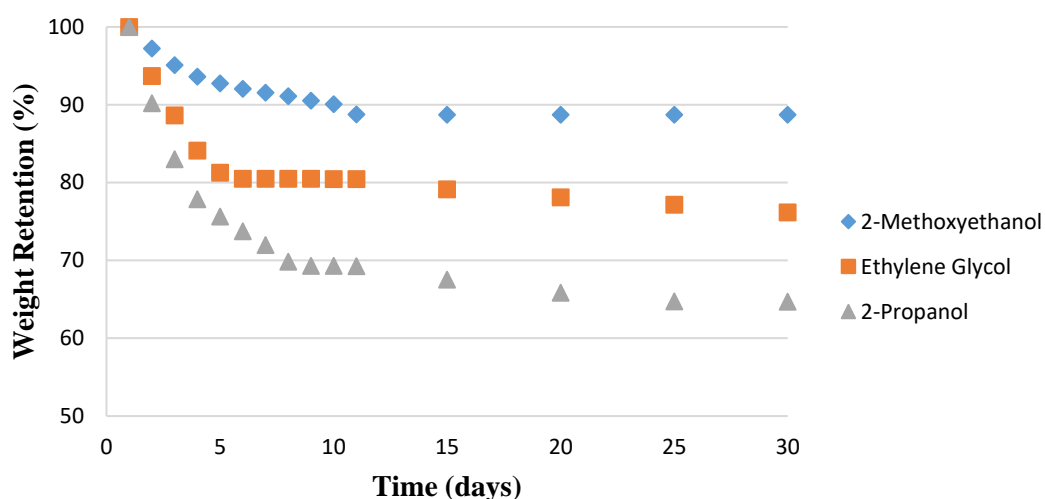


Figure 4.7. Variation of weight retention of the gels with drying time at 60 °C.

Figure 4.7 shows the appearance of the dried gels subjected to 2 weeks drying at 60 °C. Large volume shrinkage was evident. Crack formation hence the number of fragmentations increased with increasing TiO<sub>2</sub> content. The gels with high P<sub>2</sub>O<sub>5</sub> content showed better resistance against cracking. Phosphates have good glass forming properties.

The strong Ti-O-P bonds are believed to provide extra monolithicity to the gels. The dried gel monolithicity is vital for the preparation of bulk glasses. The ability to form bulk glass increases as the size of the dried gel gets bigger.

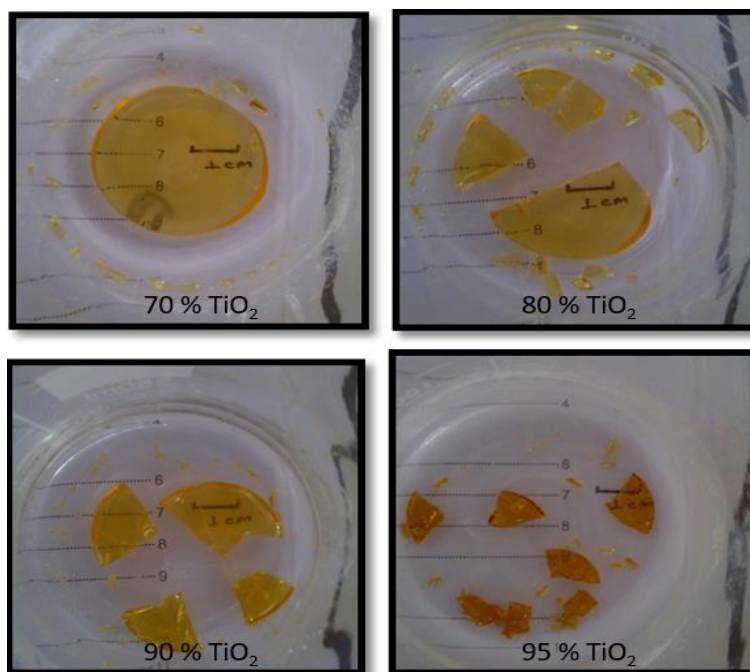


Figure 4.8. Appearance of dried gels after 2 weeks of drying at 60 °C.

### 4.3. Differential Thermal and Thermogravimetric Analyses (DTA/TG)

The dried gels synthesized by the sol-gel process are usually amorphous and they require heat-treatment at predetermined temperatures for the crystallization. Heat-treatment is especially important to get bulk glasses since the evaporation of water and solvent and crystallization process taking place during the heat-treatment may cause dramatic decrease in the volume of the dried gels. Improper heat-treatment designs encourage the formation of cracks and bulk glass could not be obtained. On the other hand, proper heat-treatment designs results in the conversion of amorphous phase to desirable crystalline phase(s). In addition, proper heat-treatment diminishes  $Ti^{+3}$  ions that give undesirable color to the glass and prevents the transparency [12].

In order to understand the thermal behavior and to optimize the heat-treatment design conditions, selected as dried TP gels were subjected to DTA and TG analyses before the application of various heat-treatment designs. The DTA-TG thermograms gave information about the removal of organics and the crystallization temperatures of the crystalline phases developed during heating. The DTA-TG thermograms of the TP gels synthesized by using 80 and 95 mol% TiO<sub>2</sub> were shown in Figure 4.9. The solvent was 2-methoxyethanol. As seen in Figures 4.9 (a) and (b), the TP gels synthesized by using 80 mol% TiO<sub>2</sub> and 95 mol% TiO<sub>2</sub> had more or less the same features in the DTA-TG thermograms suggesting that both gels had similar thermal behavior.

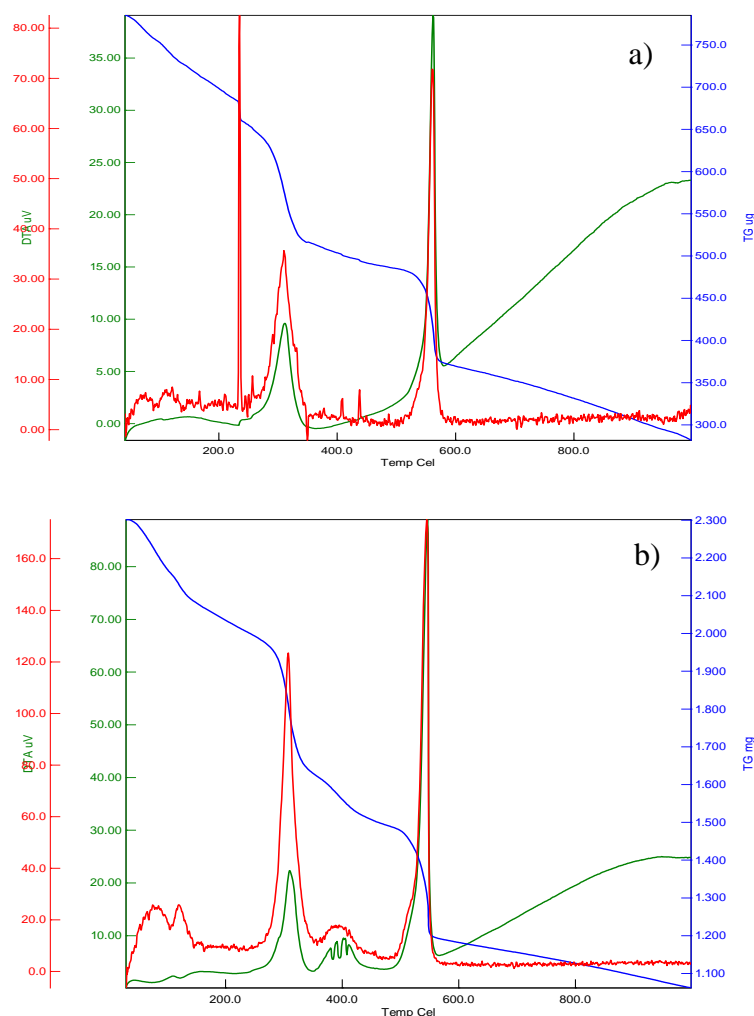
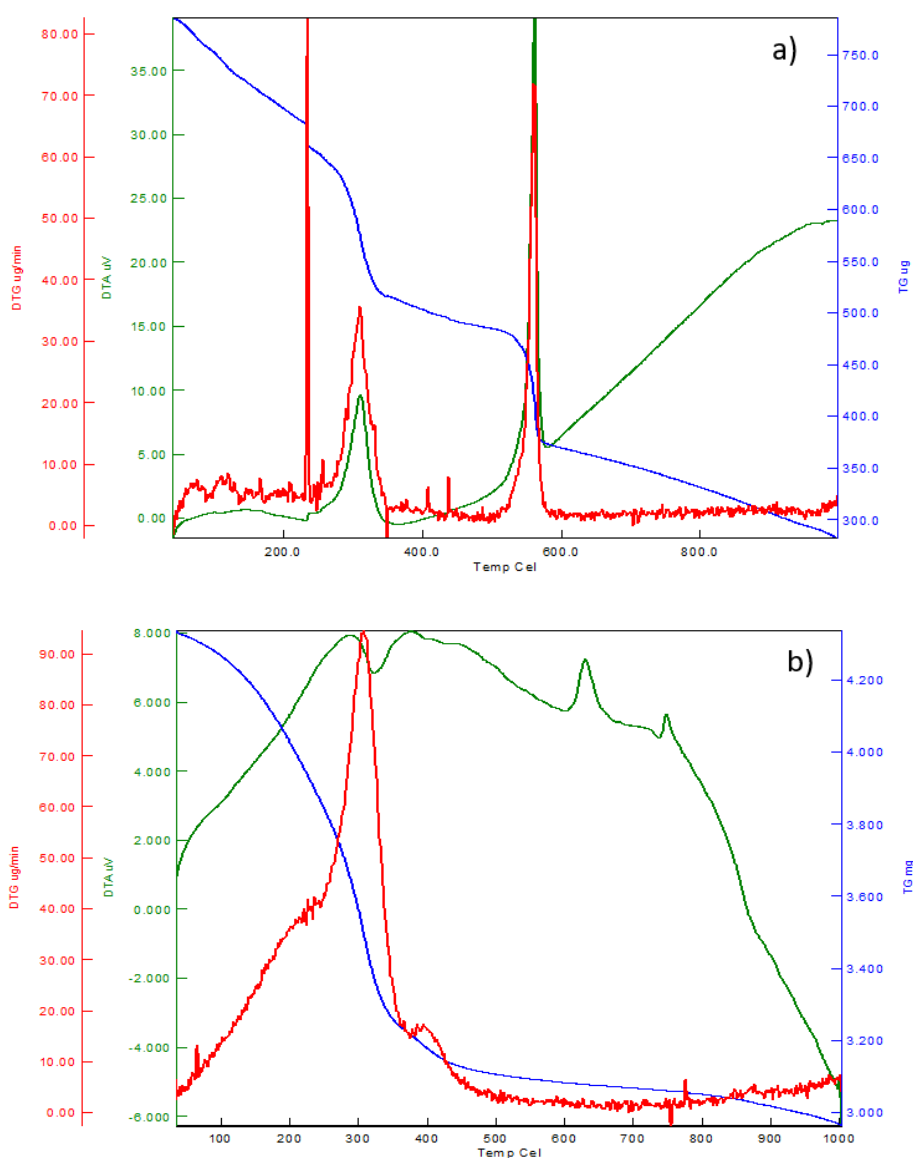


Figure 4.9. DTA-TG thermograms of the TP gels synthesized by using different TiO<sub>2</sub> contents. a) 80 mol% TiO<sub>2</sub> and b) 95 mol% TiO<sub>2</sub>.



The DTA-TG thermograms of the TP gels synthesized by using 2-propanol, 2-isopropoxy, 2-butoxy, and ethylene glycol as solvents were illustrated in Figure 4.10. TiO<sub>2</sub> content of the gels was 80 mol%. The DTA-TG thermograms of the TP gels synthesized by using different solvents, see Figure 4.9 (a) and Figures 4.10 (a)- (d), suggested that the solvent type used in the synthesis had profound influence on the peak temperatures for both endothermic and exothermic events in the DTA curves. Such intense changes in the thermograms were attributed to the differences in carbon content and boiling point of the solvents.



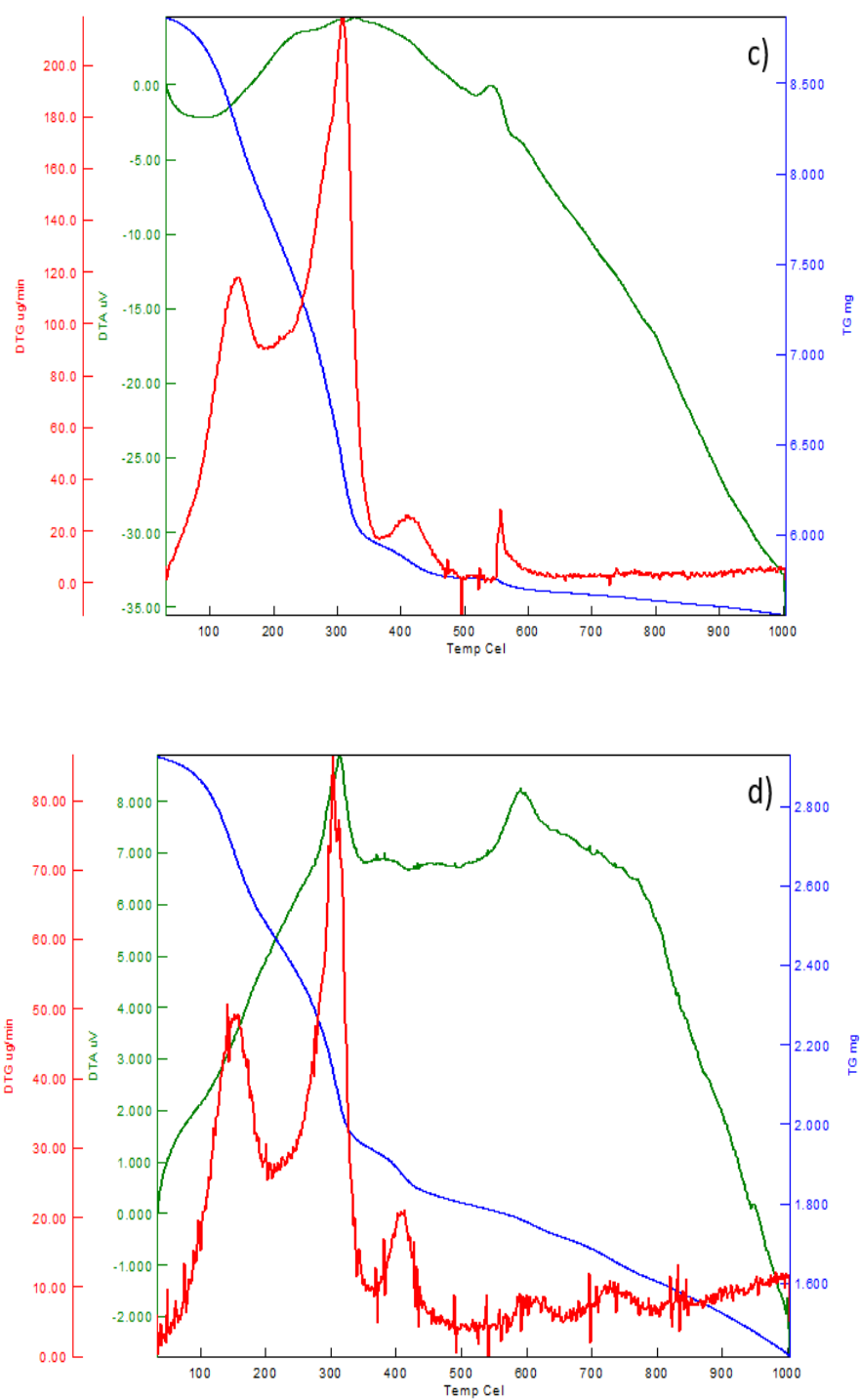


Figure 4.10. DTA-TG thermograms of the TP gels synthesized by using different solvents. a) 2-propanol, b) 2-isoproxy, c) 2-butoxy, and d) Ethylene glycol.

In general, 4 distinct weight loss stages were detected in the TG curves. 1<sup>st</sup> stage between 25 and 250 °C, 2<sup>nd</sup> stage between 250 and 360 °C, 3<sup>rd</sup> stage between 360 and 580 °C, and 4<sup>th</sup> stage between 580 and 1000 °C. From ambient to 250 °C, the sample had 21% weight loss as a result of desorption of physically adsorbed water and evaporation of remaining water in the pores. The desorption of chemically adsorbed water via hydrogen, oxygen bonds in the network structure played a role in the reduction at this stage [59].

In the 2<sup>nd</sup> stage, the sample had additional 19% weight loss and total weight loss reached to 40%. Weight loss at this stage was attributed to the solvent evaporation and the combustion of organics. The large exothermic peak detected in the DTA curve within this temperature range was attributed to the combustion of organics.

At the 3<sup>rd</sup> stage, a steep decrease in the weight of the sample was noticed and total weight loss reached up to 62% at 580 °C. Sharp exothermic peak in the DTA curve around this temperature corresponds to the oxidation of alkoxide groups that persist due to incomplete hydrolysis [59]. The weight loss between 360 and 580 °C was attributed to the oxidation of alkoxide groups bonded to the Ti atom. The burn out of remaining organics, i.e., unreacted TTIP and TEP, might contribute to the exothermic peak. In the DTA curves, the exothermic peaks between 400 and 550 °C belong to the crystallization of amorphous TiO<sub>2</sub> [54].

At the 4<sup>th</sup> stage, a small exothermic peak around 900 °C might be related to the rutile crystallization that is the high temperature stable polymorph of TiO<sub>2</sub>. At this stage, further weight loss was obtained, and the total weight loss of the sample reached to 81.2%. No obvious endothermic peak up to 1000 °C might imply the high resistance ability of the TP glasses against heating. Such high temperature stability and different crystallization temperatures are related to the P<sub>2</sub>O<sub>5</sub> portion in the glass structure. Strong hydrogen to oxygen atom bonding in the presence of P<sub>2</sub>O<sub>5</sub> enhanced the thermal stability of the final product [60].

Also, presence of  $P_2O_5$  decreased the mobility of  $TiO_2$  atoms and altered the crystallization temperatures by acting as an anchor. All the TP glasses revealed very high, almost the same weight loss behavior with increasing temperature. Generally, weight of the sample decreased dramatically up to 600 °C, and then it showed relatively steady behavior. As in the case of 2-butoxyethanol, more amount of strong C-O bonds and highly stable butoxy groups made the breaking of bonds and the organic evaporation process became much harder. For this solvent, the surface carbon atoms were removed but, trapped carbon atoms inside the crystallites remained. Further increase in the temperature removed the encapsulated carbon atoms and resulted in further weight loss in the TG curves. Weight loss at elevated temperatures was probably caused by the decomposition of formed carbon shield around  $TiO_2$  crystallites. Complete removal of the water and organics suggest that the TP glasses could be successfully obtained upon heating.

Another important feature obtained from the DTA curves was the glass transition temperature ( $T_g$ ). The baseline shift and the inflection point from the DTA curves usually correspond to the glass transition phenomenon. In this study, inflection from the baseline in the DTA curves was observed between 400 and 550 °C depending on the initial  $TiO_2$  content of the TP gels. Conclusively, the presence of the  $T_g$ 's in the DTA curves prove that the gels synthesized transformed to glasses. The  $T_g$  of the TP glasses prepared by using different  $TiO_2$  contents were in the range from ~520 to ~590 °C. An increase in  $T_g$  with increasing  $TiO_2$  content confirms that  $TiO_2$  enters the structural network of the glass. When  $P_2O_5$  was replaced with  $TiO_2$ , the higher electronegativity of  $TiO_2$  probably resulted in higher bonding ability of strong P-O-Ti bonds and increased  $T_g$ . The increase in  $T_g$  is ascribed due to the greater strength of the crosslinks between the cation and oxygen atoms [61] and generally indicates a stronger glass network and better chemical bonding abilities. Brow et al. [11] assigned  $T_g$  rise with  $TiO_2$  content to the structural rearrangements in the main network because of the P-O-P to Ti-O-P replacements. These interconnections within the structural network modify the glass structure and increase  $T_g$ .

#### **4.4. Effect of Heat-treatment Design**

The dried TP gels were subjected to different heat-treatment designs to determine the optimum heat-treatment conditions. Heat-treatment is especially important to get bulk glasses because improper heat-treatment conditions initiate cracks. On the other hand, proper heat-treatment designs facilitate the transformation of amorphous  $\text{TiO}_2$  phase to crystalline anatase phase, the photocatalytically favorable phase of  $\text{TiO}_2$ . Depending on the heat-treatment conditions, generally mixtures of glass and finely dispersed crystals are obtained in the products after the heat-treatment.

##### **4.4.1. Effect of Fast Heat-treatment**

Appearance of dried gels and the glasses obtained after FHTS of the dried gels with various  $\text{TiO}_2$  content are shown in Figure 4.11b. The optimum FHTD conditions presented in Table 4.1 has led to the production of transparent bulk glasses. However, less duration around the solvent evaporation temperatures and the high heating rates promoted extensive cracks formation. The gels heat treated at these conditions did not have satisfactory transparency due to the remaining non-evaporated solvents. Bulk glasses could not be obtained at the improper FHTD conditions.

Also, these glasses were yellow in color most probably due to the residual alkoxy groups. Obviously, the heat-treatment temperature or duration applied was not enough for the complete removal of the organics from the structure.  $\text{TiO}_2$  content of the gel was an important criterion for the monolithicity of the glasses exposed to FHTD. Also, the volume shrinkage of the TP glasses depended on the  $\text{TiO}_2$  content. The volume shrinkage during the heat-treatment for the glasses prepared with high  $\text{TiO}_2$  content was more than that for the glasses prepared with low  $\text{TiO}_2$  content. Therefore, more serious crack formation for the glasses with high  $\text{TiO}_2$  content is expected as compared to the glasses with low  $\text{TiO}_2$  content.

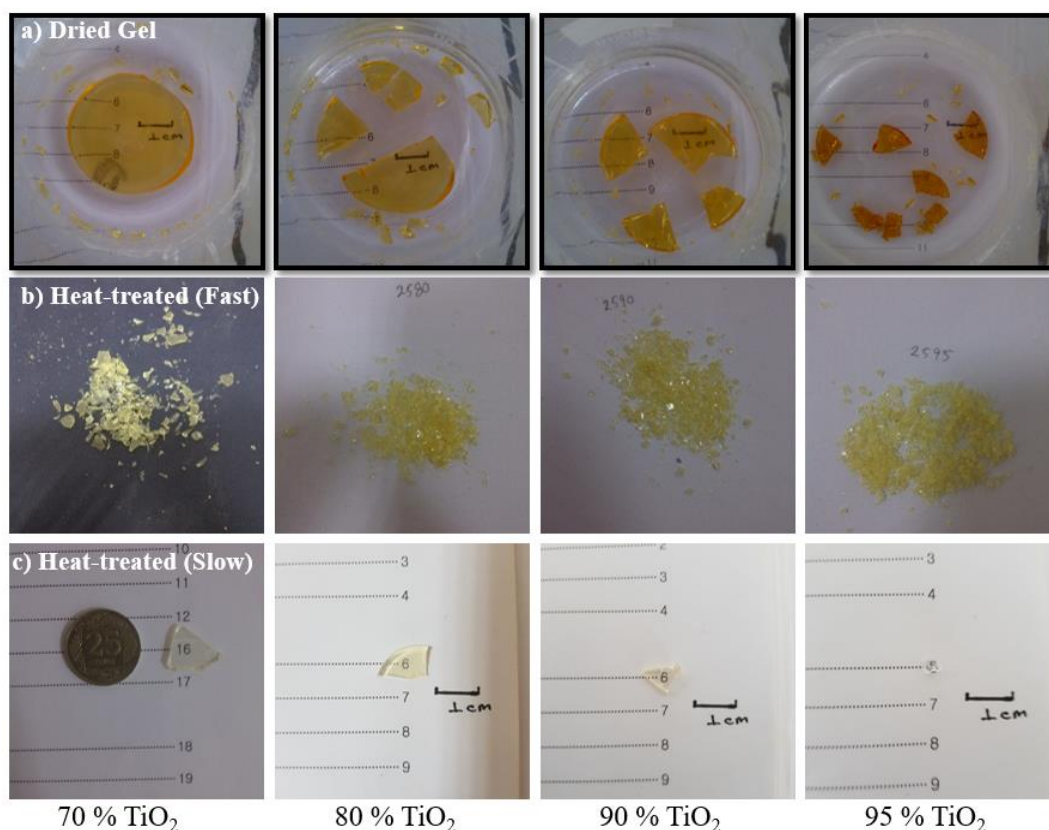


Figure 4.11. a) Appearance of the as dried TP gels of different  $\text{TiO}_2$  contents, b) appearance of the TP gels of different  $\text{TiO}_2$  contents after fast heat-treatment, and c) appearance of the TP gels of different  $\text{TiO}_2$  contents after slow heat-treatment.

#### 4.4.2. Effect of Slow Heat-treatment

Bulk and transparent glasses were successfully produced by SHTD. Slow evaporation of the solvent played a crucial role in reducing the capillary pressure differences and thus, gel monolithicity was retained. Additional heat-treatment steps and longer durations completely removed the solvents. SHTD of the dried gels yielded preparation of bulk, transparent and colorless TP glasses. Colorless feature of the glasses indicate that the solvent was effectively removed during heat-treatment. Appearance of the dried gels and the glasses exposed to SHTD are shown in Figure 4.11 c).  $\text{TiO}_2$  content of the gel was also important for the monolithicity of the glasses exposed to SHTD. It was possible to produce a single piece or bigger pieces of glass with lower  $\text{TiO}_2$  content.

## CHAPTER 5

### RESULTS AND DISCUSSION OF CHARACTERIZATION STUDIES

#### 5.1. X-Ray Diffraction (XRD)

Crystallization of the TP glasses synthesized by the sol-gel process is a complex process depending on several factors such as temperature, chemicals used, pH, and other parameters that have influence over the mobility of the atoms [25].

In this section, the influence of the most important synthesis parameters such as TiO<sub>2</sub> content, TiO<sub>2</sub> precursor type, solvent type and amount, pH, and water content on the phases present and crystallinity of the phases in the TP glasses were researched. Effect of each parameter on the crystalline phases developed and on their crystal size was determined from the XRD patterns. Also, the mechanisms involved in the crystallization process were explained.

##### 5.1.1. Effect of TiO<sub>2</sub> Content

Figure 4.12 represents the XRD patterns of the as dried TP gels synthesized by various TiO<sub>2</sub> contents. The gels were synthesized with the parameters listed in Table 4.1. The solvent used was 2-methoxyethanol. The XRD patterns of all the as dried gels indicated the characteristic features of the amorphous materials regardless of their TiO<sub>2</sub> content. That is, the XRD patterns possessed no peaks corresponding to certain crystallographic planes in crystal. Instead, noisy background and a hump between  $2\theta$  of 10° and 20°, which is an indication of short-range order, confirmed the completely amorphous nature of the samples.

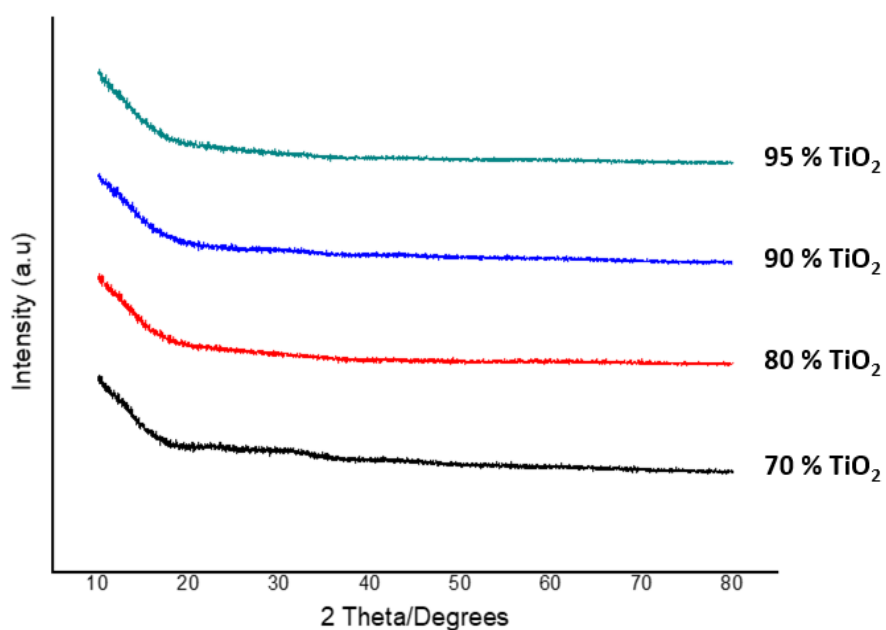


Figure 5.1. XRD patterns of the dried TP gels synthesized by various  $\text{TiO}_2$  contents.

In general, the dried gels synthesized by the sol-gel process exhibits an amorphous nature. The amorphous phase does not show sufficient photoactivity and requires a subsequent heat-treatment for the initiation and development of crystallization process [4]. By applying a regulated heat-treatment,  $\text{TiO}_2$  experiences amorphous to anatase phase transformation.  $\text{TiO}_2$  crystallites exhibit better photocatalytic activity. Therefore, heat-treatment is an essential step if the photocatalytic activity of the TP glasses is to be improved.

The XRD patterns of the TP glasses prepared by various  $\text{TiO}_2$  content subsequently heat-treated at  $600\text{ }^\circ\text{C}$  for 1 h were illustrated in Figure 5.1. All the samples indicated the XRD peaks belonging to only anatase crystalline phase (JCPDS 21-1272) along with the amorphous background. No peaks corresponding to other  $\text{TiO}_2$  phases and other crystalline phases or contaminations were detected. The characteristic peaks located at  $2\theta$  of  $25.4$ ,  $37.6$ ,  $48$ ,  $54$ ,  $55$ , and  $63^\circ$  corresponding to the (101), (004), (200), (105), (211), and (204) planes of the anatase phase, respectively, were detected for all of the glasses.



At the FHTD conditions, the TP glasses having high anatase content with fine crystallites dispersed in the amorphous base were successfully prepared.

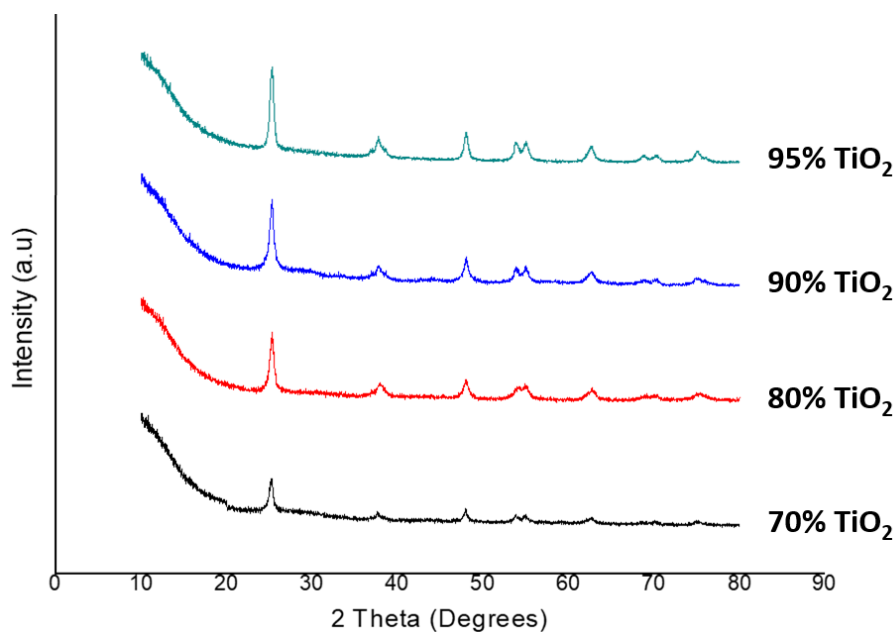


Figure 5.2. The XRD patterns of the TP glasses prepared by various TiO<sub>2</sub> contents subsequently heat-treated at 600 °C for 1 h.

As confirmed by the DTA-TG studies, a regulated heat-treatment at 600 °C for 1 h was appropriate to convert the as dried gel to glass and to develop anatase crystallites. The presence of the diffraction peaks belonging to the anatase crystallites was evident in all the glasses but, peak intensities varied depending on the TiO<sub>2</sub> content. Obviously, 600 °C was high enough to form anatase crystals along with the amorphous base and low enough to prevent anatase to rutile transition.

The transformation from amorphous to anatase TiO<sub>2</sub> takes place in the temperature ranging from 350 to 450 °C [62]. Hendrix et al. [37] stated that “The formation of anatase or rutile from amorphous TiO<sub>2</sub> does not start at a single point where all amorphous material crystallizes to anatase or rutile”.

At higher temperatures, more amorphous phase will transform to anatase. However, higher heat-treatment temperatures also transform anatase to rutile and increase the growth rate of the crystals, which leads to a smaller specific surface area”. It could be clearly seen in Figure 5.2 that anatase peak intensities exhibited an increasing trend with increasing TiO<sub>2</sub> content due to the replacement of P<sub>2</sub>O<sub>5</sub> by TiO<sub>2</sub> in the structure. The TP glasses prepared by using less TiO<sub>2</sub> content composed of P-O-Ti bonds. The replacement of P<sub>2</sub>O<sub>5</sub> by TiO<sub>2</sub> favored the development of Ti-O-Ti bonds. High amount of Ti-O-Ti bonds in the structure for higher TiO<sub>2</sub> concentrations ensured better crystallization. As Ti-O-Ti bonds increase, the glass has an improved forming rate of anatase phase [46]. Size of the anatase crystallites developed in the TP glasses with different TiO<sub>2</sub> contents was calculated by means of the Scherrer equation and given in Table 5.1.

Table 5.1. Size of the anatase crystallites developed in the TP glasses with different TiO<sub>2</sub> contents.

TiO <sub>2</sub> content (mol%)	Crystallite size (nm)
70	10.8
80	12.1
90	12.4
95	13.5

The anatase crystallites developed in the TP glasses gradually grew from 10.8 to 13.5 nm as the TiO<sub>2</sub> content increased from 70 to 95 mol%. A direct relationship between the TiO<sub>2</sub> content and crystal size was noted. Apparently, addition of TiO<sub>2</sub> increased Ti-O-Ti bonds, made atoms more mobile and enhanced their collision rate. As a result, atoms gathered more and through particle aggregation crystals grew by size.

### 5.1.2. Effect of TiO<sub>2</sub> Precursor Type

The XRD of all the as dried gels synthesized by using TTIP and TBOT indicated the characteristic features of the amorphous materials. The gels were synthesized with the parameters listed in Table 4.2. XRD analysis of the samples suggested that all the as dried gels are in amorphous nature regardless of the type of the TiO<sub>2</sub> precursor.

The XRD patterns of the TP glasses prepared by using different TiO<sub>2</sub> precursors subsequently heat-treated at 600 °C for 1 h is shown in Figure 5.3. The solvent used was 2-methoxyethanol. XRD patterns of both glasses indicated the XRD peaks belonging to only anatase crystals in the amorphous base.

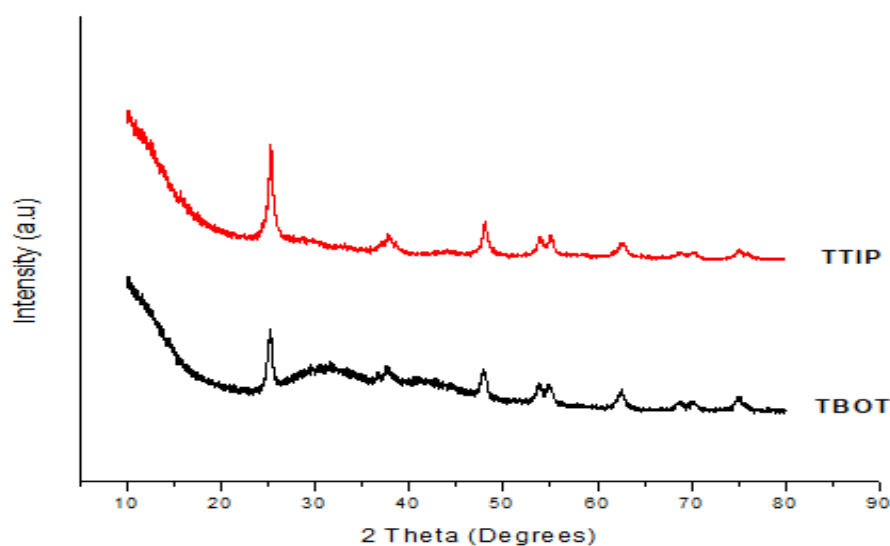


Figure 5.3. XRD patterns of the TP glasses prepared by different TiO<sub>2</sub> precursors and heat-treated at 600 °C for 1 h.

Glasses prepared by using TTIP revealed much higher peak intensities for the anatase crystal than that prepared by using TBOT, suggesting better crystallinity. The main reason for such difference might be due to the relatively shorter carbon chain of TTIP compared to TBOT. Shorter carbon chain leads to higher hydrolysis and condensation rates [63]. High carbon content of the butoxy group in TBOT probably decreased the attachment ability of the alkoxides and caused lower reaction ability. The non-reacted TiO<sub>2</sub> portion evaporated during the heat-treatment process instead of crystallization. Thus, the crystallization ability of the glass was hindered. On the contrary, high reaction ability of TTIP enhanced the anatase crystallization rate. Size of the anatase crystallites developed in the TP glasses produced by using TTIP and TBOT was 15.25 nm and 13.50 nm, respectively as shown in Table 5.2. The difference in the crystal sizes was attributed to the different hydrolysis and condensation rates of the TiO<sub>2</sub> precursors.

Table 5.2. Size of the anatase crystallites developed in the TP glasses with different TiO<sub>2</sub> precursors.

TiO <sub>2</sub> precursor type	Crystal size (nm)
TBOT	13.5
TTIP	15.2

The XRD results suggest that TTIP is more advantageous to produce the TP glasses with high anatase content than TBOT. Therefore, the TP glasses prepared by using TTIP were used for the determination of the self-cleaning properties.

### 5.1.3. Effect of Solvent Type

The XRD patterns of the TP glasses prepared by using different solvents subsequently heat-treated at 600 °C for 1 h were shown in Figure 5.4. The glasses were prepared with the parameters described in Section 4.1.3 followed by heat-treatment at 600 °C for 1 h. MW of the solvents increases in the upward direction in the figure. All the glasses, except one, exhibited the XRD peaks belonging to the only anatase crystalline phase in the amorphous background. The glass prepared by using 2-butoxyethanol did not reveal any detectable XRD peaks and it was completely amorphous even after heat-treatment at 600 °C for 1 h. This might be attributed to the very high MW of 2-butoxyethanol as well as the low activity of the butoxy group.

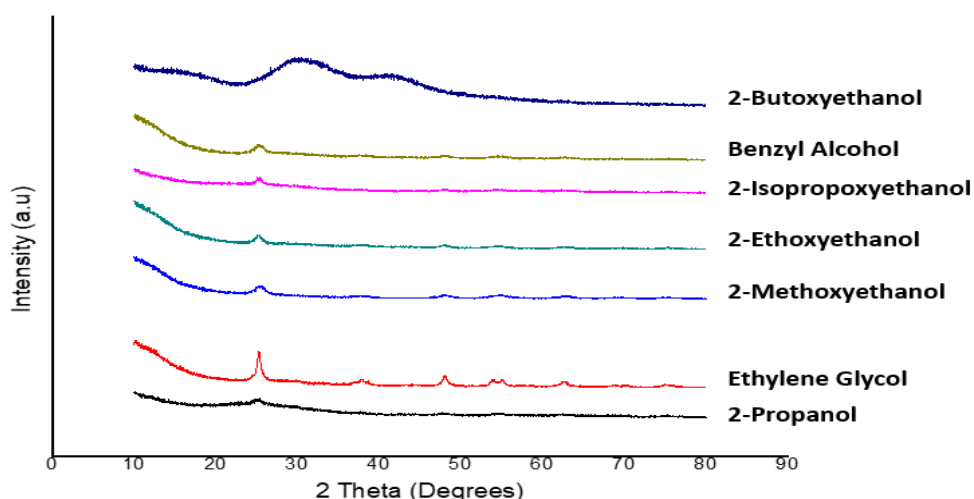


Figure 5.4. XRD patterns of the TP glasses prepared by using different solvents subsequently heat-treated at 600 °C for 1 h.

Examination of the XRD patterns did not suggest a correlation with the sample crystallinity and solvent MW or boiling point. Generally low carbon content solvents have higher crystallization ability [57]. It is also known that chemically high MW alcohols have lower solubility. The low solubility of TiO<sub>2</sub> in the solution hindered the crystallization ability thus, revealed lower intensity XRD peaks.

An assessment of the XRD patterns of the TP glasses prepared by using different solvents revealed that ethylene glycol significantly enhances the crystallization ability of the material and gives sharp, high intensity anatase peaks. It is known that by introducing nucleophilic reagents such as glycols and organic acids to alkoxides, hydrolysis rate can be significantly reduced [55]. The unique role of ethylene glycol as a nucleophilic reagent affected the crystallization process. By occupying the coordination sites and retarding hydrolysis rate, it allows TiO<sub>2</sub> ions to be more stable and dispersed homogeneously. Reagents have higher resistance to substitution of hydroxyl groups. Thus, hydrolysis rate decreases and precipitation process become more controllable. Controlling the hydrolysis and precipitation rates are important for obtaining sol-gel products with desired properties.

As a result, during the heat-treatment process more TiO<sub>2</sub> ions became mobile and reached the required activation energy for the phase transition and more atoms passing the activation energy favored the crystallization of the glass. Size of the anatase crystallites developed in the TP glasses produced by using different solvent types is given in Table 5.3. As stated previously, 2-butoxyethanol did not show any detectable crystalline peaks and was completely amorphous. Therefore, crystal size could not be measured. The highest intensity crystalline peaks and crystal sizes were obtained for the TP glasses produced by using ethylene glycol that easily coordinates to Ti<sup>+4</sup> ions and controls the hydrolysis reaction [64]. Ethylene glycol increased the number of atoms passing the energy barrier and triggered the crystallization process. As a result of high crystallization, crystallites merged and grew by size. The crystal growth ended up relatively higher crystal sizes for the glasses synthesized by using ethylene glycol.

Table 5.3. Size of the anatase crystallites developed in the TP glasses produced by using different solvents.

Solvent type	Crystal size (nm)
2-Butoxyethanol	-
Benzyl alcohol	11.5
2-Isopropoxyethanol	6.3
2-Ethoxyethanol	7.2
2-Methoxyethnaol	7.1
Ethylene glycol	14.6
2-Propanol	8.4

The XRD patterns of the TP glasses synthesized by using different solvents revealed that ethylene glycol and 2-methoxyethnaol are advantageous to produce the TP glasses with high anatase crystallinity. Therefore, the TP glasses prepared by using ethylene glycol and 2-methoxyethnaol were used for the determination of the self-cleaning properties.

#### 5.1.4. Effect of Solvent Content

The XRD patterns of the TP glasses prepared by using different solvent molarities subsequently heat-treated at 600 °C for 1 h were illustrated in Figure 5.5. Glasses were prepared with the parameters listed in Table 4.4 followed by heat-treatment at 600 °C for 1 h. The solvent used was 2-methoxyethnaol. All the glasses exhibited the peaks belonging to only anatase crystalline phase in the amorphous background.

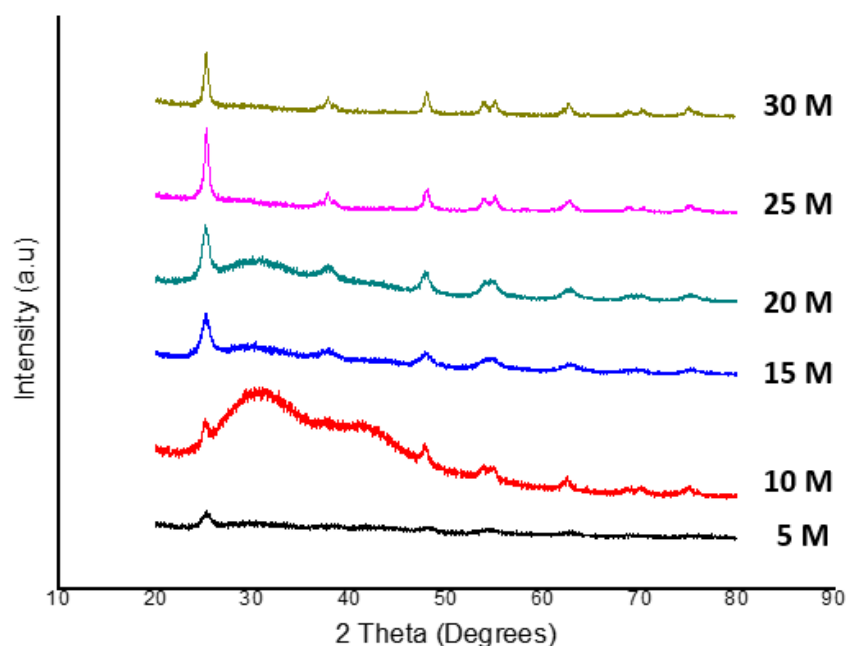


Figure 5.5. XRD patterns of the TP glasses prepared by using different solvent molarities subsequently heat-treated at 600 °C for 1 h.

The TP glasses prepared by using low solvent molar ratio such as 5 and 10 M, were mostly amorphous. Very low crystallinity was detected due to the low solubility of the solution. Probably the solubility of the solution was not high enough to dissolve Ti alkoxide efficiently. Increasing solvent molar ratio increased the crystallinity and maximum anatase peak intensity was obtained for the TP glass prepared by using 25 M ethylene glycol. At this solvent molarity, solubility of Ti ions improved and resulted linkages of more Ti-O-Ti bonds which provided better crystallinity. Further increase in the solvent molarity diminished this relationship.

Above solvent molarity of 25 M, Ti ions reached their solubility limit. At 30 M solvent molarity, decrease in the oxygen vacancies of the glass decreased the crystallization of TiO<sub>2</sub> [38]. Size of the anatase crystallites developed in the TP glasses produced by using different solvent molarities is given in Table 5.4.

Table 5.4. Size of the anatase crystallites developed in the TP glasses produced by using different solvent molarities.

Solvent molarity (M)	Crystal size (nm)
5	9.4
10	11.7
15	10.1
20	10.2
25	14.3
30	13.8

There was no apparent correlation between the solvent molarity and the crystal size for the TP glasses studied. Generally, high intensity sharp peaks correspond to high crystallinity and large crystal size. In fact, the largest crystal size was calculated for the TP glasses produced by using 25 M solvent molarity, which had the highest crystallinity.

Aggregation brought with enhanced crystallization also increased crystal size in diameter. More than 25 M solvent molarity caused a decrease in the crystal size because excess solvent molecules attached to the TiO<sub>2</sub> surfaces and hindered the nanoparticle growth [55]. Also, the increased evaporation rate at high solvent molarities might affect the crystal size.

#### **5.1.5. Effect of Water Content**

The XRD patterns of the TP glasses prepared by using different water content subsequently heat-treated at 600 °C for 1 h were illustrated in Figure 5.6. Glasses were prepared with the parameters listed in Table 4.5 followed by heat-treatment at 600 °C for 1 h. 2-methoxyethnaol was used as solvent. All the glasses exhibited the peaks belonging to only anatase crystalline phase in the amorphous background.



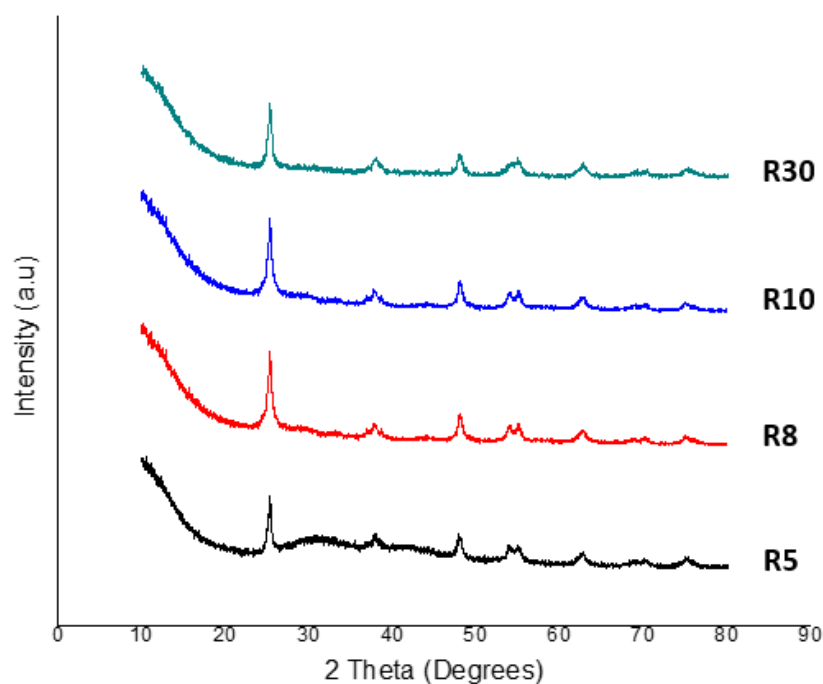


Figure 5.6. XRD patterns of the TP glasses prepared by using different water contents subsequently heat-treated at 600 °C for 1 h.

Water additions to the system decreased the solution viscosity and loosened the molecular structure. The lower viscosity allows better mobility of the atoms in the solution hence helps diffusion that favors crystallization rather than gelation. More mobile Ti atoms interacted and enhanced the formation rate of Ti-O-Ti bonds that favored the crystal growth process.

Presence of water generally accelerates the hydrolysis reactions and nucleation rates by protonating the negative charge to the alkoxide groups [65]. The higher atomic mobility finalizes with easier development of crystalline structure in the system by increasing nucleation rate [53]. Water addition also plays a role in crystallization by affecting the pH of the solution. The increase in water content lowers the pH of the solution by decreasing the  $H_3O^+$  and  $OH^-$  ions concentrations. A decrease in the pH of the solution causes the decrease in the crystal size of the anatase crystallites. Effect of solution pH on the crystallization and crystal size will be discussed in detail in Section 5.1.6.

Variation of size of the anatase crystallites developed in the TP glasses produced by using different R ratios ranging between 1 and 30 is shown in Figure 5.7. Initially an increasing trend in the anatase crystallite size was noted as the R ratio of the solution was increased. The crystal size reached to a maximum of 16.7 nm at 10 M water content. But, further increase in R decreased crystal size to 15.6 nm. Crystal growth due to the water addition is related to the mobility of Ti atoms in the solution.

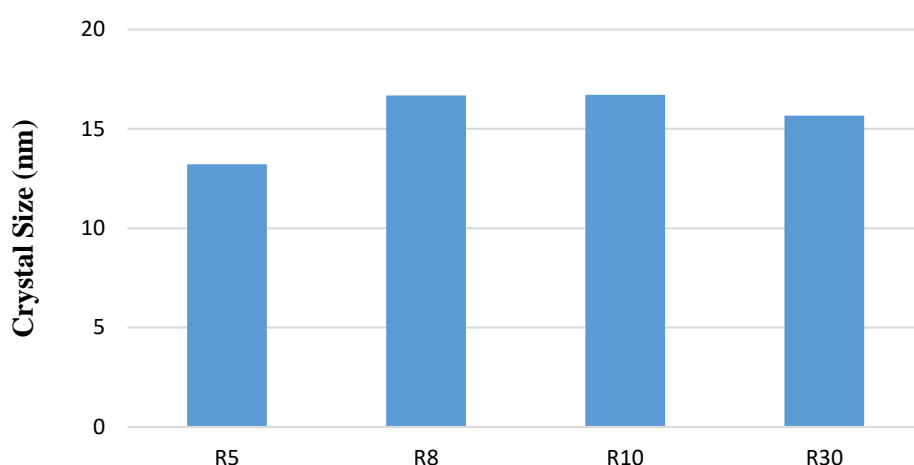


Figure 5.7. Size of anatase crystallinities developed in the TP glasses prepared by using different water/alkoxide ratios.

### 5.1.6. Effect of HCl Content

The XRD patterns of the TP glasses prepared by using different HCl molarities subsequently heat-treated at 600 °C for 1 h were illustrated in Figure 5.8. Glasses were prepared with the parameters listed in Table 4.6. The solvent used was 2-methoxyethanol. All the glasses exhibited the peaks belonging to only anatase crystalline phase in the amorphous background. Yanagisawa et al. [66] stated that chloride anion enhances only the nucleation of anatase under acidic conditions. Nonetheless, Sugimoto et al. [67] managed to produce samples having anatase and rutile phases even at room temperature by changing the solution pH.

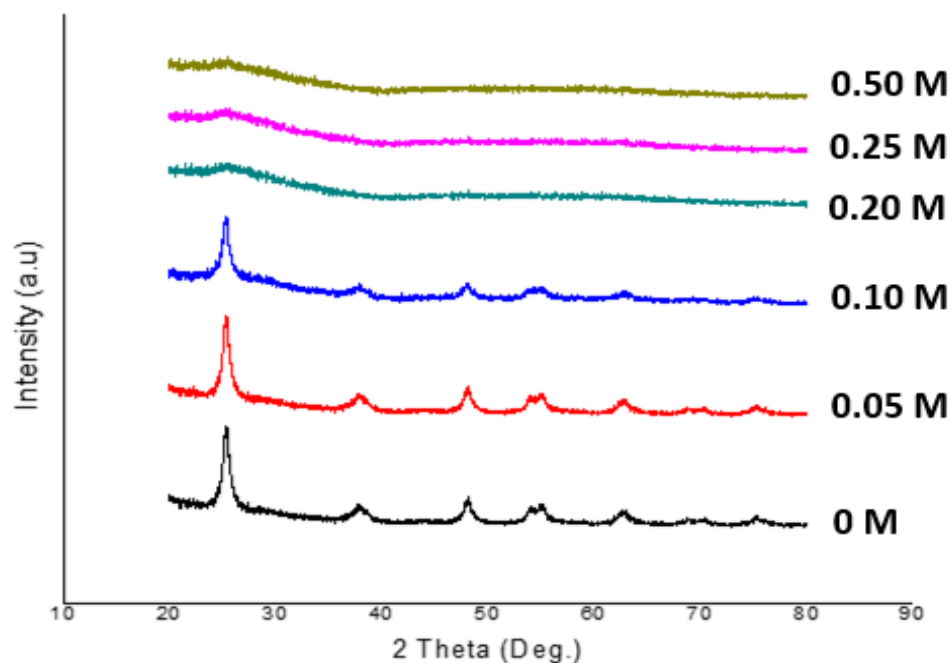


Figure 5.8. XRD patterns of the TP glasses prepared by using different HCl molarities subsequently heat-treated at 600 °C for 1 h.

Surprisingly, the TP glass prepared without HCl exhibited high anatase crystallinity. However, it should be noted that the pH of this glass was not neutral. In fact, the glass showed an acidic behavior with a pH of 4.06. Table 5.5 shows measured pH values of the TP glasses with respect to their the HCl molarities. When the HCl molarity of the solution was increased to 0.05 M, the best crystallization was obtained.

Small additions of HCl favored the anatase crystallization together with amorphous phase. Acid catalyst tend to increase hydrolysis rate and favor the crystallization [7]. As shown in Table 5.5, HCl additions decreased the pH of the solution. The increase in crystallinity with trivial decrease in pH was attributed to the hydroxide ions ( $\text{OH}^-$ ) and protons ( $\text{H}^+$ ) in the sol-gel process [15]. Further increase in the HCl molarity hence decrease in the pH of the solution lead to a gradual decrease in anatase peak intensities. Apparently, addition of HCl over 0.10 M was excess and resulted in the synthesis of completely amorphous structures.

Table 5.5. Solution pH and size of the anatase crystallites developed in the TP glasses produced by using different HCl molarities.

HCl molarity (M)	Solution pH	Crystallite size (nm)
0	4.1	12.3
0.05	3.1	12.1
0.10	2.4	10.1
0.20	1.9	-
0.25	1.8	-
0.50	1.4	-

It is obvious that solution pH did not have a major effect on the gelation behavior but, at high acidic environment it resulted in the formation of amorphous phase rather than crystalline TiO<sub>2</sub> even after heat-treatment at 600 °C. Chemically, sol-gel solutions exhibit low solubility at low pH. Therefore, in such high acidic environment, more TiO<sub>2</sub> precursor is needed to obtain the same dissolution rate. Since TiO<sub>2</sub> concentrations used in the solution was kept constant, Ti ions were not adequately dissolved in the solution and lost their crystallization ability.

Consequently, by affecting the hydrolysis and condensation rates, high acidic environment slowed down the nucleation rates and led to the formation of amorphous phase. The biggest crystal size of 12.3 nm was obtained for the TP glasses prepared without using HCl. By adding as small as 0.05 M HCl to the solution, crystal size decreased to 12.1 nm. The TP glasses prepared by using 0.10 M HCl possessed the smallest anatase crystallites with nominal size of 10.1 nm. High acidic conditions lead to the development of larger size crystallites compared to less acidic conditions due to the improvement of the mobility that allows the development of larger crystallites through agglomeration. However, in this study, an inverse relationship between the HCl molarity and crystal size was recognized. An explanation for the inverse relationship might be related to the isoelectric point of TiO<sub>2</sub>. It is known that TiO<sub>2</sub> has an isoelectric point between pH 5-6, and as the solution pH approaches this value, a growth tendency in crystal size occurs [49].

Since the TP glass prepared without using HCl has the closest pH value of 4.1 to the isoelectric point of TiO<sub>2</sub>, the crystallite with the largest crystal size was obtained. Another explanation related to the crystal size dependence on the acid concentration is that crystal size is mainly governed by the aggregation. In the presence of acid, aggregation process is inhibited thanks to the repulsion formed by adsorbed H<sup>+</sup> ions [54]. For these reasons, at highly acidic environment, crystal growth was prevented and the crystallites with lower size developed. Despite the high anatase crystallization, the TP glass prepared without using HCl was excluded from further investigations due to severe colorization and lack of transparency (foaming). The TP glasses prepared by using 0.05 HCl M were used for determination of the self-cleaning properties.

#### **5.1.7. Effect of Heat-treatment Design**

The effects of different heat-treatment designs including various heat-treatment temperatures and durations as well as different heating rates were studied to prepare the TP glasses with desirable characteristics. The influences of different heat-treatment designs on the crystallization were examined through XRD analysis and optimum preparation conditions were researched. The data was gathered for the TP gels containing 80 mol% TiO<sub>2</sub>. Solvent used was 2-methoxyethanol. Heat-treatment improves the crystallinity hence, photocatalytic activity of TiO<sub>2</sub>. Also heat-treatment causes TiO<sub>2</sub> phase transformations from amorphous to anatase and from anatase to rutile. Additionally, heat-treatment is also an important step for the removal of organics from the resultant product.

##### **5.1.7.1. Effect of Heat-treatment Temperature**

The most common way to improve the crystallinity is increasing heat-treatment temperature. Getting high degree of crystallinity at the lowest possible temperatures is desirable since crystallinity leads improvement in the surface properties of the resultant product. The XRD patterns of the as dried gel and the gels subsequently heat-treated at various temperatures were illustrated in Figure 5.9.

It was noted that the heat-treatment temperature had a profound effect on the crystalline phases developed in the TP glasses due to the kinetics of the sol-gel reactions taking place. The XRD analysis of the as dried gel indicated the characteristic features of the amorphous materials. Before the heat-treatment, no peak could be seen in the XRD pattern, suggesting that the as dried gel was amorphous. The heat-treated glasses indicated the XRD peaks belonging to the anatase and/or rutile phase depending on the heat-treatment temperature. No XRD peaks belonging to the brookite phase, another polymorph of  $\text{TiO}_2$ , or contaminations were detected up to 1000 °C. Similar results were reported by Hendrix et al. [37, 38].

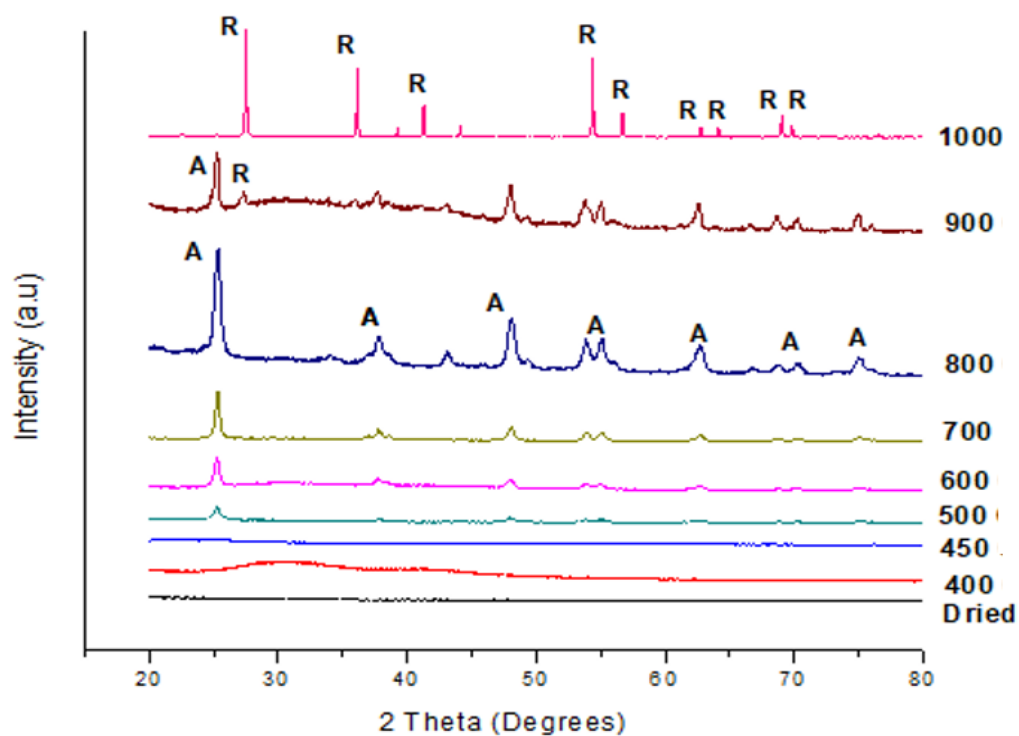


Figure 5.9. XRD patterns of the as dried gel and the gels subsequent heat-treated at various temperatures. A: Anatase, R: Rutile.

The TP glass heat-treated at 400 °C did not indicate any detectable diffraction peak. Apparently, heat-treatment temperature of 400 °C was insufficient for the initiation of  $\text{TiO}_2$  crystallization. Insufficient heat-treatment temperatures are not appropriate for the complete removal of alkoxy groups.

Remaining alkoxy groups act as structural impurities, avoid crystallization process, therefore generally amorphous products are obtained. It is apparent in Figure 5.9 that anatase formation from amorphous phase initiated when the heat-treatment temperature was increased to 450 °C. Barely noticeable, small diffraction peak detected in the TP glass heat-treated at this temperature was attributed to the crystallization of anatase phase. Development of anatase crystals suggest the amorphous to anatase transformation take place around 450 °C. Anatase formation was evident for the TP glasses heat-treated at temperatures up to 1000 °C. Though, their XRD peak intensities were different. Generally, high intensity and narrow peaks mean better crystallinity. At the temperature range of 450 to 700 °C, the intensity of anatase peaks became stronger.

The XRD analysis of the TP glasses heat-treated at the temperature range of 450 to 900 °C revealed that anatase crystallinity increases as heat-treatment temperature increases. This positive relationship might be related to the effective removal of the alkoxy groups. By affecting the condensation rate of OH groups on the TiO<sub>2</sub> surface, high heat-treatment temperatures facilitated the crystallization process. Also, at high heat-treatment temperatures, chemically bonded hydroxyl groups condensate with each other and result more bonds between Ti and O atoms, which enhance the crystallization ability through the re-arrangements of atoms [37].

Increasing trend of anatase crystallinity diminished when heat-treatment temperature was raised to 900 °C. Rutile phase was detected in the XRD patterns of the TP glasses heat-treated at temperatures of 900 and 1000 °C. The intensity of the XRD peaks belonging to anatase phase decreased but those belonging to the rutile phase increased as the heat-treatment temperature increased from 900 to 1000 °C, suggesting the irreversible phase transformation from thermodynamically metastable anatase phase to the most stable rutile phase [38]. The transformation from anatase to rutile occurs in a wide range of temperature from 600 to 1100 °C depending on the preparation conditions.

By modifying preparation conditions of TiO<sub>2</sub>, Qourzal et al. [68] reported amorphous to anatase transition temperatures below 400 °C, and anatase to rutile transition temperatures below 600 °C. As compared to the data presented in literature, much higher phase transition temperatures for TiO<sub>2</sub> were recognized in this study. The TP glasses prepared in this thesis work showed anatase crystallization at ~450 °C and rutile crystallization at ~900 °C. A possible reason is related to the remaining alkoxy groups which surrounded TiO<sub>2</sub> crystallites and delayed their crystallization ability through shielding effect. Another reason might be related to the presence of P<sub>2</sub>O<sub>5</sub> into the system. When P<sub>2</sub>O<sub>5</sub> takes a part in the structure, it enhances the thermal stability, acts as an anchor, and alters the temperatures where crystallization takes place.

More energy is needed for the formation of crystalline phases from amorphous TiO<sub>2</sub>, thus the temperature stability of the anatase phase is much higher [37]. When TiO<sub>2</sub> is chemically bonded to a substrate like P<sub>2</sub>O<sub>5</sub>, the substrate stabilized the different structures of TiO<sub>2</sub> and suppresses the transformation of amorphous TiO<sub>2</sub> to anatase and anatase to rutile by decreasing the mobility of TiO<sub>2</sub> atoms like an anchor [37, 69]. Such alteration especially in the rutile crystallization temperature indicates that high temperature stable anatase phase could be obtained through the introduction of P<sub>2</sub>O<sub>5</sub> to TiO<sub>2</sub>. Thus, higher temperatures are required for the evolution of anatase and rutile phases when P<sub>2</sub>O<sub>5</sub> is present. Anatase nucleates, as initial kinetic product, grows first in the TP glasses. Increasing the heat-treatment temperature induces phase transformation from anatase phase to rutile phase. Besides thermodynamics and kinetics, another possible explanation of this sequential transition might be related with the size of the crystallites hence surface area. Generally, phase transition temperature of smaller crystallites is substantially lower than bigger crystallites since small crystallites start fusing at relatively lower temperatures [70]. Higher surface area to volume ratio of anatase crystallites provides much higher surface energy compared to the rutile crystals. High surface energy necessitates much lower activation energy for the crystallization process, therefore anatase phase was the initial product and followed by the rutile phase [70].



The primarily formed TiO<sub>2</sub> crystallites usually contain large portion of defect sites, high temperature facilitates bond breaking as well as atoms rearrangement. Therefore, the phase transformation occurs easily. As an evidence, the TP glass prepared at heat-treatment temperature of 900 °C indicated small but easily detectable diffraction peak located at 2θ of 27.3° corresponding to the rutile phase. The increasing trend of anatase phase diminished around 900 °C due to the rutile crystallization. When the heat-treatment temperature was further increased to 1000 °C, anatase crystals have almost fully converted to rutile crystals. The calculations revealed that ~99% of the crystallites were rutile. Crystal size of the TP glasses heat-treated at various temperatures were calculated by using (101) and (110) plane diffraction peaks of anatase and rutile, respectively by means of the Scherrer equation. The variations in crystal sizes with the heat-treatment temperatures were shown in Figure 5.10.

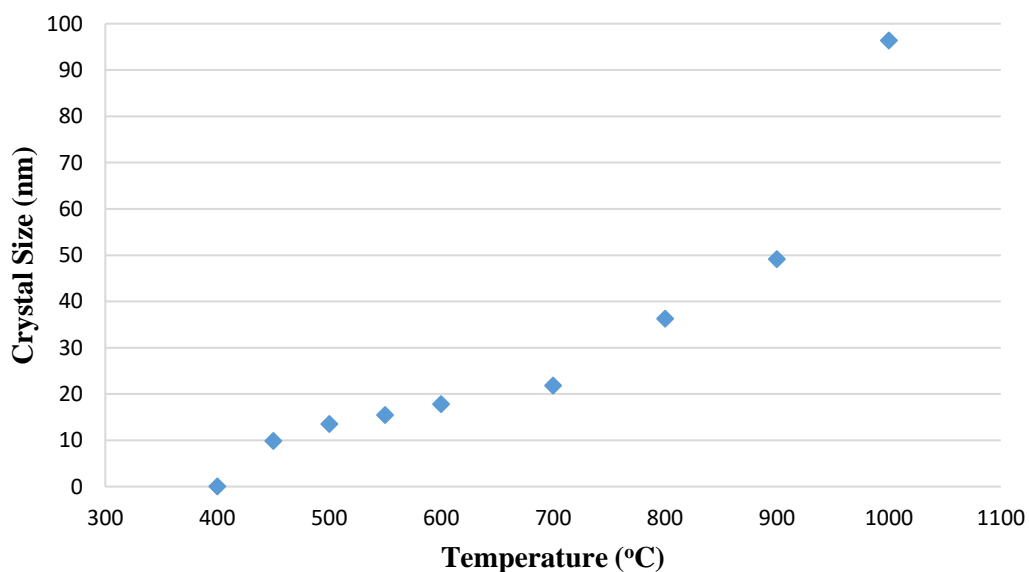


Figure 5.10. Calculated crystal sizes with respect to heat-treatment temperature.

As seen in Figure 5.10, the crystal size of the crystallites developed in the TP glasses was highly affected by the heat-treatment temperatures applied. It is obvious that the crystal size increases as the heat-treatment temperature increases.

Apparently, higher heat-treatment temperatures facilitated the development of bigger crystallites in the range from 400 to 1000 °C. The peak intensity of the samples became stronger and the width of diffraction peak was slightly narrower, indicating the formation of better crystallization with increasing heat-treatment temperatures. The nanoparticle growth process is highly related to heat and mass transfer. While amorphous grain boundary hinders the crystal growth, high temperatures improve the mass transfer rate and enlarge the size of the crystallites [71]. Therefore, the relationship between the temperature and the crystal growth was mainly based on the aggregation of TiO<sub>2</sub> crystals during heat-treatment.

The calculated crystal sizes of the anatase and rutile crystallites developed during heat-treatment of the TP glasses at various temperatures, heating rates, and durations were given in Table 5.6. The crystal size of the anatase crystallites developed during heat-treatment at various temperatures ranged between ~9 and 60 nm. This broad distribution of crystal size indicates that the amorphous to anatase transition was a solid-state crystal growth with slow nucleation rates [65]. Sizes of the crystallites in the TP glasses heat-treated at and below 700 °C were relatively small.

Above 700 °C, anatase crystallites grew faster and reached to 36.2 and 49.1 nm at 800 and 900 °C, respectively. Intense increase in the crystallite sizes was attributed to the thermally promoted crystal growth and the aggregation of TiO<sub>2</sub> grains. At the high temperatures, chemically bonded hydroxyl groups condensed with each other so that more bonds formed between the Ti and O atoms. Through rearrangements, the crystal structures slowly developed. Once a crystal was large enough to be stable, it further increased in size by taking up more TiO<sub>2</sub> atoms, either through more rearrangements, or by merging with other crystals. Despite this agglomeration behavior, anatase crystallite sizes up to 900 °C were still in the nano-range (<50 nm). The findings are in good agreement with those reported by Gorska et al. [72]. Increasing the heat-treatment temperature to 1000 °C led to development of very large rutile crystallites with a size of ~96.3 nm. Such drastic increase in the crystal size was due to the anatase to rutile transformation.

The crystal size of both anatase and rutile crystallites increased as heat-treatment temperature is increased because of aggregation of TiO<sub>2</sub> crystallites upon heat-treatment. Results suggest that at elevated temperatures, rutile crystals tend to grow more by size than anatase crystals.

Table 5.6. Crystal sizes of the anatase and rutile crystallites developed during heat-treatment of the TP glasses at different temperatures, heating rates, and durations.

Heat-treatment temperature (°C)	Heating rate (°C/min)		Heat-treatment time (h)	Crystallite size (nm)		Crystallinity fraction (%)	
	Stage 1	Stage 2		Anatase	Rutile	Anatase	Rutile
400	12	180	1	-	-	0	-
450	12	180	1	9.8	-	7.4	-
500	12	180	1	13.5	-	17.1	-
550	12	180	1	15.4	-	-	-
600	2	2	1	8.4	-	-	-
600	2	100	1	8.5	-	-	-
600	2	180	1	14.6	-	-	-
600	12	150	1	15.1	-	-	-
600	12	180	1	17.7	-	26.8	-
600	12	180	2	18.2	-	-	-
600	12	180	3	15.1	-	-	-
600	12	180	10	14.4	-	-	-
600	12	250	1	16.3	-	-	-
600	300	300	1	15.4	-	-	-
700	12	180	1	21.8	-	32.3	-
800	12	180	1	36.2	-	34.7	-
900*	12	180	1	49.1	65.4	23.5	7.1
1000*	12	180	1	60.7	96.3	1.1	98.9

\*Rutile development observed

Increasing the heat-treatment temperature to 1000 °C led to development of very large rutile crystallites with a size of ~96.3 nm. Such drastic increase in the crystal size was due to the anatase to rutile transformation. The crystal size of both anatase and rutile crystallites increased as heat-treatment temperature is increased because of aggregation of TiO<sub>2</sub> crystallites upon heat-treatment. Results suggest that at elevated temperatures, rutile crystals tend to grow more by size than anatase crystals.

The glasses containing rutile phase were excluded from the rest of the studies since the purpose of this study was to prepare the TP glasses containing small amount of fine anatase crystallites dispersed within the amorphous structure. The heat-treatment temperature of 600 °C was taken as the most appropriate heat-treatment temperature to achieve the purpose.

### 5.1.7.2. Effect of Heat-treatment Duration

Holding time at the maximum heat-treatment temperature is another major factor influencing the crystallization and phase transition of the TP glasses. By affecting the thermodynamics and kinetics, heat-treatment duration also affects the size and morphology of the TiO<sub>2</sub> crystallites developed. The XRD patterns of the TP glasses prepared by using different holding durations at 600 °C were shown in Figure 5.11. The glasses were prepared with the parameters listed in Table 4.1. The XRD analysis of the glasses heat-treated at 600 °C for various durations indicated the characteristic XRD peaks belonging to the anatase phase. Irrespective of the heat-treatment duration, anatase phase was evident in the XRD patterns of all glasses.

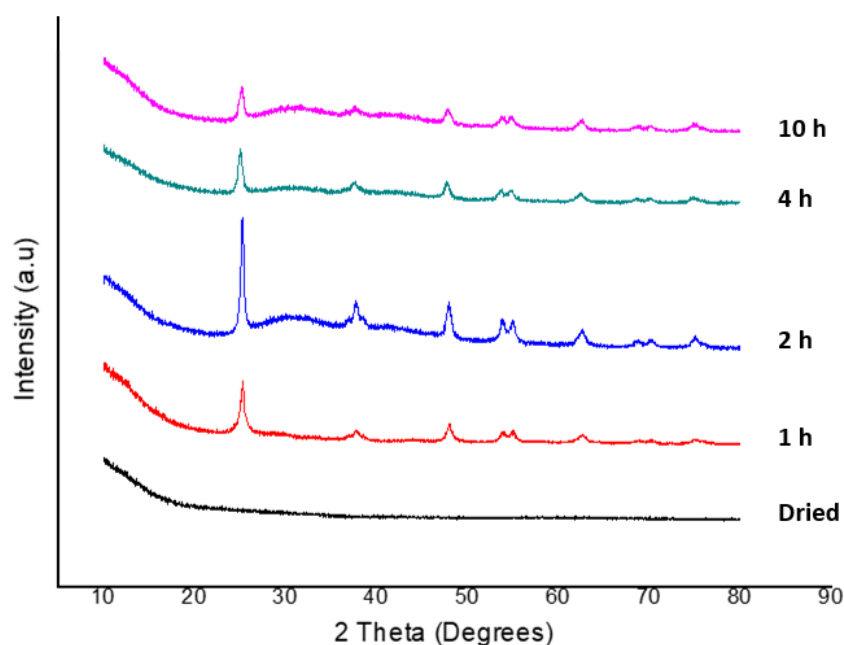


Figure 5.11. Calculated crystal sizes with respect to heat-treatment temperature.

The XRD analysis suggested that holding the dried TP gel 1 h at 600 °C provided an increase in the transmitted energy, increased the number of TiO<sub>2</sub> atoms passing the activation energy thereby triggered the anatase crystallization. It was anticipated that by increasing the heating durations at 600 °C, anatase crystallization is improved.

As shown in Figure 5.11, the intensities of the anatase peaks heightened and became stronger as the heat-treatment duration was increased from 1 to 2 h. The apparent rate constants increased with heat-treatment durations and reached to a maximum value for the glass heat-treated for 2 h at 600 °C. The application of holding durations more than 2 h at 600 °C, disrupted this positive relationship and resulted in a decrease in anatase peak intensities implying excessive heat-treatments rather deteriorate the anatase crystallization. Most likely, exposing high temperatures for longer durations led to a fairly high pressure over the structure. TiO<sub>2</sub> crystallites failed to withstand the exerted pressure, collapsed, lost their stability, and therefore their crystallization ability was disrupted. It was noted that, heat-treatment duration did not initiate the anatase to rutile phase transition of the TP glasses at 600 °C. This finding confirms that the main factor affecting the anatase to rutile phase transition is the heat-treatment temperature.

The calculated crystal sizes of the anatase crystallites developed during heat-treatment of the TP glasses at various durations ranged between ~14 and 19 nm as shown in Table 5.6. The calculated crystal size of the anatase crystallites developed during 1 h heat-treatment at 600 °C was 17.7 nm. The TP glass heat-treated for 2 h had slightly bigger crystals (18.2 nm) due to the particle aggregation followed by crystal growth. The crystal size did not show a significant variation when heat-treatment duration was increased beyond 2 h. In fact, further increase in the heat-treatment duration at 600 °C resulted in a slight decrease in the crystal size probably due to the exertion of a pressure to which TiO<sub>2</sub> crystallites could not withstand. As a result, structure collapsed, and crystallite size was adversely affected. 2 h heat-treatment duration at 600 °C was taken as the optimum heating time for obtaining the TP glasses.

### 5.1.7.3. Effect of Heat-treatment Schedule and Heating Rate

The heat-treatment schedule and heating rates applied are two of the other major factors influencing the crystallization and phase transition of the TP glasses since they affect the thermodynamics and kinetics of the phases developed. Heat-treatment schedule applied for the crystallization of the TP glasses consisted of two stages. Stage-1 was applied at temperatures between 25 and 280 °C whereas, Stage-2 was applied at temperatures between 280 and 600 °C. The first stage controls the phase(s) developed, during which primary crystallites develop. A slow reaction rate causes the development of rutile phase but, faster reaction rates promote the development of anatase phase. The second stage regulates morphology and size of the precipitates that are developed by the aggregation of primary crystallites. The XRD patterns of the TP glasses prepared by applying different heat-treatment schedules were shown in Figure 5.12. Glasses were prepared with the parameters listed in Table 4.1.

The XRD analysis of the glasses heat-treated at various heat-treatment schedules indicated the characteristic XRD peaks belonging to the anatase phase.

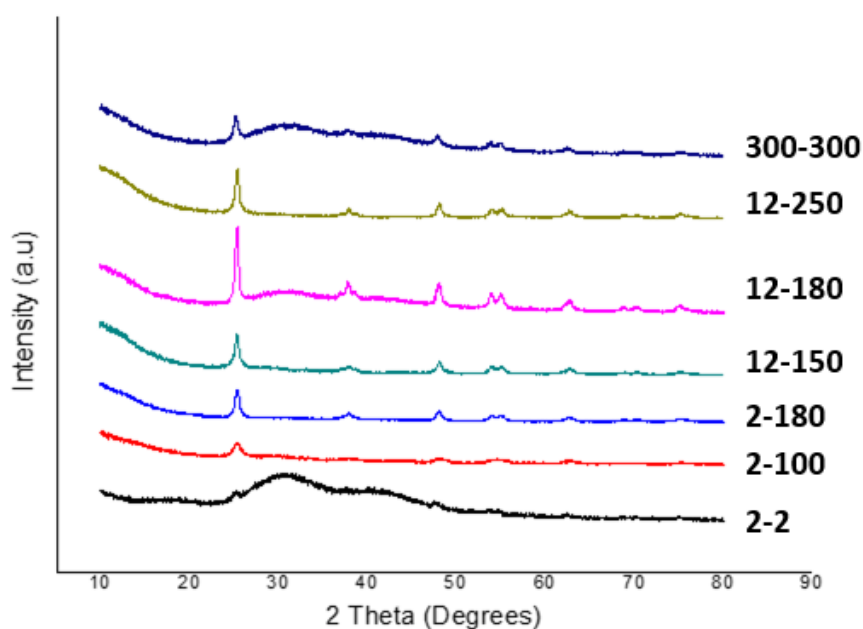


Figure 5.12. XRD patterns of the TP glasses prepared by applying different heat-treatment schedules.

The heating schedules were named with respect to the applied heating rates in both stages as X-Y; where X represents the heating rate in the first stage, Y represents the heating rate in the second stage. A slow schedule of 2-2 resulted in the development of very weak anatase peaks along with broad halo peaks which imply that the sample is composed of highly amorphous phase. It was apparent that the transferred energy was barely enough to overcome the amorphous to anatase transition activation energy. Slow heating rates can provide a relatively mild condition for the TiO<sub>2</sub> crystallization [20]. The intensities of the anatase peaks improved significantly when a schedule of 12-180, taken as the optimum schedule, was applied. Optimum heating rates facilitate the phase transition by increasing the mobility of atoms during the transformation.

With increasing heating rate, higher transmitted energy due to the faster reaction rate allowed TiO<sub>2</sub> crystallites to exceed the activation energy and promoted the anatase crystallization [25]. However, application of schedules with faster heating rates such as 12-250 and 300-300 deteriorated crystallization and weakened anatase crystal intensity. Amorphous to anatase transition is limited by the kinetics at very fast heating rates [20]. At such high heating rates, anatase crystallites did not find enough time to align themselves thus, their crystallization was hindered. When compared to very fast heating rates, at optimum schedule of 12-180, TiO<sub>2</sub> crystallites had longer time before reaching to 600 °C. The additional time provided the required energy to develop crystals as well as the sufficient time for crystals to align properly.

The calculated crystal size of the TP glasses heat-treated at different schedules, and heating rates were shown in Table 5.6. At the schedule of 2-2, glasses with low amount of crystallinity having crystal sizes below 10 nm were obtained due to the insufficient transmitted energy. The application of schedule 12-180 increased the mobility of TiO<sub>2</sub> atoms and through thermal growth crystallites reached to 17.8 nm in size. This was essentially attributed to the particle aggregation followed by the crystal growth [21].

Fast schedules of 12-260 and 300-300 resulted in lower crystal sizes of 16.4 and 15.5 nm, respectively. At such fast heat-treatment schedules, most probably the sufficient time to align the anatase crystals was not provided thus, the crystal growth process was diminished. Heating schedules of 12-180 at the maximum temperature of 600 °C for 2 h was taken as the optimum heat-treatment design for obtaining glasses with small amount of fine anatase crystallites dispersed within the amorphous structure.

The XRD studies revealed that it is possible to obtain the TP glasses with small amount of fine anatase crystallites dispersed within the amorphous structure by applying a regulated heat-treatment design to the TP gels. By tailoring parameters applied in the heat-treatment schedule anatase crystallization might be remarkably improved. Heat-treatment temperature is the most dominant factor and has more influence on the TiO<sub>2</sub> crystallites developed in the TP glasses.

## **5.2. Scanning Electron Microscope (SEM) and Energy Dispersive Spectroscopy (EDS) Analysis**

Effects of processing parameters and heat-treatment conditions on the shape, size, and morphology of the crystalline phases developed in the TP glasses were examined by SEM. The findings were taken into consideration to elucidate the growth process of anatase crystallites. In addition to morphological analysis, the TP glasses prepared by using various TiO<sub>2</sub> contents were subjected to elemental analysis by applying EDS.

### **5.2.1. Effect of TiO<sub>2</sub> Content**

The SEM images of the TP glasses prepared by various TiO<sub>2</sub> contents subsequently heat-treated at 600 °C for 1 h were illustrated in Figure 5.13.



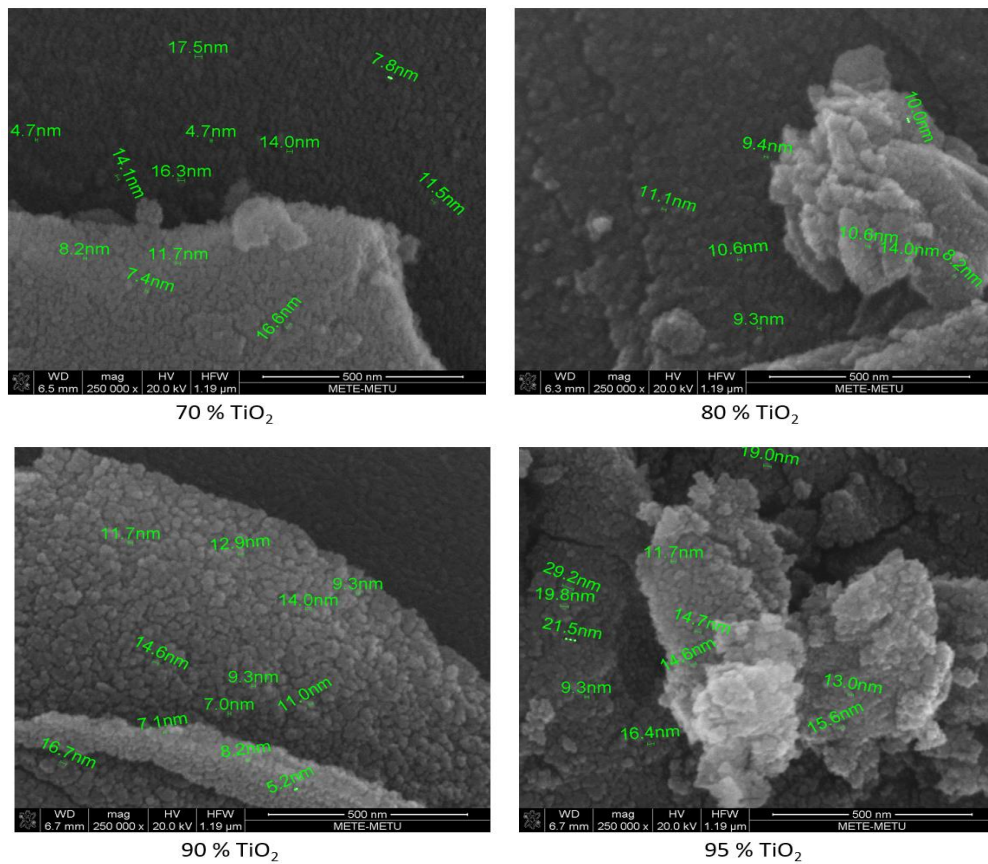
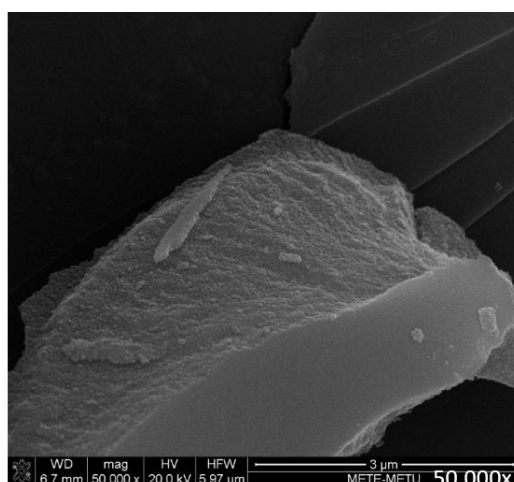
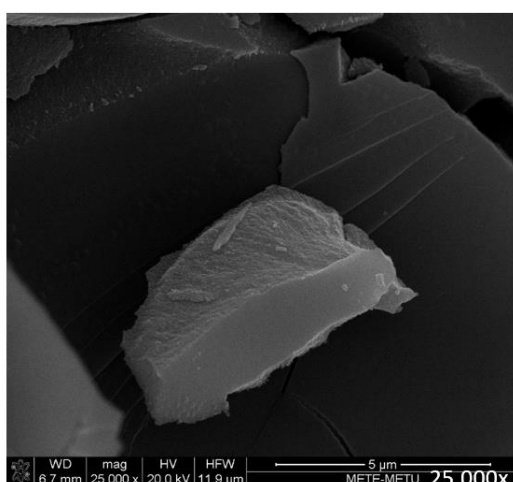
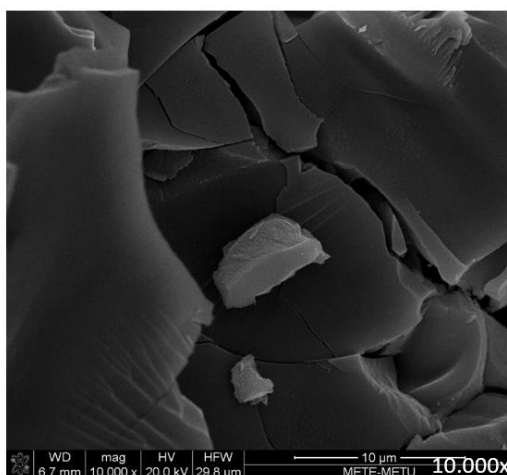
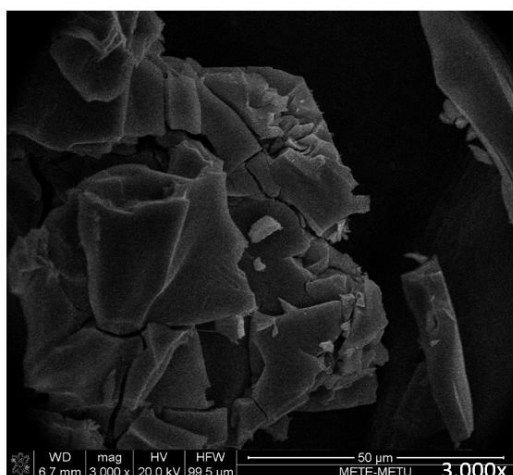


Figure 5.13. SEM images of the TP glasses prepared by various TiO<sub>2</sub> contents subsequently heat-treated at 600 °C for 1 h.

The SEM examinations revealed that the glasses prepared by using various TiO<sub>2</sub> contents have a mixture of amorphous and crystalline phases. The findings agree with the results obtained in the XRD studies. Irregular shaped glass pieces along with various sizes of randomly distributed crystallites in the range from 7 to 30 nm were observed in the SEM images. Crystal size measurements approved that the developed crystallites were in the nano-size. Representative morphology for the TP glass prepared by using 80 mol% TiO<sub>2</sub> is separately shown at different magnifications in Figure 5.14. The images taken at low magnifications revealed that the developed crystallites are highly agglomerated. Solvent evaporation during the heat-treatment stage was the main reason for the clustering of the crystallites [73].

When magnification was increased to 50.000, spherical shaped, sequential crystallites belonging to the anatase  $\text{TiO}_2$  were noticed. Further increasing the magnification up to 250.000 confirmed the anatase crystal development and morphology in detail. As seen in Figure 5.14, the morphology of the TP glasses was affected by  $\text{TiO}_2$  content. The crystallites grew bigger and agglomeration of the crystallites increased as  $\text{TiO}_2$  content increased. Probably, increasing number of Ti-O-Ti bonds with  $\text{TiO}_2$  additions improved the crystallization. High  $\text{TiO}_2$  content in the system favored the extension of Ti-O-Ti chains and resulted in 3D polymeric skeletons with tight packing. As a result of enhanced interaction, crystallites have merged, and the agglomeration process promoted crystal growth.



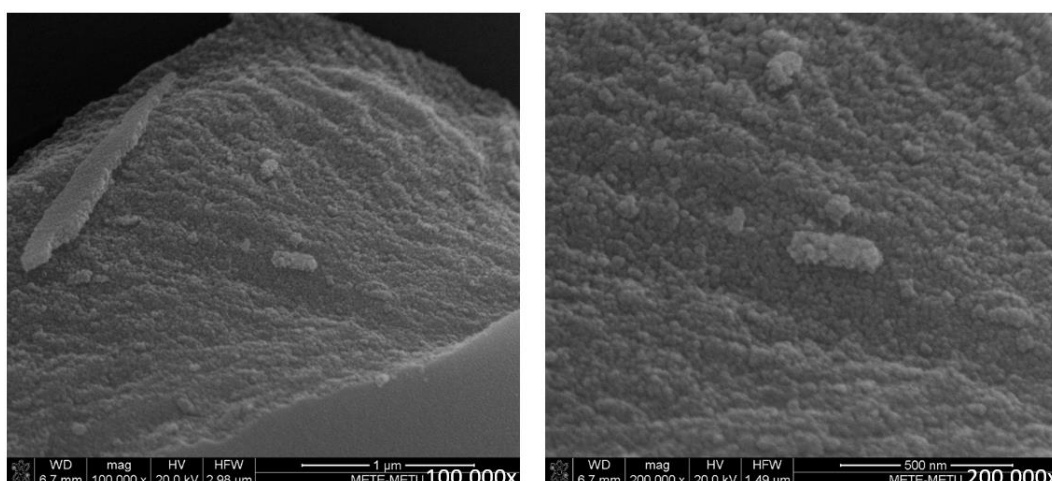


Figure 5.14. SEM images of the TP glasses prepared by using 80 mol% TiO<sub>2</sub> subsequently heat-treated at 600 °C for 1 h.

The EDS spectra of the TP glasses prepared by various TiO<sub>2</sub> contents subsequently heat-treated at 600 °C for 1 h were illustrated in Figure 5.15. Batch and analyzed compositions of the TP glasses prepared by various TiO<sub>2</sub> content were tabulated in Table 5.7. Both compositions in terms of the TiO<sub>2</sub> content were more or less the same. The highest deviation of 6% between the batch and analyzed compositions was calculated for the glass containing 80 mol% TiO<sub>2</sub>. This difference varied depending on which portion of the glass was analyzed as well as the amount of agglomeration since the crystals were not distributed in the structure uniformly.

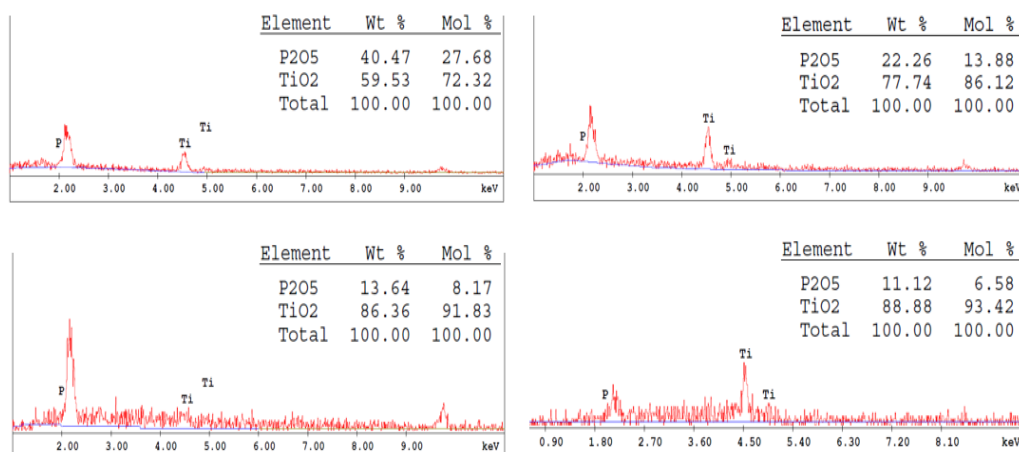


Figure 5.15. EDS spectra of the TP glasses prepared by various TiO<sub>2</sub> contents subsequently heat-treated at 600 °C for 1 h. a) 70 mol%, b) 80 mol%, c) 90 mol%, and d) 95 mol% TiO<sub>2</sub>.

Table 5.7. Batch and analyzed compositions of the TP glasses prepared by various TiO<sub>2</sub> contents.

TiO <sub>2</sub> content in batch (mol%)	TiO <sub>2</sub> content analyzed by EDS (mol%)
70	72.3
80	86.1
90	91.8
95	93.4

The analyzed composition of the TP glass containing 95 mol%, unlike other glasses, was lower than the intended batch composition probably due to the low reaction ability of the P<sub>2</sub>O<sub>5</sub> precursor. Relatively low reaction ability of TEP prevented all P<sub>2</sub>O<sub>5</sub> for entering the sol-gel reactions and participation the glass network. Some amount of TEP remained unreacted. Unreacted portion of TEP was removed by evaporation during the applied heat-treatment process and caused such difference between the batched and analyzed compositions. For the TP glasses containing very high TiO<sub>2</sub> content, such as 90 and 95 mol%, P<sub>2</sub>O<sub>5</sub> amount was not enough to form strong Ti-O-P bonds.

### 5.2.2. Effect of Solvent Type

The SEM images of the TP glasses prepared by using ethylene glycol and 2-methoxyethanol subsequently heat-treated at 600 °C for 1 h were shown in Figure 5.16. Both glasses possessed crystallites in the range from 5 to 50 nm. Examinations of the SEM images revealed an undeniable relation between the solvent type and morphology. The use of ethylene glycol as solvent resulted in the development of homogeneously dispersed nanocrystals as shown in Figure 5.16 (b). However, the use of 2-methoxyethanol as solvent resulted in the development of highly agglomerated nanocrystals as shown in Figure 5.16 (a). The agglomeration process might be influenced by the dielectric constant of the reaction medium. Low dielectric constant of 2-methoxyethanol (16.93 F/m) led to extensive agglomeration while high dielectric constant of ethylene glycol (37.7 F/m) resulted in less agglomeration. Similar results are obtained by Klomdee et al. [74].

In addition, as a nucleophilic reagent, ethylene glycol probably retarded the hydrolysis rate which allowed  $\text{TiO}_2$  to be more stable and favored their homogeneous dispersion. Ethylene glycol slowed down the hydrolysis and condensation reactions. Slow hydrolysis prevented the agglomeration of  $\text{TiO}_2$  crystallites.

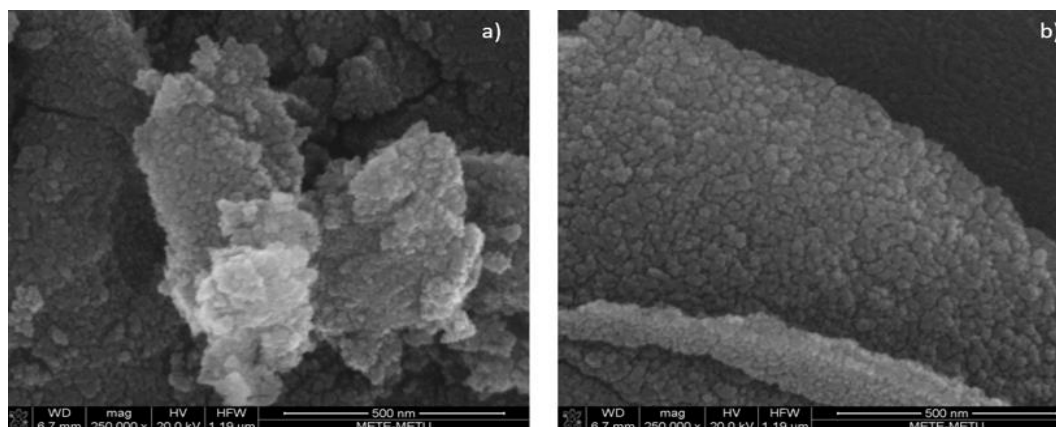


Figure 5.16. SEM images of the TP glasses prepared by using a) 2-methoxyethanol, b) Ethylene glycol. The glasses were subsequently heat-treated at 600 °C for 1 h.

### 5.2.3. Effect of Water Content

Figure 5.17 represents the SEM images of the TP glasses prepared by using R ratio of 8 and 10. The glass was subsequently heat-treated at 600 °C for 1 h and  $\text{TiO}_2$  content was 80 mol%. Samples having different R ratios revealed same surface morphologies.

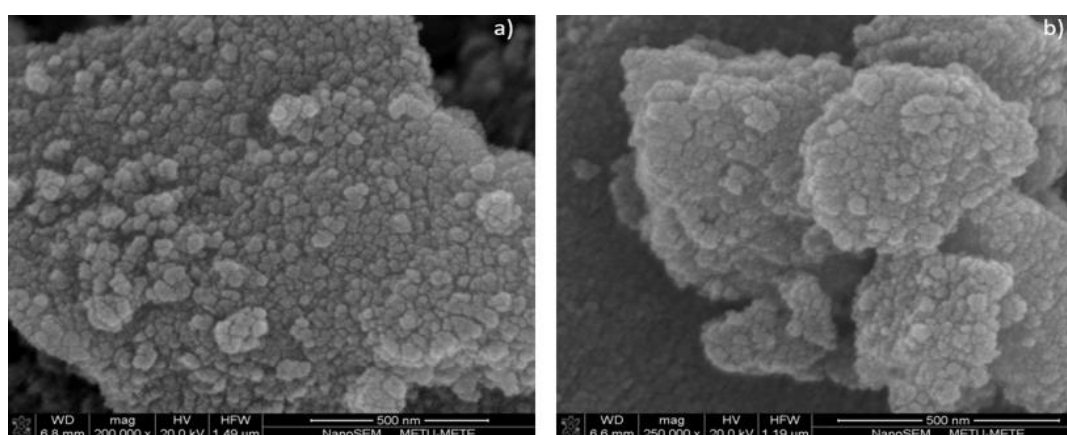


Figure 5.17. SEM images of the TP glass prepared by using different water content, subsequently heat-treated at 600 °C for 1 h.

Highly agglomerated surface morphologies were observed for all the TP glasses irrespective to their water content, implying the water content of the initial solution and 600 °C heat-treatment temperature did not have substantial effects in the morphology of the TP glasses. Size and shape of the agglomerates are totally irregular and random in distribution while individual crystallites were nearly spherical in shape. The water content of the initial solution did not play a significant role also in the size of the crystals developed. Morphological features of the TP glasses prepared by using different water contents agree with those reported by Mohammadi et al. [25].

#### 5.2.4. Effect of Heat-treatment Temperature

The SEM images of the TP glasses heat-treated at 500, 550, 600, 700, and 800 °C for 1 h were shown in Figure 5.18. TiO<sub>2</sub> content of the glasses was 80 mol%. SEM images of the TP glasses heat-treated at different temperatures revealed different surface morphologies implying that heat-treatment temperature affected the crystallization. Several researchers reported that heat-treatment temperature has an influence on the crystal growth and the shape of the crystallites developed [75].

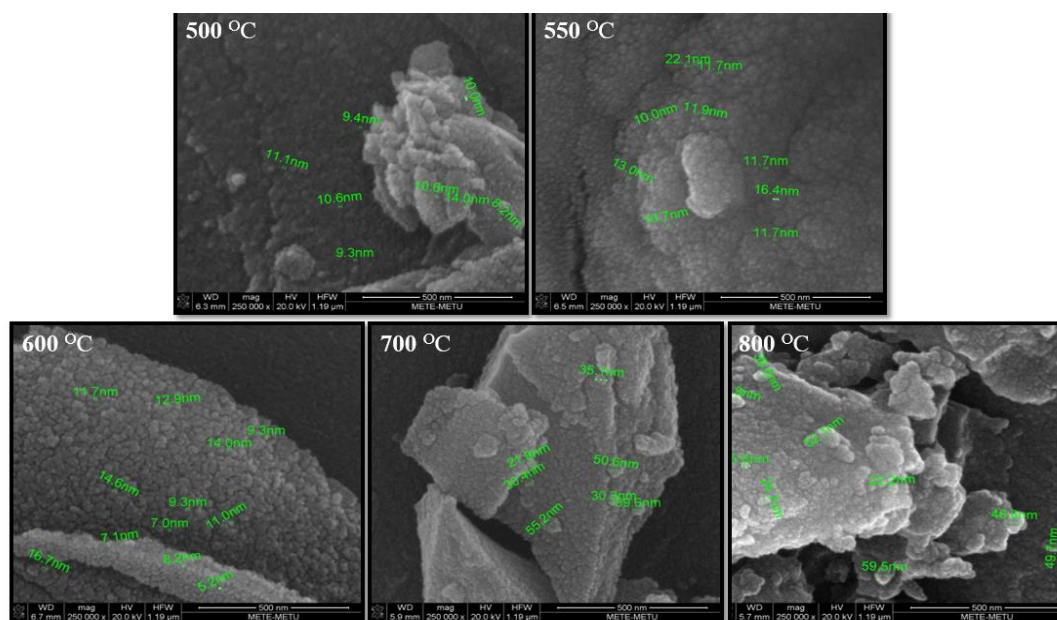


Figure 5.18. SEM images of the TP glasses heat-treated at temperatures of a) 500, b) 550, c) 600, d) 700, and e) 800 °C.

Crystal formation was evident for all the TP glasses heat-treated between 500 and 800 °C. Bigger particle size with spherical morphology was obtained as the heat-treatment temperature increased. As seen in Figure 5.18, the TP glasses had wide size distribution ranging from 5 to 70 nm. Broad size distribution suggests that the phase transition was a solid-state crystal growth with slow nucleation rates [65].

Average crystal sizes of 12, 14, 16, 38, and 50 nm were obtained for the TP glasses heat-treated at 500, 550, 600, 700, and 800 °C, respectively. Enhanced crystal growth rate at elevated temperatures were observed. At temperatures equal and less than 600 °C, nuclei growth was insignificant. The measured crystal sizes were almost the same as the calculated ones by using the Scherrer equation. However, at elevated temperatures a significant difference between the measured and calculated crystal sizes was noted. It was apparent that the calculated crystal sizes from XRD patterns were relatively larger.

In the Scherrer calculations, taking the largest peak into consideration instead of the average, and calculation of the primary crystallite size are probably the reasons for such difference. The largest crystal sizes measured in SEM images were ~70 nm. Development of large crystallites is attributed to the agglomeration of crystallites. The heat-treatment gives rise to the growth and agglomeration of the crystallites [75]. The agglomerated crystallites formed clusters. Due to severe agglomeration it was not possible to make a precise measurement through SEM images for the TP glasses heat-treated at higher temperatures. The strong increase in the crystal size for the TP glasses heat-treated above 800 °C was attributed to the development of rutile crystals.

#### **5.2.5. Effect of Heat-treatment Duration and Heating Rate**

The SEM images of the TP glasses heat-treated at 600 °C for different durations were shown in Figure 5.19. TiO<sub>2</sub> content of the glasses was 80 mol%. SEM images of the TP glasses heat-treated at different durations revealed different surface morphologies implying that heat-treatment temperature affected the crystallization.



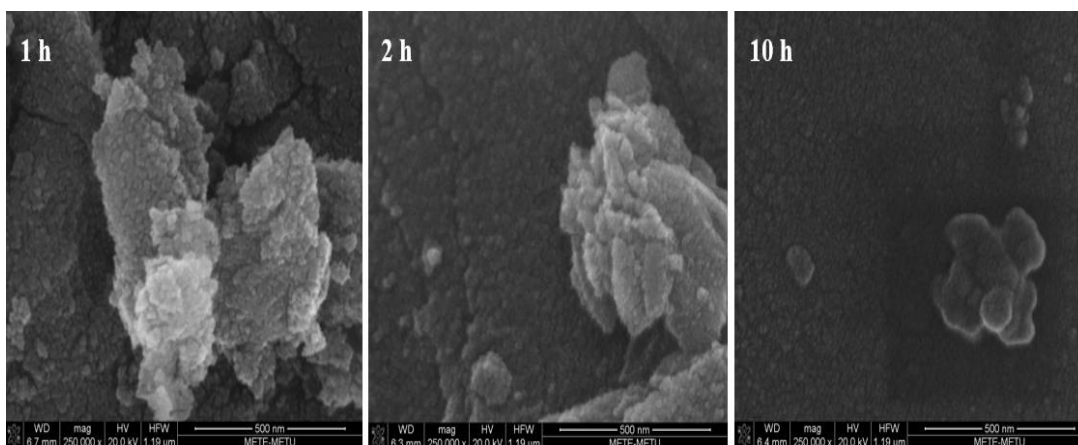


Figure 5.19. SEM images of the TP glasses heat-treated at 600 °C for different durations.

Increasing heat-treatment duration at 600 °C caused a decrease in the crystal size of the crystallites developed. Holding for a long time at high temperatures have created a pressure which crystals walls could not withstand and deteriorated the crystal growth by resulting a collapse formation. Slow heating rates allowed primary crystallites to align and subsequently aggregate to a larger size. For faster heating rates, the primary crystallites (of anatase) did not have sufficient time to align and formed featureless aggregates. Apparently, data obtained from the SEM analysis were consistent with that obtained from the XRD studies.

### 5.3. Brauner Emmett Teller (BET) Specific Surface Area (SSA) Analysis

SSA is one of the practical factors to evaluate the photocatalytic activity of materials. High SSA favors for the self-cleaning properties since the number of possible reaction sites per unit volume increases. SSA also plays an important role in the adsorption behavior of the material. It is related to the size of the crystallites. Smaller crystallites generally have higher SSA. By changing the synthesis parameters gel porosity could be tailored in sol-gel process. Thus, materials having high SSA could be synthesized. High porosity, high SSA materials might be very advantageous in production of membranes, sensors, coatings etc.



In this section, the TP glasses prepared were subjected to Brauner - Emmett - Teller (BET) multipoint SSA measurements to understand the effects of various preparation conditions (TiO<sub>2</sub> content, TiO<sub>2</sub> precursor type, solvent type, HCl content) and heat-treatment designs (heat-treatment temperature, heat-treatment duration, heating rate) on SSA. Pore size distribution and the pore volume were measured through nitrogen adsorption/desorption test by applying Barret-Joyner-Halende (BJH) method. Data were presented in Table 5.8. The SSA of a commercially available well known TiO<sub>2</sub> powder, Degussa P-25, was also measured for comparison purpose. Effects of each parameter on the SSA of the TP glasses were explained separately in the following subsections.

Table 5.8. Effect of preparation conditions and heat-treatment design on the SSA of the TP glasses prepared.

TiO <sub>2</sub> content (mol %)	TiO <sub>2</sub> precursor type	Heat-treatment temperature (°C)	Heat-treatment duration (h)	Heating rate (°C/min)	HCl molarity (mol %)	SSA (m <sup>2</sup> /g)	Agglomeration
Solvent: Ethylene Glycol							
80	TTIP	600	1	Fast	0.05	106.8	✗
80	TBOT	600	1	Fast	0.05	24.6	✗
80	TTIP	600	1	Fast	0	6.3	✗
80	TTIP	600	1	Slow	0.05	128.1	✗
80	TTIP	600	2	Slow	0.05	89.6	✗
80	TTIP	600	10	Slow	0.05	44.4	✗
80	TTIP	800	1	Slow	0.05	37.7	✓
95	TTIP	800	1	Slow	0.05	32.1	✓
Solvent: 2-Methoxyethanol							
80	TTIP	600	1	Fast	0.05	1.6	✗
80	TTIP	600	1	Slow	0.05	3.4	✗
P25	-	-	-	-	-	37.3	✗

✗: No, ✓: Yes

Most researchers have tried to enhance SSA of TiO<sub>2</sub> nanocrystallites by changing the heat-treatment regime. Present work also deals with the influence of most important synthesis parameters such as TiO<sub>2</sub> content, TiO<sub>2</sub> precursor type, solvent type, and pH on the SSA of the TP glasses. Such changes in the sol-gel synthesis parameters influence physico-chemical properties of nanosize TiO<sub>2</sub> crystallites and consequently affect the self-cleaning properties [76].

### **5.3.1. Effect of TiO<sub>2</sub> Content**

The TP glasses prepared by using 80 and 95 mol % TiO<sub>2</sub> had SSA of 37.7 and 32.1 m<sup>2</sup>/g, respectively. XRD and SEM studies revealed that TiO<sub>2</sub> content significantly affects the crystal growth and agglomeration process. The decrease in the SSA is attributed to the agglomeration of crystallites caused by an enhancement in the collision and coalescence of TiO<sub>2</sub> atoms [65].

### **5.3.2. Effect of TiO<sub>2</sub> Precursor Type**

The use of TBOT as TiO<sub>2</sub> precursor instead of TTIP resulted in a decrease in SSA from 106.8 to 24.6 m<sup>2</sup>/g. It is obvious that the use of high molecular weight TiO<sub>2</sub> precursor, TBOT, significantly decreased the SSA of the TP glass. Such significant influence of the TiO<sub>2</sub> precursor type on SSA was attributed to the differences in the size and structure of the primary building blocks formed during the synthesis [54]. Previously, Pal et al. [70] reported that when butoxide was used as alkoxy group, SSA of the material decreased noticeably.

The reason behind this might be related to the high carbon content of TBOT. In the presence of TBOT, more carbon remained in the product due to its high carbon content and caused a decrease in SSA and porosity of the glass. The considerably high remaining carbon group for the TP glass prepared by using TBOT was also observed previously in DTA-TG studies. The SSA of the TP glass prepared by using TTIP had more SSA than that of P25 powder. Therefore, the TP glasses prepared by using TTIP are promising and good candidate for self-cleaning applications.

### 5.3.3. Effect of Solvent Type

The TP glasses prepared by using ethylene glycol and 2-methoxyethanol had SSA of 128.1 and 3.4 m<sup>2</sup>/g, respectively. Positive influence of ethylene glycol on crystallization has already been discussed in XRD studies where it was noted that the best crystallinity was obtained for the TP glasses prepared by using this solvent. High amorphous content generally causes a relatively higher SSA. However, in this study the highest SSA was obtained for the glass having the highest crystallinity. This conflicting result may be related to the hydrolysis rate. Ethylene glycol easily coordinates to Ti<sup>+4</sup> ions and controls the hydrolysis reaction [64]. Hendrix et al. [37] suggest that textural properties of the sol-gel materials could be significantly improved by introducing a nucleophilic reagent into the system, such as ethylene glycol.

When large molecules were added into the sol-gel mixture and removed through heat-treatment, much higher porosities could be obtained [37]. Besides, as observed in SEM studies, presence of ethylene glycol resulted in development of homogeneously distributed crystallites without any aggregation. The use of a solvent with a high dielectric constant such as ethylene glycol, prevented agglomeration and increased SSA of the glass to 128.1 m<sup>2</sup>/g. On the other hand, glasses prepared by using a low dielectric constant solvent for instance 2-methoxyethanol promoted agglomeration and provided the lowest SSA of 3.4 m<sup>2</sup>/g.

### 5.3.4. Effect of HCl Content

The multipoint BET analysis of HCl-free glass measured SSA of 6.3 m<sup>2</sup>/g. Incorporation of as small as 0.05 M HCl to the solution increased SSA to 106.8 m<sup>2</sup>/g. Significant improvement in SSA was realized when HCl content was increased further. As discussed in Section 5.1.6, the XRD patterns of the TP glasses prepared by using different HCl molarities did not show notable difference in terms of crystallinity. Therefore, the discrepancy in SSA was mainly originated from the structural consolidation of the glass. Most probably presence of HCl provided additional voids and increased the porosity which led to improvement in SSA.

The amount of HCl might affect the formation of oligomers and polymers that have key role in the formation of meso-porous materials [42]. Conclusively, incorporation of small amount of HCl is essential for improving the SSA of the TP glasses.

### **5.3.5. Effect of Heat-treatment Temperature**

The SSA of the TP glasses decreased as the heat-treatment temperature increased as shown in Table 5.8. The SSA of the TP glass heat-treated at 600 °C was 128.1 m<sup>2</sup>/g. It is clear that heat-treatment temperature of 600 °C was satisfactory to get a TP glass with high SSA. The SSA decreased sharply to 37.7 m<sup>2</sup>/g when the heat-treatment temperature was raised to 800 °C. The remarkable decrease in the SSA with increasing heat-treatment temperature from 600 to 800 °C was attributed to the presence of more amorphous phase remained in the TP glass heat-treated at 600 °C.

Higher amorphous content and lower crystallinity resulted in higher SSA for the glasses heat-treated at lower temperatures. It is known that generally amorphous TiO<sub>2</sub> exhibits the highest SSA as compared to TiO<sub>2</sub> polymorphs [77]. As confirmed by the XRD studies, amorphous TiO<sub>2</sub> could transform to anatase or rutile depending on the heat-treatment temperature. These phase transformations accompany with the porous structure hence, changes in the SSA. Besides the phase composition, the SSA is largely affected by the crystal size as well as the bonding characteristics with increasing heat-treatment temperatures [77]. The SSA of the TP glass was in agreement with the crystal size calculations present in XRD and SEM studies. Since the crystal size of the TP glass heat-treated at 800 °C was much bigger than that heat-treated at 600 °C, lower SSA was expected. In fact, the SSA decreased by 71% when the heat-treatment temperature was increased from 600 to 800 °C. This finding implies that other factors played a noteworthy role in the SSA of the TP glass superimposed the effect of temperature. Agglomeration of crystallites might be among the main reasons for the increase in the SSA. The crystal size values reported previously suggest that the primary particle diameter increased by means of crystal growth and the enhanced agglomeration at higher heat-treatment temperatures.

With increase in the heat-treatment temperature probably the large pores diminished through crystal growth. Heat-treatment temperature also affected the pore characteristics namely; the pore size and pore volume. Pore volume curves for the TP glasses heat-treated at 600 and 800 °C were measured by BJH method and the results were plotted in Figures 5.20 (a) and (b), respectively.

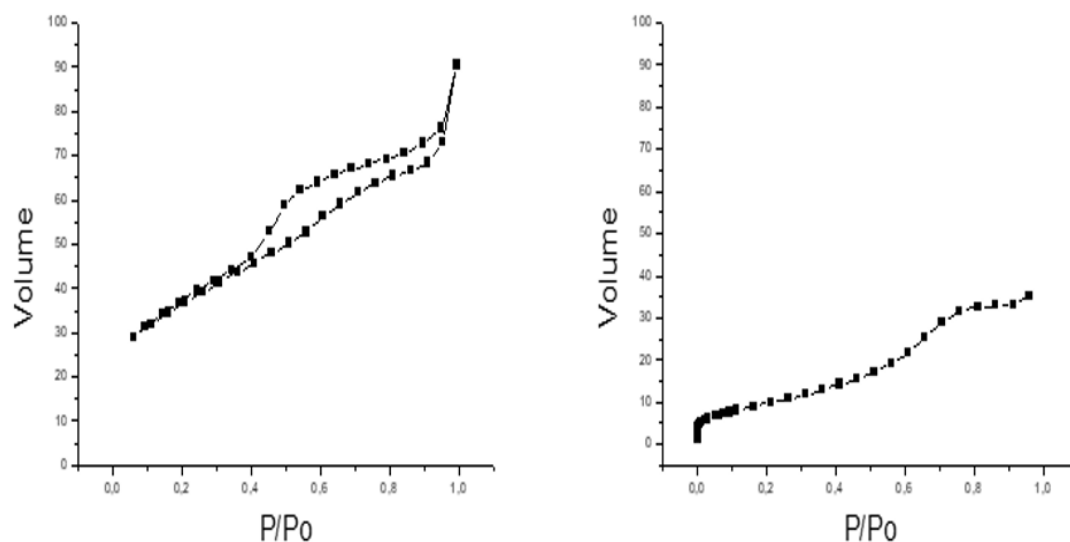


Figure 5.20. Pore volume of the TP glasses heat-treated at a) 600 °C and b) 800 °C.

Different heat-treatment temperatures resulted in changes in the relative pressure ( $P/P_0$ ) hence, influenced the pore volume as seen in Figure 5.20. The specific shapes ascribed as hysteresis isotherms evaluated and the unique characteristic of each shape provided information about the pore morphology of the glasses. Volume vs  $P/P_0$  curve of the TP glass heat-treated at 600 °C exhibited a unique shape. The hysteresis loop in Nitrogen adsorption-desorption isotherm is classified as Type-IV that is observed in a typical mesoporous material [64]. Generally, mesoporous materials have a pore diameter between 2 and 50 nm. Mesoporous structure facilitates the photodecomposition of the organic materials or undesired pollutants. Type-IV isotherm itself is divided into 4 types as H1, H2, H3, and H4. The hysteresis loop in Figure 5.20 (a) mostly resembles H4 hysteresis loop which is assigned for complex materials having both micro and mesopores together. As shown in Figure 5.20 (b), the hysteresis loop for the TP glass heat-treated at 800 °C was very different in shape.

The monolayer adsorption behavior of this glass fits well to the Type-I isotherm that is frequently encountered and generally corresponds for microporous materials having pore diameter less than 2 nm [54]. Relatively lower pore diameter obtained for the TP glass heat-treated at higher temperatures implies better sintering and densification of the product. In order to find out the pore size in the TP glass heat-treated at 600 °C, the sample was subjected to BJH measurement. The average pore size distribution curve was plotted and shown in Figure 5.21. The measurements revealed that the glass has a wide range of pore sizes mostly between 10 and 40 nm. This pore diameter range was consistent with the estimated diameters from the corresponding hysteresis loop isotherms.

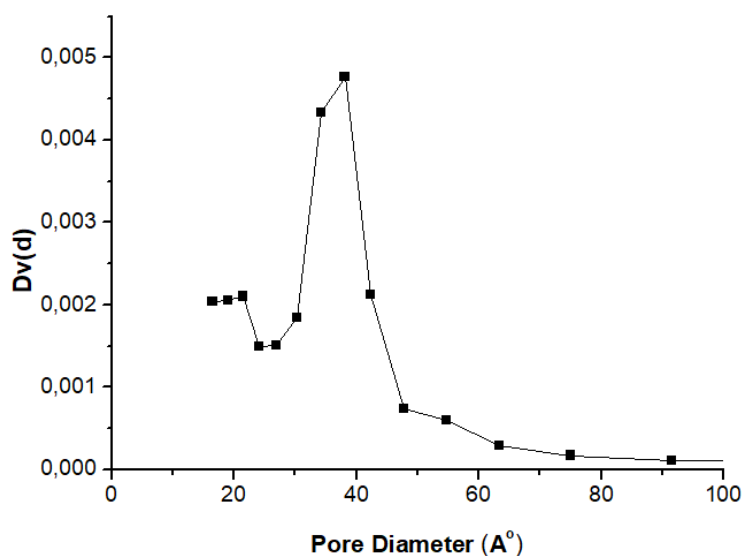


Figure 5.21. Pore size distribution of the TP glass heat-treated at 600 °C.

Relatively lower SSA ( $37.7 \text{ m}^2/\text{g}$ ) of the TP glass heat-treated at 800 °C than that for P25 powder ( $52 \text{ m}^2/\text{g}$ ) might be due to the crystal growth and severe agglomeration. The TP glass heat-treated at 600 °C exhibited 60% higher SSA than P25 powder. Superior SSA of this glass was linked to its tailored crystallinity and the presence of amorphous phase. Relatively lower size of crystallites present in this glass was the main reason for the higher SSA. Additionally, from the particle size analysis, volume weight mean size distribution of TP glass was 137 nm.

Such increase in the SSA is desirable in self-cleaning applications since high photocatalytic activity is favored by a large surface for absorbing larger amount of substrates. High SSA enhances the active surface sites and the surface charge carrier rate [27]. By enhancing interaction ability, it makes photocatalyst more accessible to the adsorbate organic molecules. Adsorption ability of the material plays a crucial role in the photocatalysis by increasing the available active reaction sites per unit volume.

### **5.3.6. Effect of Heat-treatment Duration**

As shown in Table 5.8, the SSA of the TP glasses decreased from 89.6 to 44.4 m<sup>2</sup>/g when the heat-treatment duration increased from 1 to 10 h at 600 °C. This indicates that a decrease in SSA with heat-treatment duration is mainly due to the growth of the size of TiO<sub>2</sub> crystallites. The SSA of the TiO<sub>2</sub> crystallites decreases with both heat-treatment time and heating rate. These results indicate that a decrease in the SSA is mainly due to the collapse of pores in TiO<sub>2</sub> powders. The collapse is caused by the transformation of amorphous TiO<sub>2</sub> to anatase. Slow heating rates can provide a relatively mild condition for phase transformation. Increasing heat-treatment duration from 1 to 10 h finalized with a gradual decrease in the SSA of material from 106.8 to 83.5 m<sup>2</sup>/g.

The findings of the current study did not support the results of the previous investigation reported in literature. In the previous studies, a decrease in the crystal size resulted an increase in the SSA of the material however in this work an inverse relationship was obtained. It seem that decrease in the crystal size did not influence the SSA of the material. This result may be explained by the fact that agglomeration behavior was not observed for both samples, and in fact the crystal size changes were not so much. Another explanation may be related with the pore structure. Exposing additional 9 h has deteriorated pore strenght and as a result, pore walls collapsed. This collapse formation hindered the porosity of the product and resulted in a lower SSA.

### 5.3.7. Effect of Heating Rate

As shown in Table 5.8 the SSA of the TP glasses exposed to slow heating rate is higher than that exposed to fast heating rate. The SSA of the TP glasses exposed to fast and slow heating rates were 106.8 and 128.1 m<sup>2</sup>/g, respectively. A 16.6% decrease in the SSA of the fast-heat-treated glass was attributed to the crystal growth. For this glass, relatively mild phase transformation was observed.

Faster heating rates facilitated amorphous to anatase transformation ability and enhanced crystallinity, which affected SSA of the material adversely. At slow heating rates, the phase transformation process from amorphous to anatase had longer time before TiO<sub>2</sub> crystallites reached the predetermined heat-treatment temperature. Thus, more amorphous phase transformed to anatase crystallites. Whereas at the fast heating rates, the transformation was limited by the kinetics. At the slower heating rates, when TiO<sub>2</sub> crystallites reached the heat-treatment temperature, they had comparatively more stable walls of pore because of the extra transformation.

The more stable pore walls can bear relative higher pressures without deformation and collapse. Thus, more pores could remain at the heat-treatments with slower heating rates and TiO<sub>2</sub> crystallites had higher SSA. In addition, through careful evaporation of the organics at slow heating rates the structural damage and crack formation was prevented, thus sample having more stable and strong pore walls were obtained. Since the collapse and pore deformation was avoided, more pore remained in the structure and as a result SSA of the material increased. When a comparison is made among various synthesis and heat-treatment conditions on SSA, it could be concluded that heat-treatment design is the most governing factor and it has more influence on the SSA of the TP glasses than any other factor.



## CHAPTER 6

### RESULTS AND DISCUSSION OF PROPERTY MEASUREMENTS

#### 6.1. Photocatalytic Activity Measurements

It is commonly accepted that significant differences in photocatalytic performance of the TiO<sub>2</sub> crystallites having the same crystal phase could be found, which indicates that there are several factors affecting the photocatalytic activity of the TiO<sub>2</sub> beyond the type of the crystalline phase. In this section, the influence of the most important process parameters namely; pH, water content, solvent type, and the heat-treatment design parameters such as temperature, time, and heating rate on the photocatalytic activity of the TP glasses were determined.

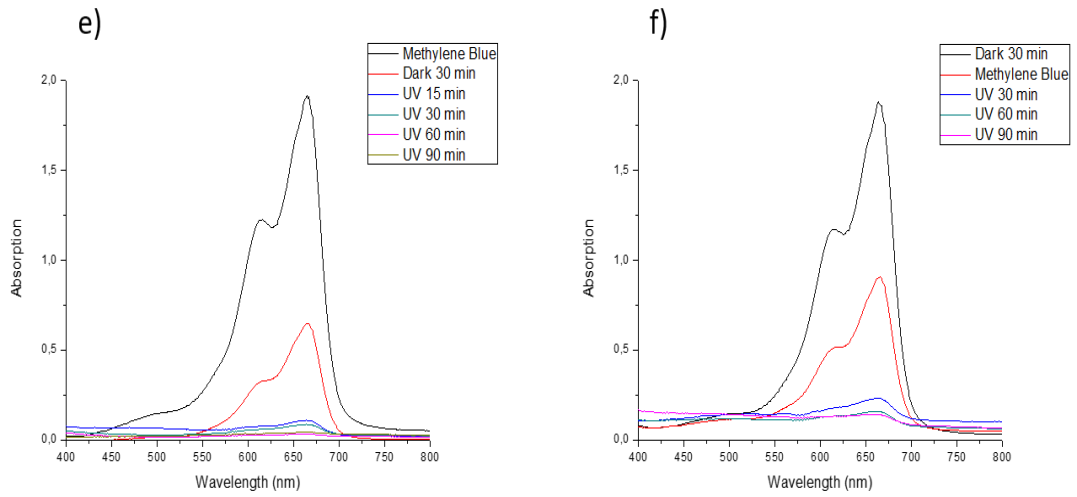
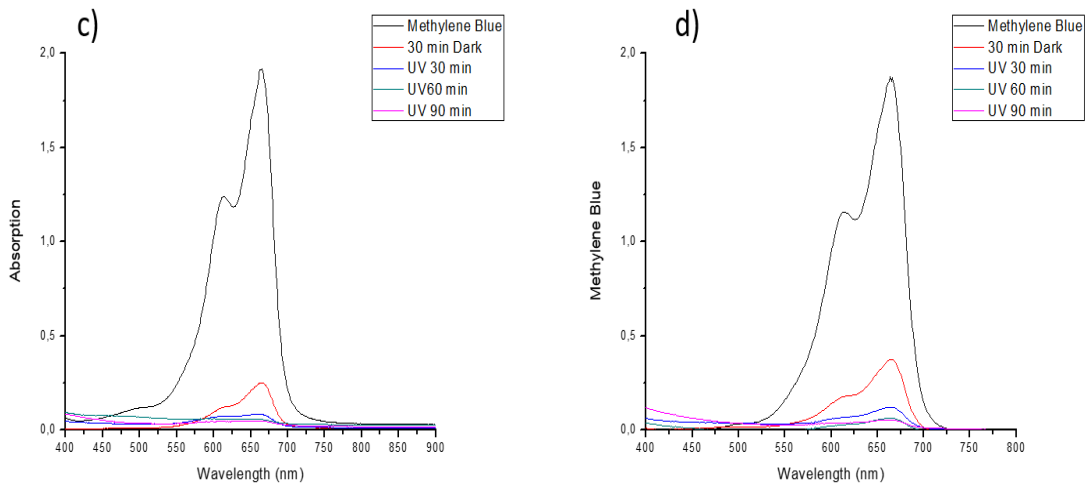
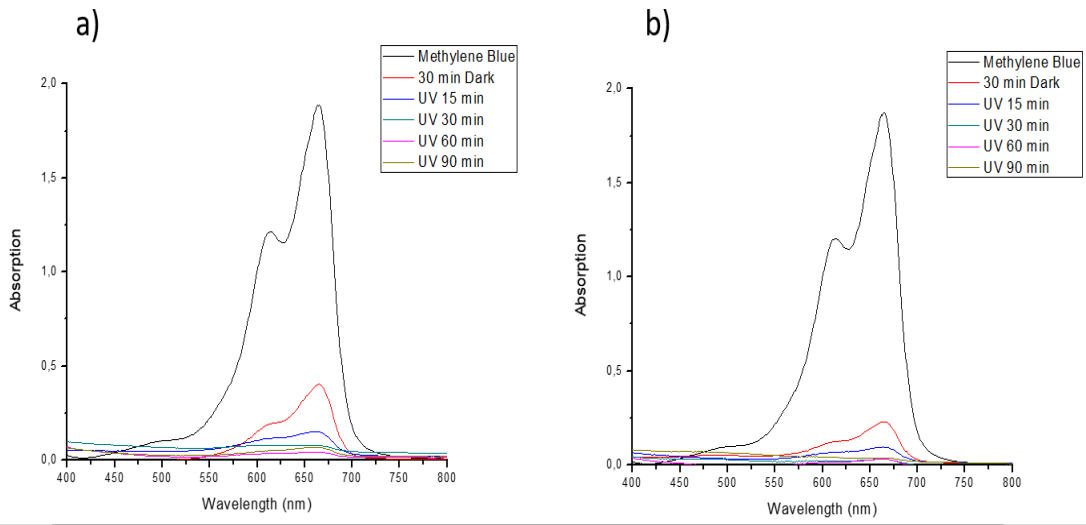
The TP glass containing mainly anatase crystallites with large surface area, high crystallinity, and small crystal size were the primary interest since anatase shows higher photocatalytic activity than the other polymorphs of TiO<sub>2</sub> [33]. The photocatalytic activity of TiO<sub>2</sub> depends strongly on crystallinity, crystal phase, crystal size, TiO<sub>2</sub> and Ti<sup>+4</sup> contents, SSA, morphology as well as measurement conditions such as light intensity, catalyst amount, and distance between the UV source and catalyst etc. [79]. Anpo et al. [36] reported that photocatalytic activity increases with decreasing anatase crystal size in the range of 4-50 nm. They concluded that with a decrease in the particle size of anatase TiO<sub>2</sub> photocatalytic activity increases, especially when the anatase size is less than 10 nm. Photocatalytic performance of the glasses was measured with respect to the degradation properties of aqueous methylene blue (MB) solution under UV illumination as described in Section 3.5.1.

The MB degradation values of the TP glasses prepared by using different heat-treatment temperatures, durations, heating rates, TiO<sub>2</sub> contents and solvent types after 30, 60, and 90 min UV light illumination were summarized in Table 6.1.

Table 6.1. MB degradation values of the selected TP glasses after 90 min UV light illumination.

TiO <sub>2</sub> content (mol%)	Solvent type	Temperature (°C)	Time (h)	Heating rate (°C/min)	Water molarity	Solvent molarity	HCl molarity (mol%)	SSA (m <sup>2</sup> /g)	Photo catalytic activity (%)
70	E.G*	600	1	12-180	8	25	0.05	-	87.3
80	E.G	400	1	12-180	8	25	0.05	163.4	45.4
80	E.G	450	1	12-180	8	25	0.05	121.6	63.3
80	E.G	500	1	12-180	8	25	0.05	91.5	83.2
80	E.G	550	1	12-180	8	25	0.05	87.3	88.1
80	E.G	600	1	12-180	8	5	0.05	-	90.4
80	E.G	600	1	12-180	8	10	0.05	-	79.2
80	E.G	600	1	12-180	8	15	0.05	-	84.8
80	E.G	600	1	12-180	8	20	0.05	-	91.7
80	E.G	600	1	12-180	8	25	0.05	73.7	92.2
90	E.G	600	1	12-180	8	25	0.05	-	93.3
90	E.G	600	2	12-180	8	25	0.05	-	96.1
95	E.G	600	1	12-180	8	25	0.05	-	92.9
80	E.G	600	1	12-180	8	30	0.05	-	87.4
80	E.G	600	1	12-180	10	25	0.05	-	90.5
80	E.G	600	1	12-180	8	25	0	-	81.0
80	E.G	600	1	12-180	8	25	0.10	-	36.0
80	E.G	600	1	2-150	8	25	0.05	-	79.5
80	E.G	600	1	12-150	8	25	0.05	-	82.4
80	E.G	600	1	12-250	8	25	0.05	-	85.7
80	E.G	600	2	12-180	8	25	0.05	-	94.3
80	E.G	600	3	12-180	8	25	0.05	-	89.1
80	E.G	600	10	12-180	8	25	0.05	-	81.2
80	E.G	700	1	12-180	8	25	0.05	51.7	89.8
80	E.G	800	1	12-180	8	25	0.05	44.8	82.7
80	E.G	900	1	12-180	8	25	0.05	-	79.4
80	E.G	1000	1	12-180	8	25	0.05	-	72.3
80	2-M**	600	2	12-180	8	25	0.05	-	51.0
P-25	-	-	-	--	-	-	-	39.1	97.0

\*E.G: Ethylene glycol, \*\*2-M: 2-methoxyethanol



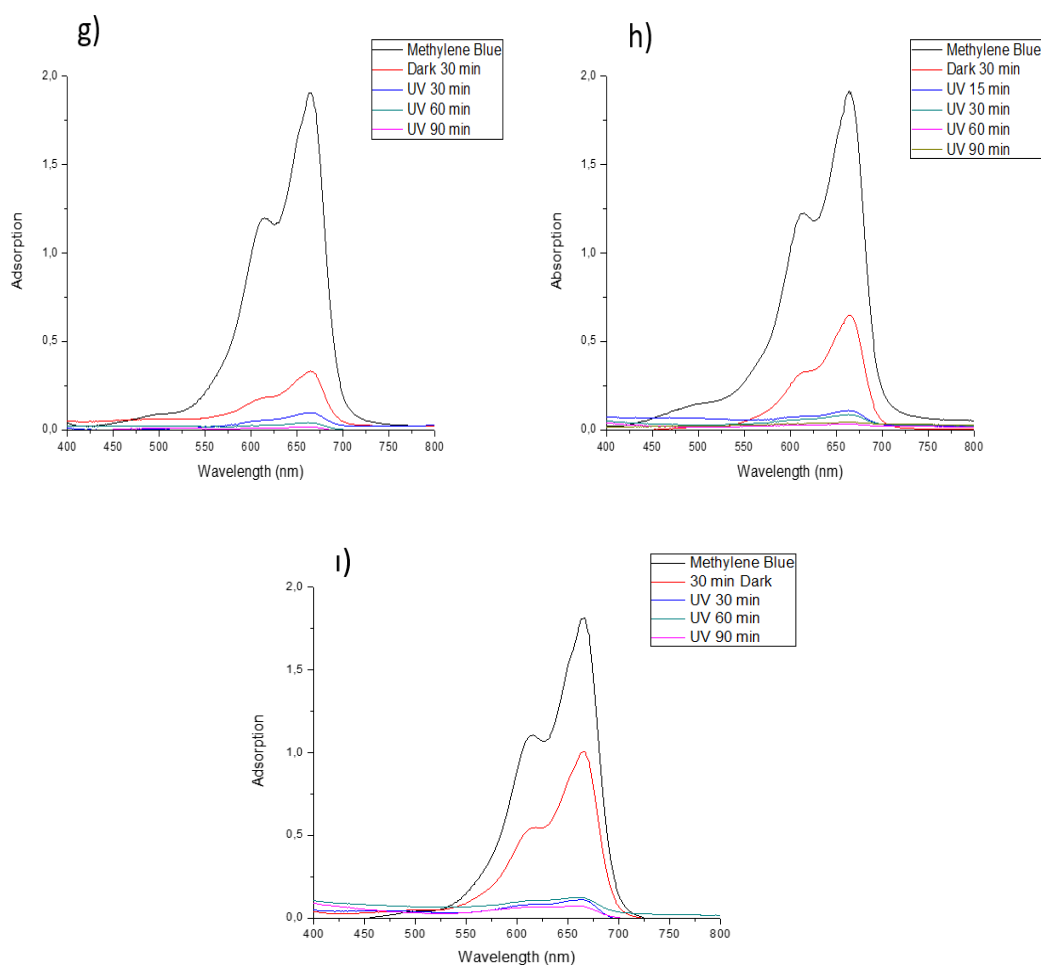


Figure 6.1. MB absorbance spectra of the selected TP glasses a) EG70-601, b) EG80-601, c) EG90-601, d) EG95-601, e) EG80-602, f) 2M80-600, g) EG80-603, h) EG80-610, and i) P25 powder.

Before UV illumination, the glasses were kept 30 min in dark in MB solution. The decrease in MB concentration in dark is not a photocatalytic process [1]. High adsorption ability of the glasses was attributed to their high SSA and high ion exchange abilities. For all TP glasses, increasing UV illumination time resulted in higher MB degradation rates. This observation in MB degradation is an indication of the first order kinetics of glasses. Upon exposure of the TP glasses to UV light, hydroxyl radicals continuously decomposed MB molecules until all MB molecules completely degraded. MB absorbance spectra of the selected TP glasses are shown in Figure 6.1.

### 6.1.1. Effect of TiO<sub>2</sub> Content

The values for the MB degradation after 90 min UV illumination for the TP glasses prepared by various TiO<sub>2</sub> content subsequently heat-treated at 600 °C for 1 h were tabulated in Table 6.1. The variation of MB degradation after 90 min UV illumination for the TP glass prepared with different TiO<sub>2</sub> contents was shown in Figure 6.2. As seen in Figure 6.2 and Table 6.1, the lowest MB degradation of 87.3% was calculated for the TP glass prepared by using 70 mol% TiO<sub>2</sub>. MB degradation increased initially as the TiO<sub>2</sub> content increased.

The TP glasses prepared by using 80 and 90 mol% TiO<sub>2</sub> degraded 82.2 and 96.1% MB, respectively. Increasing the TiO<sub>2</sub> concentration of the glass eventually improved the photocatalytic MB degradation since the amount of the photocatalyst source in the glass is increased. When TiO<sub>2</sub> content of the glass increased to 95 mol%, a decrease in MB degradation was realized. The MB degradation for this glass was 92.9%. The decrease in degradation might be due to the reaction limitations of TiO<sub>2</sub> above 90 mol% concentration. The non-reacted TiO<sub>2</sub> probably evaporated during the heat-treatment stage and did not contribute to the photocatalytic activity.

Adequate amount of catalyst increases the generation of electron/hole pairs, increases the formation of OH radicals and enhances the photocatalytic activity. Conversely, an excess amount of catalyst decreases the activity by reducing the UV light penetration via shielding effect of the suspended crystallites [80]. Thus, the shielding effect caused by the excessive TiO<sub>2</sub> led to opacity of the suspension and reduced the photoactivity of the TP glass. Higher agglomeration evidenced in the structure of the TP glass prepared by using 95 mol% TiO<sub>2</sub> might be another reason for lower MB degradation. High photocatalyst concentration might reduce the photocatalytic activity via particle aggregation [39]. Conclusively, there is an optimum amount of Ti<sup>4+</sup> ions to be incorporated into the glass network to increase the MB degradation, addition of Ti<sup>4+</sup> ions beyond the optimal amount has no effect on degradation.

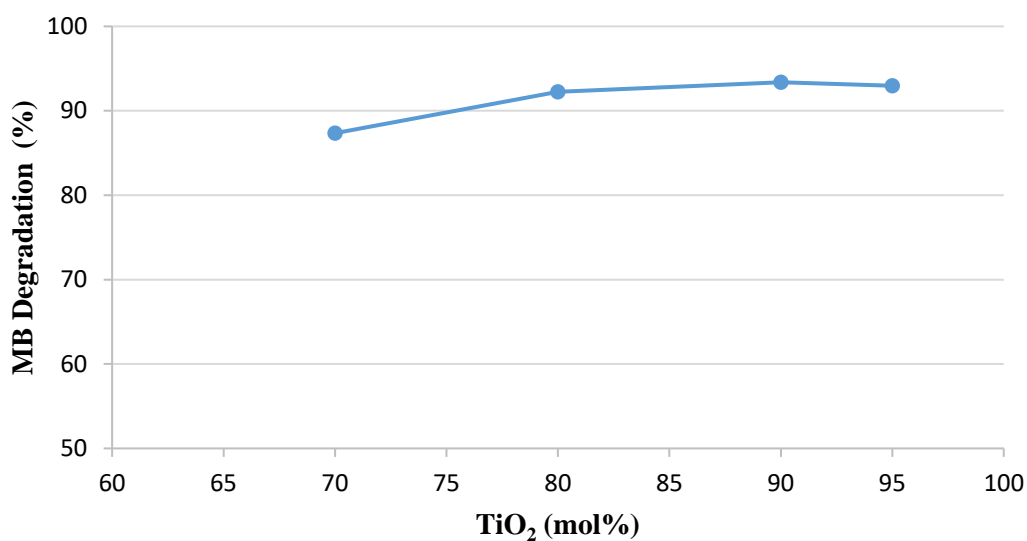


Figure 6.2. The variation of MB degradation after 90 min UV illumination for the TP glass prepared with different TiO<sub>2</sub> contents.

### 6.1.2. Effect of Solvent Type

The values for the MB adsorption in dark and the MB degradation after 90 min UV illumination for the TP glasses prepared by using different solvent types subsequently heat-treated at 600 °C for 1 h were illustrated in Figure 6.3. Adsorption and degradation values of P25 powder were included in the figure for comparison.

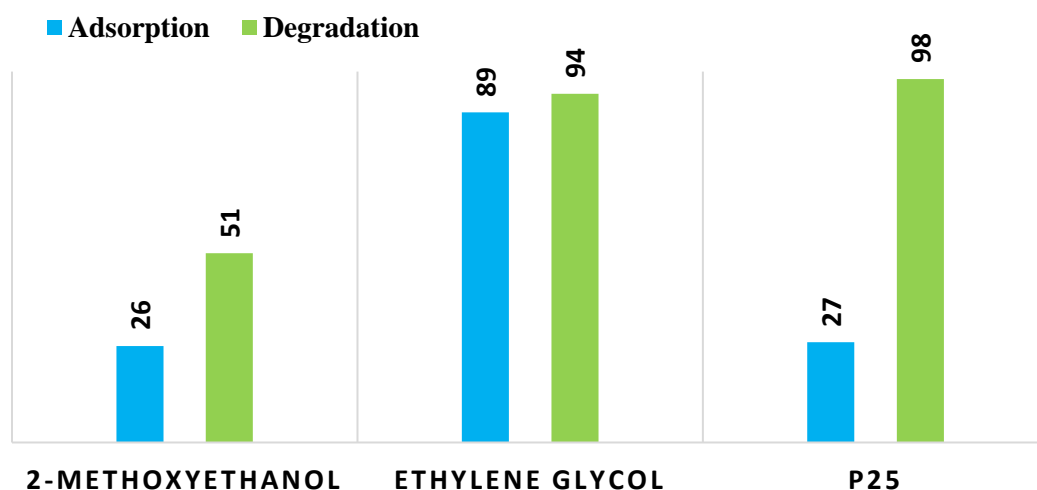


Figure 6.3. Effect of different solvent type on MB degradation.

When 2-methoxyethanol was used as solvent, the TP glass had 26% adsorption and 51% degradation of MB. Low MB adsorption of this glass was attributed to its exceptionally low SSA ( $3.4 \text{ m}^2/\text{g}$ ) and non-porous morphology. When ethylene glycol was used as solvent, MB adsorption and degradation values increased to 87% and 92%, respectively. Ethylene glycol enhanced the degradation rate by increasing the crystallinity of the glass. In addition, by preventing the precipitation and aggregation of  $\text{TiO}_2$  crystallites, it resulted in much higher SSA ( $128 \text{ m}^2/\text{g}$ ) and improved the adsorption ability by increasing the SSA. Introduction of a nucleophilic reagent to the system decreased the hydrolysis rate by occupying the coordination sites of the alkoxides and resulted in a better crystallinity as confirmed by the XRD studies. The execution of these factors resulted in the development of a glass having comparable photocatalytic activity with P25 powder.

### 6.1.3. Effect of Solvent Content

The variation in MB degradation with UV illumination time for the TP glasses prepared by using different solvent molarities subsequently heat-treated at  $600 \text{ }^\circ\text{C}$  for 1 h were illustrated in Figure 6.4. Solvent used was 2-methoxyethanol.

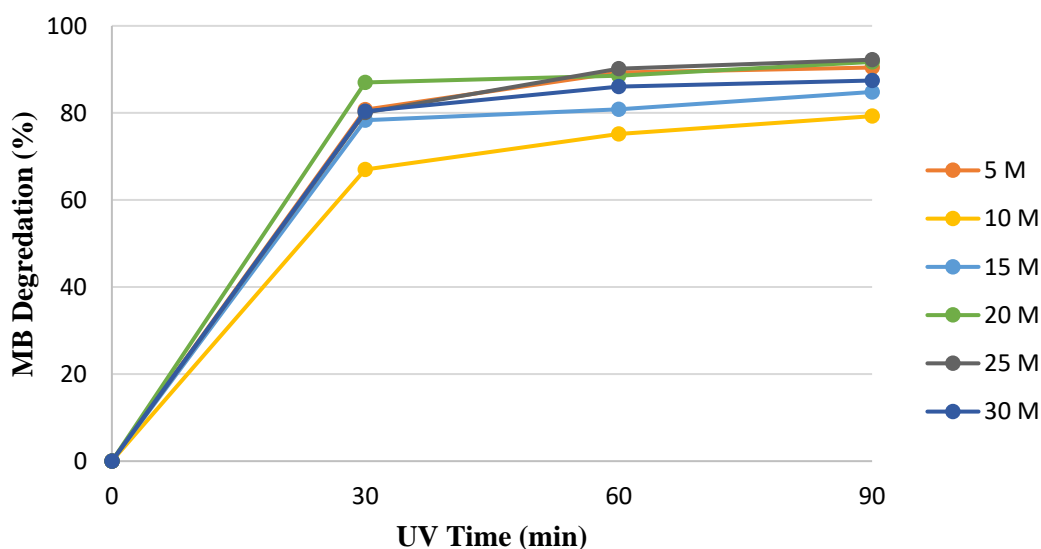


Figure 6.4. Effect of solvent content on photocatalytic activity.

The highest MB degradation rate after 90 min UV illumination was achieved for the TP glass prepared by using 25 M solvent because of the high anatase content of this glass. Enhanced activity resulted from high crystallinity of the glass, which consequently reduced the recombination of photogenerated electron-hole pairs. Low solvent concentrations were not enough to dissolve TTIP completely and unreacted portion did not contribute to the photocatalytic activity. Besides, excessive solvent concentration resulted in thick samples with low oxygen vacancies. It was generally accepted that oxygen acts as an electron scavenger and the presence of oxygen is necessary for photocatalytic activity. Without oxygen vacancies, electron-hole recombination spontaneously takes place on the surface of  $\text{TiO}_2$  and hinders photocatalytic activity [81].

#### **6.1.4. Effect of Water Content**

As shown in Table 6.1, water content caused a minor change in the photocatalytic activity, which was due to the changes in the crystal sizes. From XRD analysis, crystal sizes of 17.7 and 18.2 nm were obtained for the TP glasses prepared by using 8 and 10 M water. Size of crystallites plays a key role in photocatalysis, since it affects exposed SSA directly. Probably slightly lower crystal size of the TP glass prepared by using 8 M water increased the available reaction sites and resulted in higher photocatalytic degradation of 92.2%. Smaller crystallites lead to better photocatalytic performance as a result of enhanced  $e^-/h^+$  recombination rate via decreasing the distance for charge carriers to reach surface without recombination [38].

Increasing SSA increases number of possible reaction sites and decreases the distance to be travelled by separated charges until reaching the nearest surface [77, 78]. Oxygen vacancies in the structure, formed during heat-treatment, act as electron traps that decrease  $e^-/h^+$  recombination rate [81]. However, excess oxygen vacancies formed during heat-treatment act as  $e^-/h^+$  recombination center and decreased the photocatalytic efficiency. For a given R ratio, SSA increased as the heat-treatment temperature was increased.



Getting high SSA is desirable for the photocatalytic properties since the number of possible reaction sites per unit volume increases. Furthermore, water addition also affects pH of the solution, which affects the photocatalytic activity. Increase in water content triggers the decrease in pH due to the lessening of  $\text{H}_3\text{O}^+$  and  $\text{OH}^-$  ions in the solution and causes an equilibrium change that favors lower pH [82]. Detailed discussion related to the pH effect on photocatalytic activity was given in the following section.

#### 6.1.5. Effect of HCl Content

The variation in MB degradation with the HCl molarity hence pH of the solution for the TP glasses prepared by using different solvent molarities subsequently heat-treated at 600 °C for 1 h were illustrated in Figure 6.5.

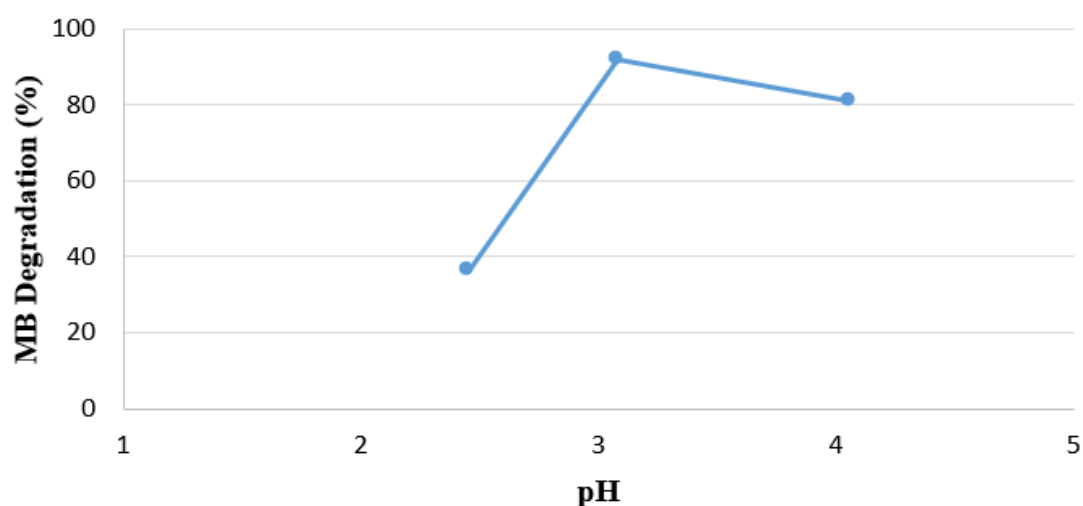


Figure 6.5. The variation in MB degradation with the pH of the solution for the TP glasses prepared by using different solvent molarities.

As confirmed by the XRD analysis, the TP glasses prepared at highly acidic conditions,  $\text{pH} < 2$ , exhibited an amorphous nature. Thus, they were excluded from photocatalytic tests. Although the TP glasses prepared by using  $\text{pH} > 2$ , had almost the same crystallinity, their photocatalytic MB degradation were considerably different and decreased in the order;  $\text{pH } 3 > \text{pH } 4 > \text{pH } 2.5$ .

The highest photocatalytic MB degradation of 92% was achieved for the TP glass prepared by using 0.05 M HCl. Introducing HCl (0.05 M) into the system enhanced the crystallization ability thanks to the hydroxide ions ( $\text{OH}^-$ ) and protons ( $\text{H}^+$ ) in the sol-gel process [82]. HCl influenced the surface electric charge of  $\text{TiO}_2$  and made electrons more likely to move into the surface of the catalyst due to the high electrostatic attraction between the positive charged  $\text{TiO}_2$  and negative charged electrons [83]. In the acidic media, electrons reacted with the oxygen molecules absorbed around the  $\text{TiO}_2$  surface to form oxidizing species such as  $\cdot\text{O}^{2-}$  and  $\cdot\text{OOH}$ . These oxidizing radicals accelerated degradation. Thus, the photocatalytic activity of  $\text{TiO}_2$  sol improved in acid media. However, the photocatalytic activity decreased to 36% with further HCl addition (0.10 M). In chemistry, it is known that generally low pH lowers the solubility. Therefore, in such acidic environment, Ti ions could not dissolve properly which might decrease the photocatalytically active Ti-O-Ti bonds. After a certain point, addition of HCl probably resulted in higher electronegativity between Ti and O atoms and made them highly polar.

#### **6.1.6. Effect of Heat-treatment Schedule**

Sol-gel derived products are mostly amorphous. It is commonly known that amorphous  $\text{TiO}_2$  has negligible photocatalytic activity due to the recombination of photoexcited electron holes at surface defects, which acts as a hole trapping centers in the photocatalytic process [29]. Amorphous  $\text{TiO}_2$  may contribute to the photocatalytic activity by increasing the lifetimes of  $e^-$  and  $h^+$  [29].

Photocatalytic activity of amorphous  $\text{TiO}_2$  could be enhanced by subjecting it to a suitable heat-treatment schedule for the crystallization of the amorphous  $\text{TiO}_2$  phase. Heat-treatment has decisive effect on the photocatalytic activity. In order to understand the effect of heat-treatment schedule on the photocatalytic activity of the TP glasses heat-treated at different heat-treatment temperatures, durations, and heating rates were subjected to MB degradation tests. Data gathered from the measurements were compared with MB degradation of P25 powder.

### 6.1.6.1. Effect of Heat-treatment Temperature

The values for the MB degradation after 90 min UV light illumination for the TP glasses heat-treated 1 h at various temperatures were listed in Table 6.2. The variation in MB degradation with heat-treatment temperature for the TP glasses heat-treated at various temperatures for 1 h was illustrated in Figure 6.6.

Table 6.2. MB degradation values after 90 min UV light illumination for the TP glasses heat-treated at various temperatures for 1 h.

Heat-treatment Temperature (°C)	MB degradation after 90 min UV illumination (%)
400	45.4
450	63.3
500	83.2
550	88.1
600	92.2
700	89.8
800	82.7
900	79.4
1000	72.3

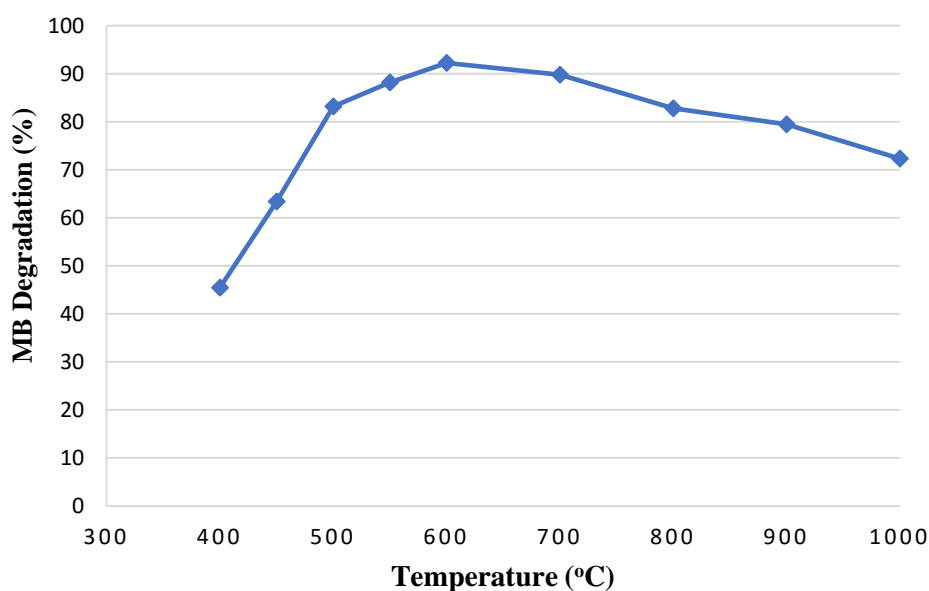


Figure 6.6. Variation in MB degradation with heat-treatment temperature for the TP glasses heat-treated at various temperatures for 1 h.

Heat-treatment temperature was a very important parameter for determining the photocatalytic activity of the TP glasses. Photocatalytic activity of the TP glasses heat-treated at 400 and 450 °C were 45.4 and 63.3%, respectively. The low photocatalytic activity of these glasses was attributed to their very high amorphous content that resulted in high concentration of defects and electron-hole trapping centers to render them inactive [29]. Decreasing the amorphous content through heat-treatment might prevent the  $e^-/h^+$  recombination rates and improve the photocatalytic activity. As illustrated in Figure 6.6, increasing the heat-treatment temperature from 400 to 600 °C greatly improved the photocatalytic activity and MB degradation reached to a maximum of 92.2%, which was a little lower than the MB degradation of 97.8% obtained for P25 powder. The superior photocatalytic activity of P25 powder is attributed to its nano sized crystallites (26 nm), high SSA (56 m<sup>2</sup>/g) and optimum pore volume (0.25 cm<sup>3</sup>/g).

In the light of literature review and previous XRD investigations, increase in the MB degradation up to 600 °C was due to the enhanced anatase crystallization. This result suggests that anatase crystals have mainly induced the photocatalytic reactions and they were the major contributing factor for enhanced photocatalytic activity. It can be proposed that photocatalytic activity was primarily a function of phase and crystallinity of the catalyst [39]. The increase in the anatase content of the samples with temperature up to 800 °C was demonstrated in XRD analysis previously. Interestingly, although the anatase content of the samples increased, photocatalytic activity did not increase. In fact, it has gradually decreased from 89.9 to 82.7% for the TP glasses heat-treated at 700 and 800 °C, respectively. This result indicates that heat-treatment at this temperature range triggered another important factor the SSA that influenced photocatalytic activity. First explanation might be related with the agglomeration phenomenon brought with the subsequent crystal growth at high heat-treatment temperatures. This can be attributed to the growth of crystal size caused by dissolution-recrystallization [84].

As previously noted, when the heat-treatment temperature was increased from 600 to 800 °C, crystal size increased from 17 to 49 nm, crystallites tended to agglomerate originating bigger crystallites with the subsequent decrease in SSA. In general, crystal size plays a key role in photocatalysis since it affects the SSA of the material directly. Smaller crystal size boosts the surface to volume ratio, increase SSA, make surface reactions more active [29]. The number of active surface sites increases by smaller particle size leading an increase on the surface charge carrier transfer rate [75].

In fact, as previously reported increasing heat-treatment temperature from 600 to 800 °C decreased SSA from 128 to 37 m<sup>2</sup>/g. It is well known that adsorption of organics plays an important role in photocatalytic degradation process [29]. Increasing heat-treatment temperature has contradictory impacts over the catalyst SSA and sometimes leads to an unpredictable effect by decreasing the photocatalytic efficiency [80]. Results suggest that the major affecting factor changed from anatase content to SSA of the glass as the heat-treatment temperature was increased. Further increasing the heat-treatment temperature to 900 and 1000 °C resulted in additional decrease in the photocatalytic activity from 79.4 % to 72.3%. In addition to the decrease in SSA, the decrease in the photocatalytic activity was also due to the anatase to rutile transition at this temperature range, which was confirmed from XRD analysis previously.

Therefore, transformation of photocatalytically favorable anatase phase to less active rutile phase decreased the photocatalytic efficiency of the product. The results suggest that the photocatalytic efficiency of the TP glasses was influenced by many factors such as the anatase content, crystal size and the SSA. The findings of this study showed that the dominance of each parameter depended on mainly 3 different temperature stages. From 400 to 600 °C, anatase content was the dominant factor while from 600 to 800 °C the SSA and at temperatures of 900 and 1000 °C anatase to rutile phase transition played the major role in determining the photocatalytic activity of the TP glass.

This result is in good agreement with that obtained by Ohtani et al. [29] who stated that “while having more crystalline anatase is beneficial for the photocatalytic activity, crystallization does not always produce materials with higher photocatalytic efficiency since during the growth of the crystals, the SSA is reduced and anatase can transform into rutile at high temperatures”. Apparently, 600 °C was the optimum heat-treatment temperature for achieving high anatase crystallinity and high SSA together. High anatase content prevented the recombination rate of photoexcited electrons and holes while the high SSA enhanced the adsorption of organic molecules onto the catalyst surface. The TP glasses having large SSA and high TiO<sub>2</sub> crystallinity exhibited high photocatalytic activity. The highest MB adsorption of 88.8% was measured after keeping the TP glass at dark for 30 min, which was significantly higher than the adsorption of 26.9% obtained for P25 powder. The whole crystallinity and less OH<sup>-</sup> group at the surface resulted in low SSA for P25 powder despite its relatively high SSA. High SSA of the TP glass provided an exceptionally high MB adsorption, about 3.3 times more than the value obtained for P25 powder. Adsorption rate influences the degradation rate, as higher number of molecules are adsorbed to surface the faster the rate of reaction [21]. Although it has slightly inferior MB degradation efficiency as compared to P25 powder, two contradictory parameters: high crystallinity and large SSA were successfully achieved in the TP glasses prepared. Thanks to its extremely high adsorption ability and considerably high degradation rate, TP glasses appear to be an alternative to P25 powder in terms of photocatalytic efficiency.

#### **6.1.6.2. Effect of Heat-treatment Duration**

The values for the MB degradation after 90 min UV light illumination for the TP glasses heat-treated at 600 °C for different heat-treatment durations were shown in Table 4.16. It was noted that the heat-treatment at 600 °C for a sufficient time improves the photocatalytic activity, but too long durations rather deteriorates it.

The highest photocatalytic MB degradation of 94.3% was achieved for the TP glass heat-treated at 600 °C for 2 h. The photocatalytic activity increases with heat-treatment durations, reaches a maximum at 2 h, and then decreases when heat-treatment duration exceeds 2 h. These results are explained in terms of the changes in the surface structure and  $Ti^{+3}$  concentrations with the heat-treatment time. This is due to the increase in  $Ti^{+3}$  concentration occurring as a result of reduction of  $Ti^{+4}$  to  $Ti^{+3}$  by organic residues such as alcohol and unhydrolyzed alkoxide groups. However, once it is used up for the reduction of  $Ti^{+4}$  or burnt out on further heating in air, the  $Ti^{+3}$  concentration starts to decrease due to reoxidation of  $Ti^{+3}$ , resulting in the decrease in the photocatalytic activity [85]. These phenomena is the major reason that the photocatalytic activity shows a maximum at 600 °C for 2 h. The TP glass heat-treated at 600 °C for 2 h has high crystallinity and more SSA therefore, it shows the maximum photocatalytic activity. As shown in the XRD patterns, higher anatase crystallinity obtained with additional 1 h heat-treatment probably caused such increase. Increasing heat-treatment durations should promote the formation of anatase crystallites with regular crystal surfaces, which will have less surface defects and give highly efficient photocatalysis by suppressing  $e^-/h^+$  recombination [86].

Existence of  $Ti^{+3}$  states prevented the photogenerated  $e^-/h^+$  recombination thus increased the photocatalytic activity. However, after this point additional treatment decreased the photocatalytic activity of the glass and minimum degradation of 81.2% was obtained for the TP glass heat-treated at 600 °C for 10 h. Very long heating at high temperature resulted in collapse pore structure and decreased SSA. Besides, after the reduction of  $Ti^{+4}$  states, further heating has resulted in a drop in the  $Ti^{+3}$  concentrations through re-oxidation. Decrease in the  $Ti^{+3}$  concentrations with excess heating time resulted in decrease in the photocatalytic activity. It was found that heat-treatment at a suitable time improved the photocatalytic activity of the TP glass but, too long durations deteriorated it.

Despite the decrease in SSA, the highest photocatalytic activity obtained for the TP glass heat-treated at 600 °C for 2 h indicates that at a certain temperature, amount of anatase phase played a more dominant role than SSA for determining the photocatalytic efficiency of the material.

### **6.1.6.3. Effect of Heating Rate**

The values for the MB degradation after 90 min UV light illumination for the TP glasses prepared by using different heating rates were shown in Table 6.1. Increasing heating rate in Stage 1 (from 25 to 280 °C) did not have much influence but, that in Stage 2 (from 280 to 600 °C) affected the photocatalytic activity. Increasing heating rate in Stage 2 up to 180 °C/h improved the anatase crystallinity. Thus, the highest photocatalytic activity of 92.2% was achieved. As previously discussed in the XRD studies, further increment in the heating rate deteriorated the crystallinity.

Probably at such high heating rates, TiO<sub>2</sub> crystallites could not find enough time to align properly. Moreover, abrupt evaporation of the solvent and water caused a shrinkage which subjected the glass to high pressure so that intense cracks formed. Although fast heating rate results in a better crystallinity, the TP glasses heat-treated at slow heating rates had much bigger SSA. Therefore, the TP glasses heat-treated at slow heating rates showed slightly higher photocatalytic activity than those at fast heating rates.

## **6.2. Band Gap Measurements**

The energy corresponding to electron excitation from VB to CB can be used to determine the optical band gap energy,  $E_g$ , value. The  $E_g$  values for the TP glasses were measured using UV-Vis diffuse reflectance spectra. The direct and indirect  $E_g$  values were calculated by plotting energy versus  $F(R)$ ,  $(F(R)*E)^{1/2}$  and  $(F(R)*E)^2$  graphs and extrapolating the linear portion of the transmittance curves.  $E_g$  values for the TP glass as calculated by using Kubelka-Munk transform method were shown in Figure 6.7.



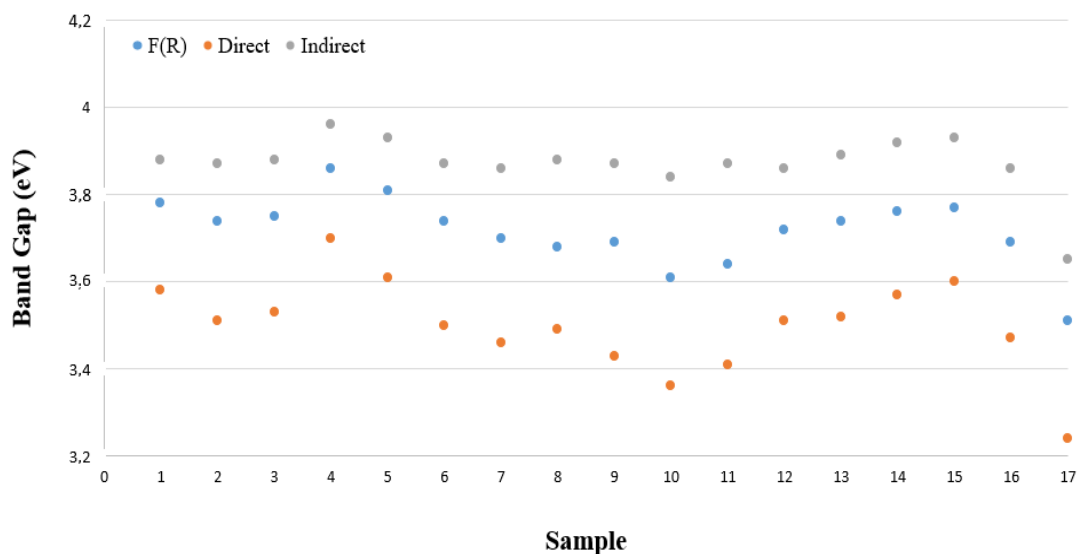


Figure 6.7. Band-gap energy of the TP glasses.

$E_g$  values for the TP glasses dispersed in a wide range between 3.2 to 4.0 eV depending on the calculation method. The lowest  $E_g$  values were obtained by direct calculation method and varied with respect to the preparation and heat-treatment conditions for the TP glasses. Generally, smaller  $E_g$  values are beneficial for photocatalysis since it enables larger active light spectrum where catalyst is active. The active light spectrum broadens with decreasing  $E_g$ . This broadening makes the catalyst active even in visible light.

### 6.2.1. Effect of TiO<sub>2</sub> Content

The values for the direct  $E_g$  for the TP glasses prepared by various TiO<sub>2</sub> content subsequently heat-treated at 600 °C for 1 h were tabulated in Table 6.3.

Table 6.3. The values for the direct  $E_g$  for the TP glasses prepared by various TiO<sub>2</sub> content subsequently heat-treated at 600 °C for 1 h.

TiO <sub>2</sub> content (mol %)	Direct band gap (eV)
70	3.53
80	3.50
90	3.41
95	3.51

It is obvious that increase in TiO<sub>2</sub> content of the TP glass lead a decrease in E<sub>g</sub> until 95 mol % TiO<sub>2</sub> content. When the TiO<sub>2</sub> content was increased to 95 mol % TiO<sub>2</sub>, E<sub>g</sub> increased. Probably the TP glass prepared by using 90 mol % TiO<sub>2</sub> had the most structural defects and oxygen vacancies so that it provided the smallest E<sub>g</sub> values. It is known that amorphous, anatase and rutile phases of TiO<sub>2</sub> have E<sub>g</sub> values of 3.5, 3.2 and 3.0 eV, respectively. A difference in the absorption edge between anatase and rutile crystallites leads to a shift in conduction edge and results in the difference in E<sub>g</sub> values [24]. Significantly larger E<sub>g</sub> values calculated for the TP glasses were attributed to the presence of P<sub>2</sub>O<sub>5</sub>.

TiO<sub>2</sub> and P<sub>2</sub>O<sub>5</sub> exhibit different energy levels and P<sub>2</sub>O<sub>5</sub> has larger E<sub>g</sub> values than TiO<sub>2</sub>. Therefore, when the two oxides came together, band gap becomes larger and electrons require more energy to be excited from VB to CB [27]. Larger E<sub>g</sub> of the TP glass means a decrease in the light spectra that could be absorbed and thus it might be a disadvantage for applications requiring indoor light as the light source. On the other hand, larger E<sub>g</sub> value leads to the use of absorbed energy in a more effective way. Larger E<sub>g</sub> lowers the probability for recombination, increases the hydroxyl and superoxide formation efficiency and enables TiO<sub>2</sub> to catalyze different reactions [37].

### **6.2.2. Effect of Heat-treatment**

The values for the direct E<sub>g</sub> for the TP glasses heat-treated at various temperatures for 1 and 2 h were tabulated in Table 6.4. The E<sub>g</sub> values varied between 3.36 and 3.70 eV and decreased with increasing heat-treatment temperature. The E<sub>g</sub> value of the TP glass heat-treated at 600 °C for 2 h was slightly lower, 3.47 eV.

The difference in the E<sub>g</sub> values was due to the difference in crystallite size and phase composition of the glasses caused by different heat-treatment temperatures and durations. The largest E<sub>g</sub> was obtained for the TP glass heat-treated at 400 °C. Higher CB levels were mainly caused by the higher amorphous content of the glass. This finding agrees with the results reported by Prasai et al. [87].

Table 6.4. Values for the direct  $E_g$  for the TP glasses heat-treated at various temperatures.

Heat-treatment temperature (°C)	Heat-treatment duration (h)	Direct band gap (eV)
400	1	3.70
500	1	3.61
600	1	3.50
600	2	3.47
700	1	3.43
1000	1	3.36

The increase in the size of the crystallites with increasing heat-treatment temperatures also contributes to lowering  $E_g$ . Venkatacham et al. [75] reported that the  $E_g$  depends on the size of nanoparticles by the quantum size effect and shift of the absorption edge signifies the changes in  $\text{TiO}_2$  particle sizes. Heat-treatment caused surface alterations and affected the  $E_g$  values by changing the oxygen stoichiometry in the oxide mixture [40]. The TP glasses heat-treated at various temperatures exhibited bigger  $E_g$  values than crystalline anatase and rutile phases of  $\text{TiO}_2$ . Metal oxides typically show lower  $E_g$  values with the change in phase, such as from amorphous to anatase to rutile [88].

In this study, the largest  $E_g$  value of 3.70 eV was obtained for the TP glass with high amorphous content and the smallest  $E_g$  value of 3.36 eV was obtained for the TP glass with high rutile content. The  $E_g$  value of P25 powder was 3.26 eV. Relatively lower  $E_g$  of P25 powder was attributed to the decrease in the  $e^-/h^+$  recombination rate with coexistence of anatase and rutile phases [7].

### 6.3. Transmittance Measurements

The transmittance of the TP glasses was measured using UV-Vis spectrophotometer. Transmittance spectra were measured in the wavelength range between 200 and 1000 nm. Effect of different parameters on the transmittance of the TP glasses was examined.

### 6.3.1. Effect of TiO<sub>2</sub> Content and Heat-treatment Temperature

Figure 6.8 represents the transmittance of the TP glasses prepared by using 80 and 90 mol% TiO<sub>2</sub> subsequently heat-treated at temperatures between 600 and 1000 °C.

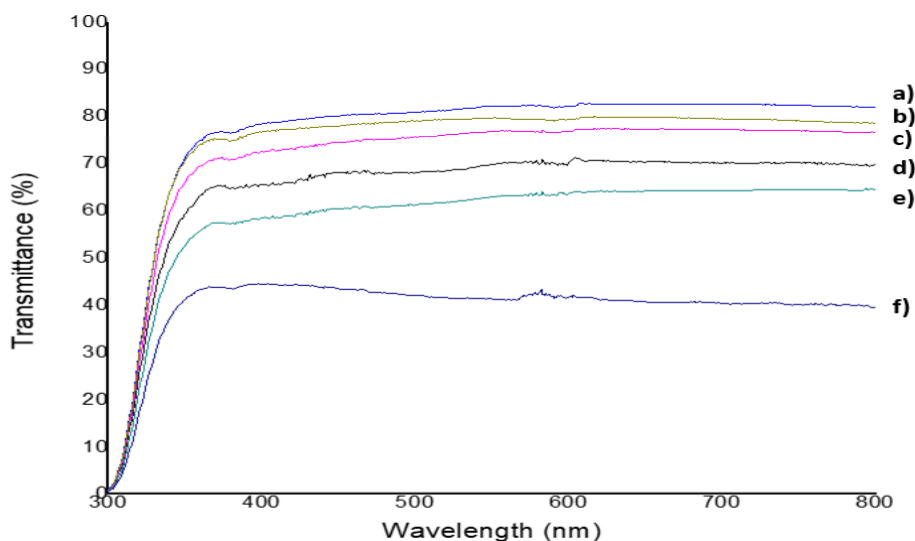


Figure 6.8. The transmittance of a) 90 mol% 2-methoxyethanol 600 °C, b) 80 mol% 2-methoxyethanol 600 °C, c) 90 mol% ethylene glycol 600 °C, d) 80 mol% ethylene glycol 600 °C, e) 80 mol% ethylene glycol 800 °C, f) 80 mol% ethylene glycol 1000 °C.

The optical transmission of the TP glass prepared by using 90 mol% TiO<sub>2</sub> was more than that of the TP glass prepared by using 80 mol% TiO<sub>2</sub> due to the presence of more amount of small anatase crystallites. Increasing heat-treatment temperature to 1000 °C resulted in a decrease in the transmittance probably because of the difference in crystal structure. Rutile crystals in the structure decreased the transmission ability of the glass by scattering effect. Low transmission was accompanied by the rutile crystals, which has the highest refractive index of TiO<sub>2</sub> polymorph [86].

### 6.3.2. Effect of Solvent Type

The TP glasses prepared by using 2-methoxyethanol, 2-propanol, ethylene glycol, 2-ethoxyethanol, 2-isopropoxyethanol, 2-butoxyethanol, and benzyl alcohol were subjected to the transmittance tests. The transmittance spectra of the glasses were illustrated in Figure 6.8.

The highest transmission was obtained for the TP glass prepared by using 2-methoxyethanol. The visual transparency of the TP glass prepared by using this solvent was previously shown in Figures 4.1 - 4.3. Although the glass was completely transparent to the naked eye, it showed a relatively lower transmittance value of 80% compared with an ordinary window glass (94%), i.e. soda lime glass. This decrease might be related with the high amount of surface microcracks formed during the heat-treatment process. It is known that reflection and absorption result a decrease in overall transmission. Samples produced by using 2-propanol and ethylene glycol as solvents exhibited even lower transmittance values attributable to their higher absorption ability caused by high SSA and porosity of these glasses.

#### **6.4. Hydrophilicity**

The hydrophilicity and degradation of organic molecules on the surface were two reasons why TiO<sub>2</sub> can be used for self-cleaning application [38]. The degradation process through photocatalytic oxidation prevents organic substances from accumulation and hydrophilic feature helps to wash off contaminants more easily.

Previously, photocatalytic activity of TP glasses was evaluated through decolorization of aqueous MB solution and under UV irradiation. In this section hydrophilicity of the TP glasses were assessed by measuring the contact angle of a water droplet on the glass surface to evaluate the self-cleaning ability. In order to measure the hydrophilicity (or surface wettability) and interfacial changes, distilled water droplets were dropped on the surface of the TP glasses by using a manual syringe and contact angle of the samples were measured. The contact angle measurements were done only for the glasses prepared by using 80, and 90 mol% TiO<sub>2</sub> and by using 2-methoxyethanol and ethylene glycol since they provided sufficient photocatalytic activity. Contact angle values were measured directly after placing a droplet on the glass surface. The values were tabulated in Table 6.5. The interaction between the distilled water droplets and the glass surface were shown in Figure 6.9.

Table 6.5. Contact angle values of the TP glasses.

TiO <sub>2</sub> content (mol %)	Solvent type	Drop	Contact angle (Degree)
80	2-Methoxyethanol	1 <sup>st</sup> drop	0
80	2-Methoxyethanol	2 <sup>nd</sup> drop	0
80	Ethylene glycol	1 <sup>st</sup> drop	11.3
80	Ethylene glycol	2 <sup>nd</sup> drop	18.3
90	2-Methoxyethanol	1 <sup>st</sup> drop	0
90	2-Methoxyethanol	2 <sup>nd</sup> drop	0
90	Ethylene glycol	1 <sup>st</sup> drop	10.7
90	Ethylene glycol	2 <sup>nd</sup> drop	12.7

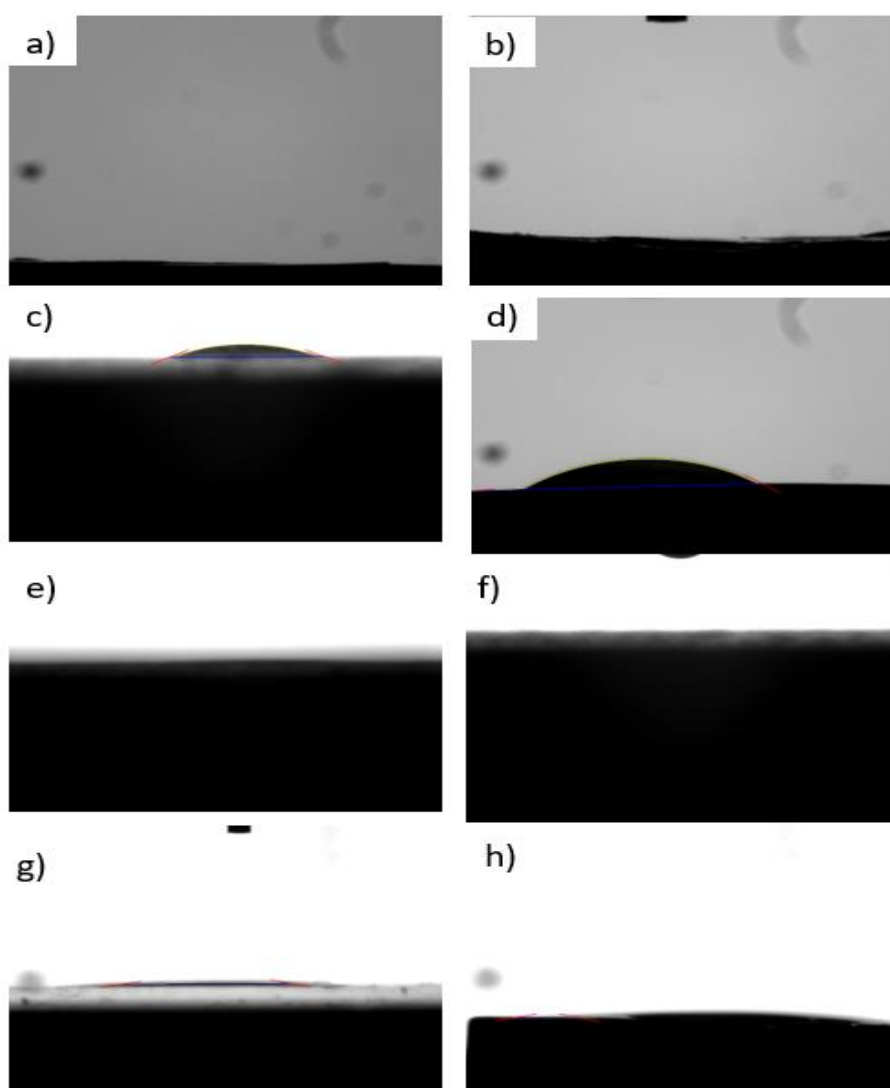


Figure 6.9. The interaction between the distilled water droplets and the glass surface.

In general, glasses possess high surface energy hence wet easily. Materials having high surface energy tend to absorb low energy compounds such as water vapor and organic contaminants from the environment [41] and usually a liquid with lower surface tension results in smaller contact angle. For the TP glasses prepared by using 2-methoxyethanol and ethylene glycol, measured contact angles were  $0^\circ$  and  $11.3^\circ$ , respectively. Smaller contact angles indicate better hydrophilicity. In this case, it can be said that the TP glasses have high hydrophilicity since they have contact angles below  $20^\circ$ .

When the second droplet was dropped after the first measurement, contact angle values of the TP glasses prepared by using 2-methoxyethanol and ethylene glycol increased to  $12.7^\circ$  and  $22.8^\circ$ , respectively. This is attributed to the adsorption of a portion of the 1<sup>st</sup> drop by the glass porosity. When the 2<sup>nd</sup> droplet was dropped, it had higher interaction with the wet glass surface.

For the TP glass prepared by using 2-methoxyethanol, all water droplets have spread out from the surface and resulted in complete wetting with a contact angle of  $\sim 0^\circ$ . The super-hydrophilic behaviour was associated with the chemisorption of water molecules and can be explained by the oxygen vacancy generated on the photoexcited  $\text{TiO}_2$  surface [89]. When water was dropped on the glass surface they take up the oxygen vacancies and make the surface hydrophilic.

The contact angle values of the glasses decreased with increasing  $\text{TiO}_2$  content implying better hydrophilicity. Lower contact angle with increasing  $\text{TiO}_2$  content of the glass is related to the increased crystallinity. High photocatalytic activity and hydrophilicity make the TP glasses promising materials for self-cleaning applications.





## CHAPTER 7

### CONCLUSIONS

Bulk  $\text{TiO}_2\text{-P}_2\text{O}_5$  glasses containing high amount of  $\text{TiO}_2$  can be successfully synthesized through the sol-gel process. The synthesis parameters and conditions have profound influence on the microstructure and crystallization behavior of the TP glasses. A regulated heat-treatment causes the development of anatase  $\text{TiO}_2$  crystals in the structure at temperatures above 400 °C. It is possible to control crystallinity, crystal size, morphology, and surface area by tailoring processing parameters such as heat-treatment temperature, duration, and heating rate which influence the photocatalytic activity of the TP glasses. Heat-treatment at temperatures above 900 °C results anatase to rutile transformation. The immobilization of  $\text{TiO}_2$  crystals by the  $\text{P}_2\text{O}_5$  facilitates high temperature stable anatase phase.

From 400 to 600 °C; anatase content, from 600 to 800 °C; specific surface area, and at and above 900 °C; rutile content are the chief factors influencing the photocatalytic activity of the TP glass. The TP glasses exhibit both photocatalytic activity and photo-induced hydrophilicity. A photocatalytic Methylene Blue (MB) degradation of 96.1% is achieved after exposing the TP glass to UV light for 90 min.

MB degradation of the TP glass was slightly inferior to that of a commercially available  $\text{TiO}_2$  powder, Degussa P25. But the glass had superior adsorption ability, about 3 times as much as P25. High photocatalytic activity of the TP glass was attributed to compatibility of sufficient anatase crystallinity to initiate photocatalytic reactions and its high specific surface area. TP glass could be used as an alternative material to  $\text{TiO}_2$  powder and coatings in self-cleaning applications.



## REFERENCES

- [1] J. Fu, "Photocatalytic properties of TiO<sub>2</sub>-P<sub>2</sub>O<sub>5</sub> glass ceramics," *Mater. Res. Bull.*, vol. 46, pp. 2523–2526, 2011.
- [2] A. Fujishima and K. Honda, "Electrochemical photolysis of water at a semiconductor Electrode", *Nature*, vol. 238, pp. 37-38, 1972.
- [3] A. C. Lee, R. H. Lin, C. Y. Yang, M. H. Lin, and W. Y. Wang, "Preparations and characterization of novel photocatalysts with mesoporous titanium dioxide (TiO<sub>2</sub>) via sol-gel method," *Mater. Chem. Phys.*, vol. 109, pp. 275–280, 2008.
- [4] J. Fu, "Photocatalytic properties of glass ceramics containing anatase-type TiO<sub>2</sub>," *Mater. Lett.*, vol. 68, pp. 419–422, 2012.
- [5] D. E. Harrison and F. A. Hummel, "Reactions in the system TiO<sub>2</sub>-P<sub>2</sub>O<sub>5</sub>," *J Am. Cer. Soc.*, vol. 333, pp. 487–490, 1954.
- [6] A. Tang, H. Huang, D. Wei, Z. Tang, and M. Zhang, "Sol-gel preparation and optical properties of amorphous TiO<sub>2</sub>-P<sub>2</sub>O<sub>5</sub> films," *Mater. Res. Innov.*, vol. 20, pp. 235–239, 2016.
- [7] O. Carp, C. L. Huisman, and A. Reller, "Photoinduced reactivity of titanium dioxide", *Prog. Solid State Chem.*, vol. 32, pp. 33-177 2004.
- [8] T. Hashimoto, M. Wagu, K. Kimura, and H. Nasu, "Titanophosphate glasses as lithium-free nonsilicate pH-responsive glasses - Compatibility between pH responsivity and self-cleaning properties," *Mater. Res. Bull.*, vol. 47, pp. 1942–1949, 2012.
- [9] A Mansingh, J. K. Vaid, and R. P. Tandon, "AC Conductivity of vanadium phosphate glasses," *J. Non-Cryst. Solids*, vol. 7, pp. 179–90, 1974.
- [10] T. Hayashi, T. Yamada, and H. Saito, "Preparation of titania-silica glasses by the gel method", *J Mat Sci.*, vol. 18, pp. 3137-3142, 1983.

- [11] R. K. Brow, D. R. Tallant, W. L. Warren, A. McIntyre, and D. E. Day, "Spectroscopic studies of titanophosphate and calcium titanophosphate glasses," *Phys. Chem. Glasses* vol. 38, pp. 300–306, 1997
- [12] T. Hashimoto, H. Nasu, and K. Kamiya, "Ti<sup>+3</sup> free multicomponent titanophosphate glasses as ecologically sustainable optical glasses," *J. Am. Ceram. Soc.*, vol. 89, pp. 2521–2527, 2006.
- [13] L. Gao and Q. Zhang, "Effects of amorphous contents and particle size on the photocatalytic properties of TiO<sub>2</sub> nanoparticles," *Scr. Mater.*, vol. 44, pp. 1195–1198, 2001.
- [14] S. C. Pillai and S. Hehir (Eds), "Sol-gel materials for energy, environment and electronic applications", *Advances in sol-gel derived materials and technologies*, January, 2017.
- [15] D. M. Pickup, R. J. Speight, J. C. Knowles, M. E. Smith, and R. J. Newport, "Sol-gel synthesis and structural characterisation of binary TiO<sub>2</sub>–P<sub>2</sub>O<sub>5</sub> glasses," *Mater. Res. Bull.*, vol. 43, pp. 333–342, 2008.
- [16] C. Schmutz, E. Basset, P. Barboux, and J. Maquet, "Study of titanium phosphate gels and their application to the synthesis of KTiOPO films," *J. Mater. Sci.*, vol. 3, pp. 393–397, 1993.
- [17] A. Tang, T. Hashimoto, H. Nasu, and K. Kamiya, "Sol-gel preparation and properties of TiO<sub>2</sub>–P<sub>2</sub>O<sub>5</sub> bulk glasses," *Mater. Res. Bull.*, vol. 40, pp. 55–66, 2005.
- [18] A. J. Tang, T. Hashimoto, T. Nishida, H. Nasu, and K. Kamiya, "Structure study of binary titanophosphate glasses prepared by sol-gel and melting methods," *J. Ceram. Soc. Japan*, vol. 112, pp. 496–501, 2004.
- [19] F. Foroutan, N. J. Waters, G. J. Owens, N. J. Mordan, H. Kim, N. Leeuw, and J. C. Knowles, "Novel sol-gel preparation of (P<sub>2</sub>O<sub>5</sub>)<sub>0.4</sub>–(CaO)<sub>0.25</sub>–(Na<sub>2</sub>O)<sub>x</sub>–(TiO<sub>2</sub>)<sub>(0.35–x)</sub> bioresorbable glasses (x=0.05, 0.1, and 0.15)," *J. Sol-Gel Sci.*

- Technol., vol. 73, pp. 434–442, 2014.
- [20] X. You, F. Chen, and J. Zhang, “Effects of calcination on the physical and photocatalytic properties of TiO<sub>2</sub> powders prepared by sol-gel template method,” vol. 34, pp. 181–187, 2005.
- [21] B. Viswanathan and K. J. A. Raj, “Effect of surface area, pore volume and particle size of P25 titania on the phase transformation of anatase to rutile,” *Ind. J. Chem. - Sect. A: Inorg. Phys. Theor. Anal. Chem.*, vol. 48, pp. 1378–1382, 2009.
- [22] N. Wetchakun and S. Phanichphant, “Effect of temperature on the degree of anatase-rutile transformation in titanium dioxide nanoparticles synthesized by the modified sol-gel method,” *Curr. Appl. Phys.*, vol. 8, pp. 343–346, 2008.
- [23] X. H. Xia, Y. Liang, Z. Wang, J. Fan, Y. S. Luo, and Z. J. Jia, “Synthesis and photocatalytic properties of TiO<sub>2</sub> nanostructures,” *Mater. Res. Bull.*, vol. 43, pp. 2187–2195, 2008.
- [24] A. Simpraditpan, T. Wirunmongkol, S. Pavasupree, and W. Pecharapa, “Effect of calcination temperature on structural and photocatalyst properties of nanofibers prepared from low-cost natural ilmenite mineral by simple hydrothermal method,” *Mater. Res. Bull.*, vol. 48, pp. 3211–3217, 2013.
- [25] M. R. Mohammadi, D. J. Fray, and A. Mohammadi, “Sol-gel nanostructured titanium dioxide: Controlling the crystal structure, crystallite size, phase transformation, packing and ordering,” *Microporous Mesoporous Mater.*, vol. 112, pp. 392–402, 2008.
- [26] J. P. Nikkanen, T. Kanerva, and T. Mäntylä, “The effect of acidity in low-temperature synthesis of titanium dioxide,” *J. Cryst. Growth*, vol. 304, pp. 179–183, 2007.
- [27] T. C. Totito, “Photocatalytic activity of supported TiO<sub>2</sub> nanocrystals,” University of the Western Cape, November, 2013.

- [28] S. Qiu and S. J. Kalita, "Synthesis, processing and characterization of nanocrystalline titanium dioxide," *Mater. Sci. Eng. A*, vol. 435–436, pp. 327–332, 2006.
- [29] B. Ohtani, Y. Ogawa, and S. Nishimoto, "Photocatalytic activity of amorphous - anatase mixture of titanium (IV) oxide particles suspended in aqueous solutions," *J. Phys. Chem. B*, vol. 5647, pp. 3746–3752, 1997.
- [30] A. Fujishima, X. Zhang, and D. A. Tryk, "TiO<sub>2</sub> photocatalysis and related surface phenomena". *Surf. Sci. Rep.*, vol. 63, pp. 515-582., 2008.
- [31] X. Chen and S. Mao "Titanium dioxide nanomaterials: synthesis, properties, modifications, and applications", *Chem. Rev.*, vol. 107, pp. 2891 – 2959., 2007.
- [32] A. L. Linsebigler, G. Lu, and J. T. Yates, "Photocatalysis on TiO<sub>2</sub> surfaces : Principles , mechanisms, and selected results photocatalysis on TiO<sub>n</sub> Surfaces", *Chem. Rev.*, vol. 95, pp. 735–758, 2002.
- [33] K. J. Choi and S. W. Hong, "Preparation of TiO<sub>2</sub> nanofibers immobilized on quartz substrate by electrospinning for photocatalytic degradation of ranitidine", *Res. Chem. Interm.*, vol. 38, pp. 1161-1169, 2011.
- [34] J. Drelich, E. Chibowski, D. D. Meng, and K. Terpilowski, "Hydrophilic and superhydrophilic surfaces and materials", *Soft Matter.*, vol. 7, pp. 9804-9828, 2011.
- [35] R. Wang, K. Hashimoto, A. Fujishima, M. Chikuni, E. Kojima, A. Kitamura, M. Shimohigoshi, and T. Watanabe, "Light-induced amphiphilic surfaces," *Nature*, vol. 388, no. 6641, pp. 431–432, 1997.
- [36] M. Anpo, N. Aikawa, S. Kodama, and Y. Kubokawa, "Photocatalytic hydrogenation of alkynes and alkenes with water over titanium dioxide. Hydrogenation accompanied by bond fission". *J. Phys. Chem.*, vol. 88, pp. 2569 - 2572, 1984.

- [37] Y. Hendrix, A. Lazaro, Q. Yu, and J. Brouwers, "Titania-Silica composites: A review on the photocatalytic activity and synthesis methods," *World J. Nano Sci. Eng.*, vol. 05, pp. 161–177, 2015.
- [38] P. Periyat, B. Naufal, and S. G. Ullattil, "A review on high temperature stable anatase TiO<sub>2</sub> photocatalysts," *Mater. Sci. Forum*, vol. 855, pp. 78–93, 2016.
- [39] C. Su, B. Y. Hong, and C. M. Tseng, "Sol-gel preparation and photocatalysis of titanium dioxide," *Catal. Today*, vol. 96, pp. 119–126, 2004.
- [40] L. Koudelka, P. Mošner, J. Pospíšil, L. Montagne, and G. Palavit, "Structure and properties of titanium-zinc borophosphate glasses," *J. Solid State Chem.*, vol. 178, pp. 1837–1843, 2005.
- [41] E. A. Abou Neel, W. Chrzanowski, and J. C. Knowles, "Effect of increasing titanium dioxide content on bulk and surface properties of phosphate-based glasses," *Acta Biomater.*, vol. 4, pp. 523–534, 2008.
- [42] D. S. Brauer, N. Karpukhina, V. R. Law, and R. Hill, "Effect of TiO<sub>2</sub> addition on structure, solubility and crystallisation of phosphate invert glasses for biomedical applications". *J. Non-Cryst. Sol.*, vol. 356, pp. 2626-2633, 2010.
- [43] M. Navarro, M. Ginebra, M. P. Clement, J. Martinez, S. Avila, and J. Planell, "Physicochemical degradation of titania-stabilized soluble phosphate glasses for medical applications". *J. Am. Ceram. Soc.*, vol. 86, pp.1345-1352, 2003.
- [44] K. Sunada, T. Watanabe, and T. Hashimoto, "Studies on photokilling of bacteria on TiO<sub>2</sub> thin film", *J. Photochem. Photobiol. A: Chem.*, vol. 156, pp. 227-233, 2003.
- [45] F. Foroutan, "Sol-gel synthesis of phosphate-based glasses for biomedical applications," PhD Thesis, Division of Biomaterials and Tissue Engineering, UCL Eastman Dental Institute, University College London, 2015.
- [46] R. K. Brown, D. R. Tallant, W. L. Warren, A. McIntyre, and D. E. Day, "Spectroscopic studies of the structure of titanophosphate and calcium

- titanophosphate glasses", *Phys. Chem. Glasses*, vol. 38, pp. 300, 1997.
- [47] S. Sakka, "Sol-gel process and applications", Second Ed. Elsevier, 2013.
- [48] D. Carta, D. M. Pickup, J. C. Knowles, M. E. Smith, and R. J. Newport, "Sol-gel synthesis of the  $P(2)O(5)$ -CaO-Na(2)O-SiO(2) system as a novel bioresorbable glass", *J. Mat. Chem.*, vol. 15, pp. 2134-2140, 2005.
- [49] E. A. Barringer and H. K. Bowen, "High-purity, monodisperse TiO<sub>2</sub> powders by hydrolysis of titanium tetrathoxide. 2. Aqueous interfacial electrochemistry and dispersion stability," *Langmuir*, vol. 1, pp. 420-428, 1985.
- [50] L. L. Hench and J. K. West, "The sol-gel process". *Chem. Rev.*, vol. 90, pp. 33-72, 1990.
- [51] B. E. Yoldas, "Hydrolysis of titanium alkoxide and effects of hydrolytic polycondensation parameters," *J. Mater. Sci.*, vol. 21, pp. 1087-1092, 1986.
- [52] H. Klug, and L. E. Alexander, "X-ray diffraction procedures", 2<sup>nd</sup> edn., John Wiley and Sons, Inc., New York, 1974.
- [53] L. Agartan, D. Kapusuz, J. Park, and A. Ozturk, "Effect of H<sub>2</sub>O/TEOT ratio on photocatalytic activity of sol-gel-derived TiO<sub>2</sub> powder," *Nanomater. Energy*, vol. 2, pp. 280-287, 2013.
- [54] M. E. Simonsen and E. G. Sogaard, "Sol-gel reactions of titanium alkoxides and water: Influence of pH and alkoxy group on cluster formation and properties of the resulting products," *J. Sol-gel Sci. Technol.*, vol. 53, pp. 485-497, 2010.
- [55] D. D. Dunuwila, C. D. Gagliardi, and K. A. Berglund, "Application of controlled hydrolysis of titanium(IV) isopropoxide to produce sol-gel-derived thin films," *Chem. Mater.*, vol. 6, pp. 1556-1562, 1994.
- [56] A. C. Pierre, "Introduction to sol-gel processing", Kluwer Academic Publishers, USA, 1998.



- [57] I. Y. Terabe K, Kato K, Miyazaki H, Yamaguchi S, Imai A, "Microstructure and crystallization behaviour of TiO<sub>2</sub> precursor prepared by the sol-gel method using metal alkoxide," *J. Mater. Sci.*, vol. 29, pp. 1617–1622, 1994.
- [58] M. Gopal W. J. Moberly Chan, L. C. De Jonghe, "Room temperature synthesis of crystalline metal oxides," *J. Mater. Sci.*, vol. 32, pp. 6001–6008, 1997.
- [59] V. Guzmán-Velderrain, Y. O. López, J. S. Gutiérrez, A. L. Ortiz, V. H. Collins-Martínez "TiO<sub>2</sub> films synthesis over polypropylene by sol-gel assisted with hydrothermal treatment for the photocatalytic propane degradation," *ChemPhysChem*, vol. 13, pp. 120–132, 2014.
- [60] S.P. Tung and B.J. Hwang, "Synthesis and characterization of hydrated phosphor–silicate glass membrane prepared by an accelerated sol–gel process with water/vapor management," *J. Mater. Chem.*, vol. 15, pp. 3532, 2005.
- [61] A. V. Gayathri Devi, V. Rajendran, and N. Rajendran, "Structure, solubility and bioactivity in TiO<sub>2</sub>-doped phosphate-based bioglasses and glass-ceramics," *Mater. Chem. Phys.*, vol. 124, pp. 312–318, 2010.
- [62] G. H. Awan and S. Aziz, "Synthesis and applications of TiO<sub>2</sub> nanoparticles", *Pakistan Eng. Congr., 70<sup>th</sup> Annu. Sess. Proc.*, vol. 70, pp. 403–412, 2007.
- [63] Z. Li, Y. Zhu, J. Wang, Q. Guo, and J. Li, "Size-controlled synthesis of dispersed equiaxed amorphous TiO<sub>2</sub> nanoparticles," *Ceram. Int.*, vol. 41, pp. 9057–9062, 2015.
- [64] N. Uekawa, N. Endo, K. Ishii, T. Kojima, and K. Kakegawa, "Characterization of titanium oxide nanoparticles obtained by hydrolysis reaction of ethylene glycol solution of alkoxide," *J. of Nanotechnology*, vol. 2012, pp 1-8, 2012.
- [65] H. Yin, Y. Wada, T. Kitamura, S. Kambe, S. Murasawa, H. Mori, T. Sakata, and S. Yanagida, "Hydrothermal synthesis of nanosized anatase and rutile TiO<sub>2</sub> using amorphous phase TiO<sub>2</sub>," *J. Mater. Chem.*, vol. 11, pp. 1694–1703, 2001.
- [66] K. Yanagisawa, K. Ioku, and N. Yamasaki, "Formation of anatase porous

- ceramics by hydrothermal hot-pressing of amorphous titania spheres,” *J. Am. Ceram. Soc.*, vol. 80, pp. 1303–1306, 1997.
- [67] T. Sugimoto, X. Zhou, and A. Muramatsu, “Synthesis of uniform anatase TiO<sub>2</sub> nanoparticles by gel–sol method 1. Solution chemistry of Ti(OH)(4-n)+(n) complexes,” *J. Coll. Interf. Sci.*, vol. 252, pp. 53–61, 2002.
- [68] S. Qourzal, A. Assabbane, and Y. Ait-Ichou, “Synthesis of TiO<sub>2</sub> via hydrolysis of titanium tetraisopropoxide and its photocatalytic activity on a suspended mixture with activated carbon in the degradation of 2-naphthol,” *J. Photochem. Photobiol. A: Chem.*, vol. 163, pp. 317–321, 2004.
- [69] P. Cheng, M. P. Zeheng, Q. Huang, Y.P. Jin, and M.Y. Gu, "Enhanced photoactivity of Silica-Titania binary oxides prepared by sol-gel method". *J. Mat. Sci. Lett.*, vol 22, pp. 1165-1168, 2003.
- [70] M. Pal and J. G. Serrano, P. Santiago, and U. Pal, “Size-controlled synthesis of spherical TiO<sub>2</sub> nanoparticles: Morphology, crystallization, and phase transition,” *J. Phys. Chem.* vol. 111, pp. 96–102, 2007.
- [71] S. Liu, J. Lu, Q. Feng, and W. Tang, “Effect of ethanol on synthesis and electrochemical property of mesoporous Al-doped titanium dioxide via solid-state reaction,” *Chinese J. Chem. Eng.*, vol. 19, pp. 674–681, 2011.
- [72] P. Gorska, A. Zaleska, E. Kowalska, T. Klimczuk, W. Sobczak, E. Skworek, W. Januszd, and J. Hupka, "TiO<sub>2</sub> photoactivity in vis and UV light: The influence of calcination temperature and surface properties". *Applied Catalysis B: Environmental* 2008, vol. 84, pp. 440 – 447, 2008.
- [73] S. S. Arbuj, R. R. Hawaldar, U. P. Mulik, B. N. Wani, D. P. Amalnerkar, and S. B. Waghmode, “Preparation, characterization and photocatalytic activity of TiO<sub>2</sub> towards methylene blue degradation,” *Mater. Sci. Eng. B*, vol. 168, pp. 90–94, 2010.
- [74] J. Klongdee, W. Petchkroh, K. Phuempoonsathaporn, P. Praserthdam, A. S.

- Vangnai, and V. Pavarajarn, "Activity of nanosized titania synthesized from thermal decomposition of titanium (IV) n-butoxide for the photocatalytic degradation of diuron," *Sci. Technol. Adv. Mater.*, vol. 6, pp. 290–295, 2005.
- [75] N. Venkatachalam, M. Palanichamy, and V. Murugesan, "Sol-gel preparation and characterization of nanosize TiO<sub>2</sub>: Its photocatalytic performance," *Mater. Chem. Phys.*, vol. 104, pp. 454–459, 2007.
- [76] M. Kanna and S. Wongnawa, "Mixed amorphous and nanocrystalline TiO<sub>2</sub> powders prepared by sol-gel method: Characterization and photocatalytic study," *Mater. Chem. Phys.*, vol. 110, pp. 166–175, 2008.
- [77] S. Qui and S. J. Kalita, "Synthesis, processing and characterization of nanocrystalline titanium dioxide," *Mat. Sci. Eng.*, vol. 435-436, pp. 327-332, 2006.
- [78] J. Mosa, M. Aparicio, A. Durán, and Y. Castro, "Mesostuctured HSO<sub>3</sub>-functionalized TiO<sub>2</sub>-P<sub>2</sub>O<sub>5</sub> sol-gel films prepared by evaporation induced self-assembly method with high proton conductivity," *Electrochim. Acta*, vol. 173, pp. 215–222, 2015.
- [79] "Z. Chen, G. Zhao, H. Li, and G. Han, "Effects of water amount and pH on the crystal behaviour of a TiO<sub>2</sub> nanocrystalline derived from a sol–gel process at a low temperature", *J. Am. Ceram. Soc.*, vol. 92, pp. 1024 – 1029, 2009.
- [80] G. S. Pozan and A. Kambur, "Effect of operating parameters and titanium source on photodegradation of phenol," *Ind. J. Chem. Technol.*, vol. 21, pp. 272–279, 2014.
- [81] D. Kapusuz, J. Park, and A. Ozturk, "Sol – gel synthesis and photocatalytic activity of B and Zr co-doped TiO<sub>2</sub>," *J. Phys. Chem. Solids*, vol. 74, pp.1026 – 1031, 2013.
- [82] L. Agartan, D. Kapusuz, J. Park, and A. Ozturk, "Effect of initial water content and calcination temperature on photocatalytic properties of TiO<sub>2</sub> nanopowders

- synthesized by the sol-gel process,” *Ceram. Int.*, vol. 41, pp. 12788–12797, 2015.
- [83] J. Yao and C. Wang “Decolorization of methylene blue with TiO<sub>2</sub> sol via UV irradiation photocatalytic degradation,” *Int. J. Photoenergy*, vol. 2010, pp. 3-4, 2010.
- [84] H. Zhang and J. F. Banfield, “Kinetics of crystallization and crystal growth of nanocrystalline anatase in nanometer-sized amorphous titania,” *Chem. Mater.*, vol. 14, pp. 4145–4154, 2002.
- [85] J. Yu, X. Zhao, and Q. Zhao, “Photocatalytic activity of nanometer TiO<sub>2</sub> thin films prepared by the sol – gel method,” *Mater. Chem. Phys.*, vol. 69, pp. 25–29, 2001.
- [86] N. Erdoğan, "Hydrothermal synthesis of TiO<sub>2</sub> nanostructures for photocatalytic and photovoltaic applications," PhD Thesis, Middle East Technical University, 2017.
- [87] B. Prasai, B. Cai, M. K. Underwood, J. P. Lewis, and D. A. Drabold, “Properties of amorphous and crystalline titanium dioxide from first principles,” *J. Mater. Sci.*, vol. 47, pp. 7515–7521, 2012.
- [88] H. Jensen, K. D. Joensen, J. E. Jurgensen, J. S. Pedersen, and G. Sogaard, “Characterization of nanosized partly crystalline photocatalysts,” *J. Nanoparticle Res.*, vol. 6, pp. 519–526, 2004.
- [89] M. A. Vargas and J. E. Rodriguez-Páez, "Amorphous TiO<sub>2</sub> nanoparticles: Synthesis and antibacterial capacity, ”*J. Non. Cryst. Solids*, vol. 459, pp. 192–205, 2017.